UCRL-19334
c.2

RECEIVED
LAWRENCE
RADIATION LABORATORY
JAN 14 1970
LIBRARY AND
DOCUMENTS SECTION

PHYSICAL PROBES OF NERVE MEMBRANE STRUCTURE

Gerald Entine
(Ph.D. Thesis)

December 1969

AEC Contract No. W-7405-eng-48

TWO-WEEK LOAN COPY

This is a Library Circulating Copy which may be borrowed for two weeks. For a personal retention copy, call Tech. Info. Division, Ext. 5545

UCRL-19334

LAWRENCE RADIATION LABORATORY
UNIVERSITY of CALIFORNIA BERKELEY

DISCLAIMER

This document was prepared as an account of work sponsored by the United States Government. While this document is believed to contain correct information, neither the United States Government nor any agency thereof, nor the Regents of the University of California, nor any of their employees, makes any warranty, express or implied, or assumes any legal responsibility for the accuracy, completeness, or usefulness of any information, apparatus, product, or process disclosed, or represents that its use would not infringe privately owned rights. Reference herein to any specific commercial product, process, or service by its trade name, trademark, manufacturer, or otherwise, does not necessarily constitute or imply its endorsement, recommendation, or favoring by the United States Government or any agency thereof, or the Regents of the University of California. The views and opinions of authors expressed herein do not necessarily state or reflect those of the United States Government or any agency thereof or the Regents of the University of California.

TABLE OF CONTENTS

	Page
ABSTRACT	-i-
I. INTRODUCTION	1
II. REVIEW OF NEUROPHYSIOLOGY	4
A. The Nerve Cell and its Action Potential	4
1) General Description	4
2) Electrochemical Potentials	7
3) Hodgkin Huxley Theory of Action Potential Propagation	9
B. Membrane Models	11
1) Internal Perfusion and the Sodium-Potassium Channels	11
2) Bilipid-Layer Model	14
3) Kavanau Pillar and Pore Model	18
4) Lettvin Passive Conduction Theory	20
III. REVIEW OF OPTICAL ABSORPTION, FLUORESCENCE, AND BIREFRINGENCE	23
A. Absorption	23
B. Fluorescence	23
C. Birefringence	24
1) Basic Equations	24
2) Intrinsic and Form Birefringence	28

TABLE OF CONTENTS (continued)

Page

3) Dependence of Index of Refraction on Wavelength 31

4) Dependence of Birefringence on Wavelength 35

IV. TECHNIQUES AND INSTRUMENTATION FOR OPTICAL STUDIES 39

A. Previous Work 39

1) Birefringence and Scattering Measurements 39

2) Ultraviolet Absorption 40

B. Introduction to our Study 41

C. Optical Instrumentation 42

1) Absorption and Fluorescence Apparatus 42

2) Light Sources 43

3) Ultraviolet Polarizers and Lenses 45

4) Birefringence Apparatus - Laser 46

5) Ultraviolet Birefringence System 46

6) High Light Intensity Optics for Visible Spectrum 48

D. Electronic Instrumentation 50

1) Continuous versus Chopped Light 50

2) Photomultiplier and Preamplifier 52

3) Bandwidth of System 53

4) Synchronization 55

5) Lamp Power Supplies 58

6) Calibration 62

TABLE OF CONTENTS (continued)

	Page
ACKNOWLEDGEMENTS	120
REFERENCES	122
SELECTED BIBLIOGRAPHY	124

PHYSICAL PROBES OF NERVE MEMBRANE STRUCTURE

Gerald Entine

Laboratory of Chemical Biodynamics
Lawrence Radiation Laboratory
University of California
Berkeley, California

December 1969

ABSTRACT

The nerve axon is an object of fascination for scientists of almost every field. The source of the nerve axon's uniqueness is its membrane, a layer only about 100 Å thick, which is generally believed to be the only part of the axon which changes significantly during the action potential. The composition, structure and mechanism of the membrane is virtually a complete mystery, and it is to these three questions that our dissertation research was directed.

The major difficulty in this problem is that the 100 Å membrane cannot be isolated from the surrounding cell structures which together are one hundred times thicker than the membrane. By studying the live nerve as it fires, we hoped to use the fact that during the action potential only the membrane changes significantly to distinguish it from the bulk of the cellular structure. Two techniques were developed, one using optical methods and one using electron spin resonance. Both of these techniques have the possibility of being specific enough to indicate directly the composition, structure and mechanism of at least some of the active parts of the membrane.

This thesis is divided into several parts. The first part contains a brief description of nerve properties and a review of some of the approaches which have been used in previous studies. Nerve membrane models are discussed in some detail as a guide to the current conjectures of the field. A review of optical absorption and fluorescence is also presented, followed by a more extensive discussion of the theory of birefringence. The derivation of the wavelength dependence is particularly pertinent, and is essential to the interpretation of the data.

The section on techniques and optical instrumentation describes not only the essential instruments, theory, experiments and results, but also the peripheral problems involved in doing a neurophysiological study. Discussion of problems such as designing sea water aquaria and dissecting giant axons from squid are less exciting than the central theme, but of great value to physicists or other non-physiologists who wish to attempt seriously to study nerves. Non-optimal instruments and negative results are also included since similar undertakings are being contemplated by several newcomers to the field.

The results of the optical work are accompanied by a review of the most recent findings of other laboratories in the field. The implications of these results encourage future expansion of these techniques.

The third section - on biradical spin labeling - arises from work done in conjunction with others in the Biodynamics Laboratory. It discusses the nature of the biradical interaction, the effect of

biradical structure and of solvents on that interaction, and its use to probe both the resting and excited nerve.

The primary conclusion of this work is that the axon membrane does exhibit a change in optical properties which follows closely the time course of the action potential. The calculations of the wavelength dependence of birefringence show it is quite possible that the birefringence changes could reveal the nature of the molecules involved in the membrane change. In our particular experiments, measurements could be made only down to 350 nm. If measurements could be made near the 280 nm protein absorption band, it would immediately determine whether proteins are the source of the signal.

The conclusions of the biradical spin labeling studies suggest that the lipid portion of lobster nerves is in a liquid rather than a structured state and that it does not change during the action potential. Suggestions are made for pursuing this technique with more refined labeling molecules.

I. INTRODUCTION

The nerve axon is an object of fascination for scientists of almost every field. Electrical engineers delight in calculating transmission line analogs of it , physical chemists revel in its ionic currents and electrochemical potentials, and physiologists wonder at the diversity of drugs which affect its properties so drastically. Nevertheless, despite the vast attention and effort directed at the axon, its basic secrets remain undisclosed.

The source of the nerve axon's uniqueness is its membrane, a layer only about 100 Å thick, which is generally believed to be the only part of the axon which changes significantly during the action potential. The composition, structure and mechanism of the membrane is virtually a complete mystery, and it is to these three questions that our dissertation research was directed.

The major difficulty in this problem is that the 100 Å membrane cannot be isolated from the surrounding cell structures which together are one hundred times thicker than the membrane. By studying the live nerve as it fires, we hoped to use the fact that during the action potential only the membrane changes significantly to distinguish it from the bulk of the cellular structure. Two techniques were developed, one using optical methods and one using electron spin resonance. Both of these techniques have

the possibility of being specific enough to indicate directly the composition, structure and mechanism of at least some of the active parts of the membrane. Although our particular experiments were not as conclusive as desired, the techniques appear quite promising, and are now being pursued by other laboratories.

This thesis is divided into several parts. The first part contains a brief description of nerve properties and a review of some of the approaches which have been used in previous studies. Nerve membrane models are discussed in some detail as a guide to the current conjectures of the field. A review of optical absorption and fluorescence is also presented, followed by a more extensive discussion of the theory of birefringence. The derivation of the wavelength dependence is particularly pertinent and is essential to the interpretation of the data.

The section on techniques and optical instrumentation describes not only the essential instruments, theory, experiments and results, but also the peripheral problems involved in doing a neurophysiological study. Discussion of problems such as designing sea water aquaria and dissecting giant axons from squid are less exciting than the central theme, but of great value to physicists or other non-physiologists who wish to attempt seriously to study nerves. Non-optimal instruments and negative results are also included since similar undertakings are being contemplated by several newcomers to the field.

The results of the optical work are accompanied by a review of the most recent findings of other laboratories in the field.

The implications of these results encourage future expansion of these techniques.

The third section - on biradical spin labeling - arises from work done in conjunction with others in the Biodynamics Laboratory. The philosophy and techniques developed for the optical work seemed very adaptable to ESR, and with the introduction of the use of biradical labels into our laboratory, we decided to devote some time to the project. Nevertheless, the optical project remained the focus of the dissertation and the spin label work was not pursued as deeply as the optical studies. This section discusses the nature of the biradical interaction, the effect of biradical structure and of solvents on that interaction, and its use to probe both the resting and excited nerve.

II. REVIEW OF NEUROPHYSIOLOGY

A. The Nerve Cell and its Action Potential

1) General Description[1]

Nerve cells are found in many different sizes and varieties in the different species of animals, but are surprisingly similar in their general structure and functional properties. Figure II-1 shows a generalized nerve cell. The cell body containing the nucleus has two distinct types of processes: the dendrites and an axon. The dendrites act as the input to the nerve cell. When stimulated by chemical transmitters from other nerve cells or receptors, they initiate the firing of the nerve and lead to the propagation of an action potential down the axon. The axon can be quite short, as in the retinal nerve cells, or as much as several feet in length.

The action potential can be readily controlled by an experimenter, and its phenomonology has been studied for several decades. Figure II-2 shows a typical experimental setup for electrical stimulation and recording of the action potential. It is found that for a given duration of stimulus, there is a threshold amplitude below which the axon does not fire, and above which the firing is total. The size of the action potential, if it occurs, is completely independent of the size of the stimulating pulse.

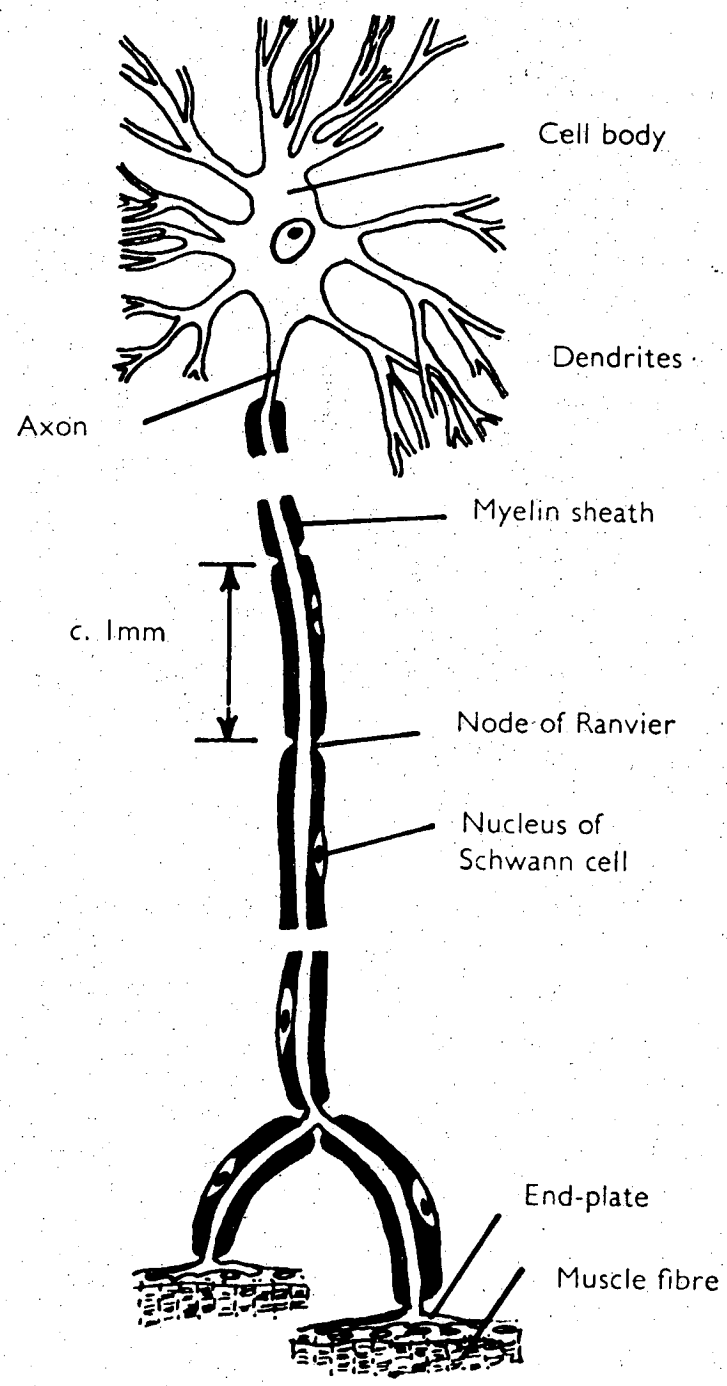

Figure II-1. Generalized nerve cell (Hodgkin, p. 21).

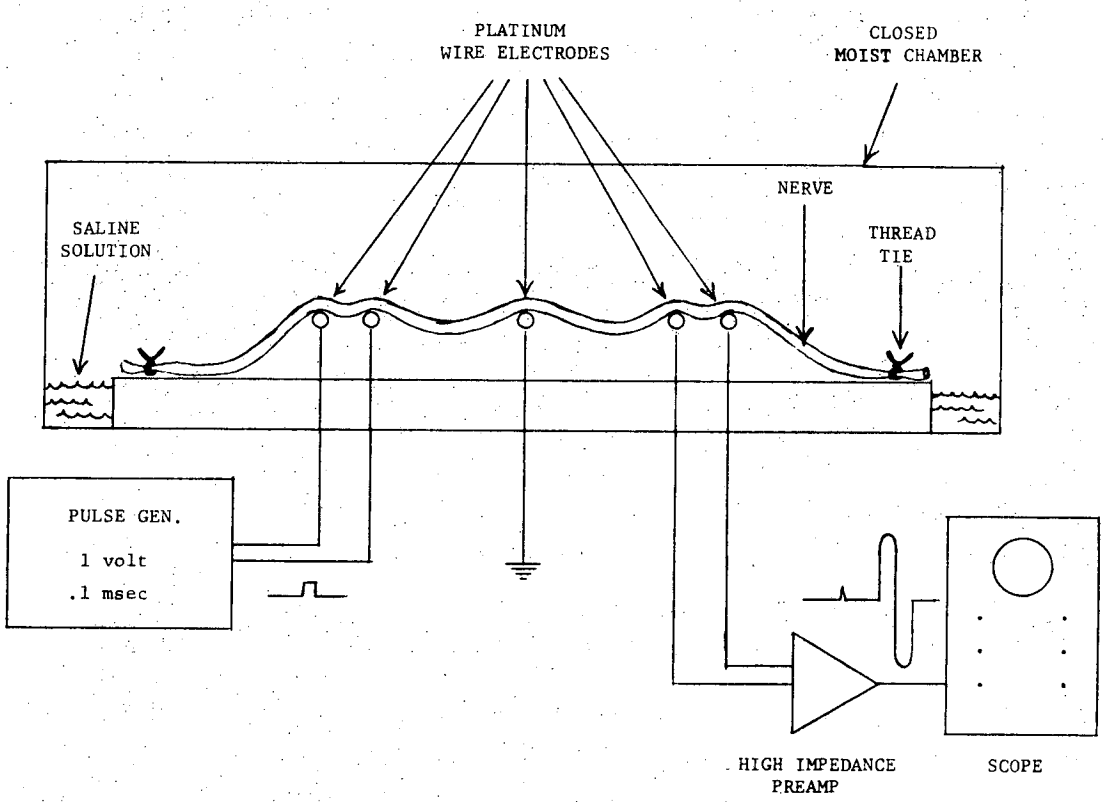

XBL-698-5303

Figure II-2. Typical nerve stimulating and recording setup.

Typically used stimulating pulses are 0.1 msec wide and 1 volt high, although these values can be varied greatly, with longer pulses requiring less amplitude. The degree to which the saline solution short circuits the electrodes and the condition of the nerve also strongly affect the amount of stimulus required to excite a nerve.

Originally, action potentials were recorded with extracellular electrodes, and this method is still the most convenient way to determine the state of the nerve. As the action potential passes the electrodes, a biphasic signal is recorded (Figure II-3a). These measurements show that the action potential lasts about 2 msec and propagates at velocities of 0.5 to 20 meters per second.

It is possible to place one electrode inside a large nerve axon and to measure the voltage between the inside and the outside of the nerve. Figure II-3b shows a typical response measured this way. It is evident that at rest, the nerve maintains its interior 60 mv negative with respect to the outside fluid. It is primarily this voltage which acts as the energy source for the action potential and accounts for its magnitude being independent of the size of the stimulus pulse.

2) Electrochemical Potentials

What generates this resting potential? By an as yet unexplained process, the nerve cell accumulates a high concentration of potassium ions, K^+, while excreting enough sodium, Na^+, to keep the internal sodium concentration much below that of the

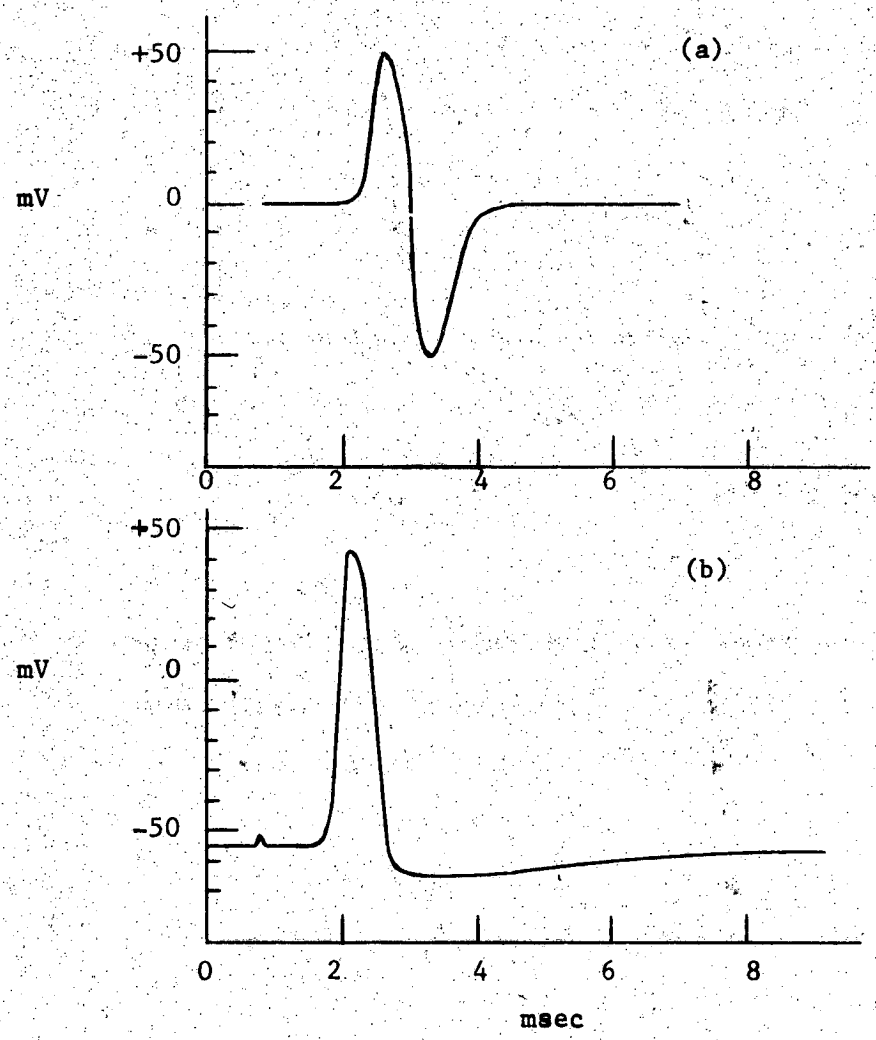

XBL 698-5302

Figure II-3. Squid nerve action potentials. (a) Extracellular electrodes. (b) Intracellular electrode.

extracellular fluid. By the Nernst equation, the membrane would have a potassium equilibrium potential V_K of

$$V_K = RT/F\ (\ln[K]_o/[K]_i) = -75 \text{ mv (for squid)}$$

and a sodium equilibrium potential V_{Na} of

$$V_{Na} = RT/F\ (\ln[Na]_o/[Na]_i) = +55 \text{ mv (for squid)}$$

where $[\ ]_o$ are the concentrations outside the cell, and $[\ ]_i$ are the concentrations inside.

The resting potential of a squid nerve is fairly close to V_K because the membrane is almost ten times as permeable to K^+ as to Na^+ in that state.

If the nerve is fired, the membrane becomes permeable to Na^+ and presumably relatively impermeable to K^+. This leads to the potential during the crest of the response approaching the +55 mv predicted by the Nernst equation.

3) Hodgkin Huxley Theory of Action Potential Propagation

Hodgkin and Huxley,[1] using the above observations and hypotheses as a starting point, developed a theory of action potential behavior which has been a major source of experiments in the field. By assuming that the nerve membrane can be switched from its potassium permeable state to its sodium permeable state by the flow of electrical current, one can attribute the propagation of the

action potential to a flow of current between the resting and active nerve. It has been shown that the rise in sodium permeability lasts less than a millisecond, and that within three tenths of a millisecond potassium ions leave the nerve faster than sodium ions enter. The potassium flow restores the resting potential and puts the membrane into a ready condition to be fired again.

The large membrane capacitance of about one microfarad per cm^2 along with the high resistance of a small cylinder of axoplasm limits the rate of conduction velocity. (This was originally discovered by Young shortly after he introduced the use of the giant squid axon to the field in 1935. He found that the propagation velocity went as the square root of the axon diameter.[2]) Changing the conductivity of the extracellular fluid causes predictable changes in velocity. Myelinated nerves propagate pulses faster than unmyelinated ones of the same diameter because the sheath reduces the effective capacitance per unit length. These observations indicate that the nerve action potential is indeed propagated by local electric currents spreading in front of the active region.

In 1939, Curtis and Cole[3] measured the conductivity of the squid axon membrane during the action potential. They found that the membrane resistance fell from its resting value of 1000 ohm-cm^2 to only 25 ohm-cm^2 during the crest of the pulse. This change, while following the general time course of the action potential,

lagged it slightly as would be expected since the leading edge of the potential is due to passive conduction of spreading currents from the adjacent active regions.

The techniques of Curtis and Cole, and Hodgkin and Huxley, were repeated with almost infinite variations by many other groups. In 1958, Hodgkin and Huxley took the results of the preceeding works and the computations of theorists and developed a set of phenomonological equations to describe the action potential in terms of sodium and potassium currents. Since that time the effects of many ionic variations have been attributed to changes in the coefficients of the terms of these equations. However, since their approach is basically a computer curve fitting one, it is generally regarded as a description of the action potential rather than a proven explanation for it.

B. Membrane Models

1) Internal Perfusion and the Sodium-Potassium Channels

In 1960, Tasaki *et al.*[4] introduced an extremely important technique into the field: internal perfusion. Until that time it was generally held that nerve axons were such delicate cells. that any attempt to remove the axoplasm would surely kill them. Tasaki decided to try it anyway. He took a giant squid axon, cut off one end, squeezed the axoplasm out like toothpaste, and re-filled it with a saline solution. Much to everyone's surprise, the axon retained its excitability, and soon the technique

allowed the internal salt concentrations of the axon to be varied at will for periods of several hours.

The advent of the technique of internal perfusion led to a host of experiments in which agents such as enzymes and toxins were added to the internal fluid. Furthermore, all of the previous experiments in which the external medium had been changed could be repeated with different internal conditions. The new data obtained in this way encouraged theorists to invent new models of membrane structure, several of which are presented here. Some of these are extensions of the original Daveson-Danielli bilipid membrane theory proposed in 1935. Some assume that the nerve structure undergoes drastic changes during the action potential, while others assume a more passive behavior. However, none of the current theories have been able to gain the general confidence of the field.

Many attempts have been made to understand the nerve membrane by application of toxins and enzymes which alter the ion flow and presumably the membrane structure. It is this type of experiment which proves that the sodium and potassium currents are separable. Rajor and Atwater[5] used pronase, an enzyme which rather nonspecifically breaks protein peptide bonds, in their work. The pronase was applied to the nerve by internal perfusion while action potential and voltage clamp measurements were being performed.

The action potentials almost immediately started to show a plateau on the falling edge, although the leading edge of the

potential remained unaffected. The width of the plateau increased for as long as the pronase was allowed to remain (maximum of ten minutes) until it reached a duration of almost 70 msec. The effect is not reversible. Such a phenomena is most easily explained by assuming that only the potassium channels were affected by the enzyme. This hypothesis was confirmed by taking voltage clamp measurements* and varying the potassium and sodium concentrations. The shape of the potassium conductance versus voltage was the same with or without pronase, but curve was shifted along the voltage axis by 60 mv toward depolarization by the pronase. Thus the actual field that the potassium channels see might be greatly affected by the protein charge state. In any event, these experiments again demonstrate the semi-isolation between the potassium and sodium currents.

Non-enzymatic agents such as tetraethylammonium ion (TEA) and tetradotoxin (TTX) present an even more striking display of ion flow separation. TEA is a non-biological substance which, as a small cation, can be confused with the naturally occuring cations which carry the membrane current. One action of TEA is to prolong the action potentials of nerve and muscle fibers by an inhibition of the voltage dependent potassium permeability. Squid axons are found to be insensitive to TEA applied externally but quite affected by internal perfusion with it. In this condition the potassium

---

*Membrane voltage controlled by experimenter using one internal and one external electrode.

conductance is normal for inward currents and essentially nil for outward currents.

Hille[6] showed that for frog nerves TEA is a specific inhibitor for potassium conductance. It has no effect on either leakage currents or sodium currents. However, its behavior on the frog's nodes of Ranvier is quite different from that described above for the squid axon. In particular, the frog nerve affects were all observed with external TEA and Hille concludes that there must be a specific receptor site on the external side of nodal membrane. Hille found that TEA seemed to have no interaction with agents which affected the non-potassium channels. For instance, TTX, which has been shown to inhibit only sodium current for all nerves when applied externally, does not affect the magnitude of potassium inhibition by TEA in various concentrations. Calcium concentration, which is also thought to work only on the sodium channels, also does not interact with TEA.

Hille therefore concludes that since the sodium, potassium, and leakage currents are chemically independent, the most easy interpretation is that the mechanisms are spatially separated.

The proof that the sodium and potassium channels are distinct puts a strong demand on the models proposed for membrane structure. So far few models provide a really plausible explanation for this separation.

2) Bilipid-Layer Model

The bilipid membrane theory of Daveson and Danielli rested on a measurement made a decade before by Gorter and Grendel.[7] These

experimentalists tried to correlate the quantity of membrane lipid in red blood cells with the surface area of these cells. Although they made two erroneous assumptions, the effects of the mistakes cancelled and they obtained the correct answer that the ratio of area of extracted lipid formed into a monolayer, to the surface area of the membrane is two to one. They concluded that the membrane is a layer of lipid two molecules thick with the polar groups pointing outward into a polar medium.

Due to surprising results of surface tension measurements of cell membranes, Daveson and Danielli proposed their theory which included a protein layer covering the outside and inside of the bilipid layer. Figure II-4 illustrates their idea. The theory

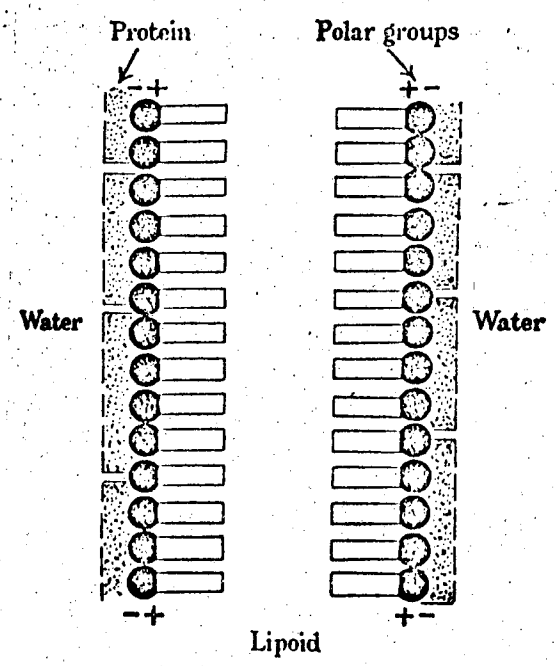

Figure II-4. Structure of cell membrane (Danielli) showing the proposed general pattern (from Davson and Danielli, 1943).

drew considerable support but still could not answer all critics. In 1959, J. D. Robertson formalized many of the arguments supporting their theory.

The Danielli and Davson unit membrane theory had been fairly well accepted up until about 6 years ago. Since that time, despite Robertson's refinement of it, it has been meeting with a fair amount of resistance and newer techniques present data which do not fit as readily into the picture. Lenard and Singer[8] were led to propose a new membrane model from the results of their ORD and CD measurements on red blood cell and bacteria membranes. Their data suggested that about one third of the protein found in these membranes is in an α helix form while the remainder is in random coil configurations. They hypothesized that since the activity of the membranes of bacteria and red blood cells are different despite their having roughly the same percentage of protein in the helix form, the ORD and CD spectra result from structural protein in the membranes.

Taking into account the hypothesis that one third of the membrane protein is in the α helix form, the Danielli-Davson-Robertson may be drawn schematically like Figure II-5a (page 1833, Ref. 8). The model Lenard and Singer propose, unlike the above model which is primarily determined by electrostatic considerations, attempts to maximize the hydrophobic interactions. The D-D-R model leaves the structural protein entirely in the unfolded state on the exterior surfaces of the membrane and thus allows a large fraction of the non-polar amino acid side chains to contact water. In such

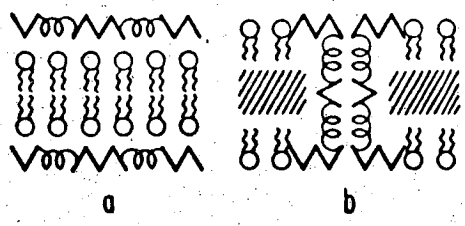

Figure II-5. (a) The Danielli-Davson-Robertson unit membrane, as modified to include the data presented in this communication. The proteins on the outer surfaces of the membrane consist of helical (ℓℓℓℓℓ) and random-coil (∧∧∨) portions. The polar lipids ( ) are oriented in a bimolecular leaflet with their polar heads (O) facing out. (b) A generalized membrane.

a case, they contend, the helices in Figure II-5a should have amino acid sequences in which approximately every second amino acid is ionic in order to interact both with water on the exposed surface and with the ionic parts of the lipid on the inner side of the protein layer. Such a condition would lead to instability of the α helix.

The model Lenard and Singer propose, Figure II-5b, holds that: 1) the ionic and polar heads of the lipid molecules and all the ionic side chains of the structural protein are on the exterior surface of the membrane in Van der Waals contact with the bulk aqueous phase; 2) sequences of structural protein consisting predominantly of non-polar side chains are in the interior of the

membrane along with the hydrocarbon tails of the phospholipids and the relatively non-polar lipids such as chloresterol; and 3) structural proteins have unique sequences which adapt them to interact with the lipid components of the membranes and the aqueous environment.

While no strong evidence is presented for this model, the above authors do point out that the amount of helicity of membrane protein can be changed by the type solvent into which they are placed, suggesting that: a) there are no structural restraints preventing the membrane from adopting a much more helical conformation than they exhibit in the membrane, and b) the conformation adopted in any condition is the one most thermodynamically favorable.

3) Kavanau Pillar and Pore Model

One membrane model which includes the idea of gross molecular rearrangement during the action potential has been proposed by Kavanau.[9] He proposes that the resting nerve membrane is a "closed" configuration in which longitudinal lipid blocks almost completely fill up the 100 Å thick region between the two protein outer envelopes. During the action potential, the lipid micelles have an internal flow in which they change from a longitudinal to a transverse form, forcing the thickness of the membrane to double, and leaving large pore areas for ion flow (Figure II-6). Viewed from the top, this structure would be in a hexagonal pattern.

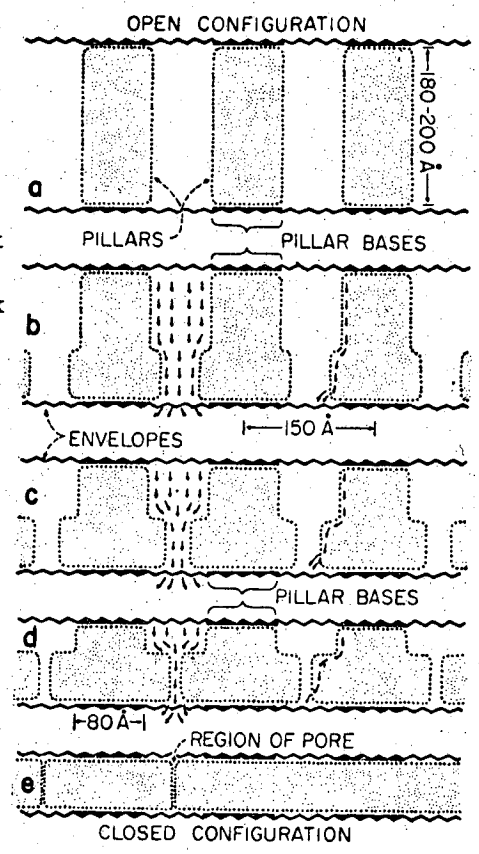

Figure II-6. Kavanau model. Heavy dots are liquid polar head groups. Arrows at left show flow of "pumped" matrix as membrane collapses. Arrows at right show flow of polar lipid heads.

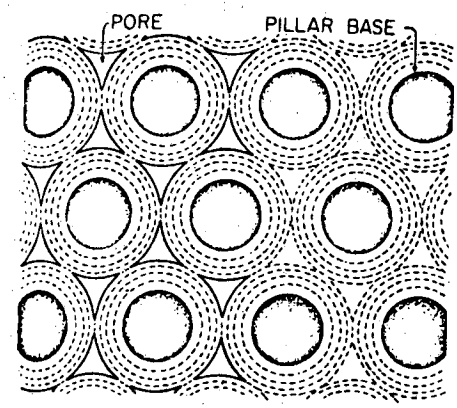

Surface view of membrane model shows successive size of pillars as membrane collapses. Pillars get large enough to touch but still leave pores.

Kavanau bases his conjecture on recent electron microscope studies which showed a hexagonal pattern. Although most studies show a membrane thickness corresponding to only the closed configuration, this is expected since that is the resting state. Certain damaged membranes show a hexagonal pattern which appears to leave pores of the size hypothesized. Undamaged membranes often show no hexagonal pattern, but Kavanau attributes this to the influence of the staining techniques on the membrane structure.

Thus Kavanau's model is not very solidly based on experimental data. However, if it were correct, the change in the orientation of the lipid micelles might be detectable optically and such optical changes could support his model.

4) Lettvin Passive Conduction Theory

Several theories have been presented which hold that the action potential is not caused by a structural change in the membrane but rather by a passive ion flux controlled by the differences of the sizes and charges of the various cations involved. Such a theory has been presented by Lettvin *et al.*[10] The membrane is viewed as the usual bimolecular leaflet with different types of pores or channels for each of the two major cations: a potassium channel which is only large enough to pass K^+, and a sodium channel which can pass Na^+ and K^+ easily but CA^{++} only with difficulty. The ions can be distinguished not only electrostatically, due to their charge and extent of hydration, but also by their steric properties, due to their radii and the deformability of their hydration cloud.

A hydrated ion is able to lock a channel either by covering one end and electrostatically binding there, or by entering a channel and binding to its walls. An ion can also act as a key for a locked channel by tumbling the locking ion out of the channel and replacing it as a channel lock.

For a sodium channel, K^+ will never be a lock, while Na^+ will be a moderate lock and CA^{++} a good lock. The normal resting state of the membrane will have a CA^{++} lock near the inner end of the Na channel. Entering Na^+, although not able to pass through the channel, will tumble near the CA^{++}. A step depolarization could cause a relaxation of the interaction between the CA^{++} and Na^+ and their environs and increase their mutual tumbling until the CA^{++} is tumbled out of the channel. Na^+ will then continue to pass through the channel from the outside medium until another Ca^{++} comes in. The time course of the Na flux starts abrubtly, due to the depolarization from the adjacent excited membrane region, but ends statistically as the scarcer Ca^{++} ions fill more and more channels.

The K channels are postulated to be unaffected by Na^+, which cannot enter them, but can be strongly locked by Ca^{++} bound on the outside of the channel by the membrane polarization field. The ease of tumbling a Ca^{++} with a K^+ can be increased by a decrease in this field and thus the step depolarization leads to the opening of these channels for K^+ flow.

The model predicts that calcium-like ions (e.g. Mg^{++}) will act like Ca^{++}, sodium-like ions (Li^{+}) act like Na^{+} and potassium-like ions (Rb^{+}) will act like K^{+}. This is indeed the case experimentally. Since Ca^{++} cannot pass through a potassium channel, Ca^{++} influx should always be associated with Na^{+} influx. This was found to be true. Finally, as external Ca^{++} concentration is raised, the rate at which Ca^{++} can diffuse into Na channels and relock them after a step depolarization is increased, and this could explain the increase in the rate at which sodium inactivation recovers following a short pulse depolarization.

III. REVIEW OF OPTICAL ABSORPTION, FLUORESCENCE, AND BIREFRINGENCE

A. Absorption

Three types of optical properties were examined in our study: absorption, fluorescence, and birefringence. Absorption changes are usually straightforward to interpret. The absorption spectra of most substances likely to be found in the nerve are well known and the spectra fairly distinct. Absorption changes of proteins, for instance, would be quite distinguishable from those due to lipids. However, it would not be possible through the use of absorption measurements alone to distinguish between related proteins.

Using polarized light for the measurement would allow exploration of the degree of alignment of the molecules. If an increase in light intensity during the action potential were found for one direction of polarization, and a decrease found for another direction, one could conclude that the molecules had rotated rather than changed only chemically.

B. Fluorescence

Fluorescence measurements could yield data similar to that obtained from absorption. The species of molecule could be determined by either the excitation spectrum or the emission spectrum .

Since the absorption of the exciting wavelength and the emission of the fluorescence would be maximal along the direction of the fluorescent molecules absorption axis, polarization studies could pinpoint the orientation of the axis and any rotation.

C. Birefringence

The third type of measurement, birefringence, is generally the hardest to interpret. It is a less commonly studied property and its theory will therefore be reviewed here in some detail. Traditionally, birefringence has been used to demonstrate alignment of molecules and structural compartments in cells. By comparing the birefringence of the specimen to the birefringence of sheets of bulk material, it is possible to estimate either the amount of material in the cell or its degree of alignment, provided the other quantity is known. In the case of the nerve membrane, not only the quantity and degree of orientation are both unknown, but also the type of molecule involved. Therefore, the traditional approach cannot yield much information. However, because of the relationship of the index of refraction of a material to its absorption, it appears possible to obtain some very specific information about the molecules from a study of the wavelength dependence of the birefringence .

1) Basic Equations[11]

When polarized light impinges normally on a substance and emerges with the same polarization as it had upon entrance

regardless of the orientation of the polarization axis, the substance is optically isotropic. There exist substances for which the emerging light is linearly polarized for only two axes of polarization. Such a substance is called birefringent, and the axes, called the optical axes, can be shown to be mutually perpendicular.

The velocity of propagation of light polarized along the two axes of a birefringent substance are unequal, and it is this variation in the index of refraction which can cause linearly polarized light to become eliptically polarized by passage through the substance. Consider a flat birefringent substance with its optic axes along the X and Y directions and linear polarized light passing normally through it.[11,11a] Let α be the angle between the axis of polarization, P, and the X axis. The incident beam is then:

$$E_o = A\cos\omega t \tag{1}$$

with components along the X and Y axes of

$$\begin{aligned} E_{ox} &= A\cos\alpha\cos\omega t &&= B\cos\omega t \\ E_{oy} &= A\sin\alpha\cos\omega t &&= C\cos\omega t \end{aligned} \tag{2}$$

The emerging light has components:

$$E_x = B\cos\omega(t - n_1 z/c)$$

$$E_y = C\cos\omega(t - n_2 z/c) \tag{3}$$

where n_1 and n_2 are the larger and smaller indices of refraction, and c is the speed of light in vacuum. For a thickness, e, the beams will emerge with a phase difference, δ, of

$$\delta = (\omega e/c)(n_1 - n_2) \tag{4}$$

and the beams emerge with wave equations

$$\begin{aligned} E_x &= B\cos(\omega t - kz) = B\cos\phi \\ E_y &= C\cos(\omega t - kz + \delta) = C\cos(\phi + \delta) \end{aligned} \tag{5}$$

These are the equations of an ellipse, so the light does emerge elliptically polarized. To see this, we must eliminate ϕ from the equation.

$$E_x/B = \cos\phi \tag{6}$$

$$E_y/C = \cos\phi\cos\delta - \sin\phi\sin\delta \tag{7}$$

Squaring equation 6 and substituting in it E_x/A for $\cos\phi$, we get

$$E_x^2/B^2 + E_y^2/C^2 - (E_x E_y/BC)(\cos\delta) - \sin^2\delta = 0 .$$

This is the equation for an ellipse for which one axis makes an angle θ with the X axis, where

$$\tan 2\theta = 2BC\cos\delta/B^2-C^2 \quad . \tag{8}$$

Thus not only the relative sizes of the major and minor axes depend on δ, but also the angle of the axes with respect to the X axis.

Consider what happens when an analyzer is placed after the substance with its transmission axis at an angle β to the X axis Eq. 12). The light emerging from the birefringent object has amplitudes (Eqs. 1 and 2)

$$\begin{aligned} &B\cos\phi \quad \text{along X} \\ &C\cos(\phi + \delta) \quad \text{along Y} \end{aligned} \tag{9}$$

The light transmitted by the analyzer is represented by

$$\cos\beta(B\cos\phi) \tag{10}$$

$$\sin\beta(C\cos(\phi + \delta) \quad . \tag{11}$$

Therefore the intensity, I, of the light transmitted by the analyzer is equal to the sum of the squares of the coefficients of $\cos\phi$ and $\sin\phi$. Equation (11) can be expanded to isolate the terms into the form

$$\text{Eq. (11)} = C\sin(\cos\phi\cos\delta - \sin\phi\sin\delta) \tag{12}$$

leading to

$$I = (B\cos\beta + C\sin\beta\cos\delta)^2 + (C\sin\beta\sin\delta)^2$$

$$I = A^2\cos^2(\alpha-\beta) - A^2\sin 2\alpha\sin 2\beta\sin^2(\delta/2) \tag{13}$$

The first term is independent of δ and is what would be transmitted through the polarizer and analyzer if no birefringent plate were interposed. The second term is dependent on all three variables, α, β, and δ.

For studying δ, we wish to maximize the second term while minimizing the first one. This condition is obtained by having the polarizer and analyzer crossed (i.e. $(\alpha-\beta) = 90°$), while having them at 45° to the optic axis (e.g., $\alpha = 45°$ and $\beta = -45°$). The intensity is then

$$I = A^2\sin^2\delta/2 = A^2\sin^2 m\pi \tag{14}$$

where m is retardation in fractions of a wavelength.

2) Intrinsic and Form Birefringence

There are two types of birefringence.[12] Intrinsic birefringence arises from oriented molecules which each are themselves optically anisotropic. Form birefringence arises from oriented

layers of isotropic material separated by layers of a second isotropic material of different refractive index. Both the layers and their separation must be small compared to the wavelength of light.

As an example of the latter type, consider a row of parallel plates of thickness K, separated by distances t_2. Let ε_1 be the dielectric constant of the plates and ε_2 the dielectric constants of the medium between the plates.

Let linearly polarized light impinge on the side of the plates with the E vector perpendicular to the plates. Since the normal component of the electric displacement D must be continuous across a boundary, D must be the some in medium 1 and medium 2. Then the electric fields are equal to

$$E = D/\varepsilon_1 \quad \text{and} \quad E_2 = D/\varepsilon_2$$

and the mean field averaged over the total volume is

$$E = \frac{t_1 \, D/\varepsilon_1 + t_2 \, D/\varepsilon_2}{t_1 + t_2}$$

Therefore, the effective dielectric constant ε for the E field perpendicular to the plates is

$$\varepsilon_\perp = \frac{D}{E} = \frac{(t_1 + t_2)\, \varepsilon_1 \varepsilon_2}{t_1 \varepsilon_2 + t_2 \varepsilon_1} = \frac{\varepsilon_1 \varepsilon_2}{f_1 \varepsilon_2 + f_2 \varepsilon_1}$$

where f_1 is the fractional volume occupied by material 1 and f_2 is the fractional volume occupied by material 2.

Next, consider the case when the E field is parallel to the plates. The tangential component of E must be continuous across the boundary, so $E_1 = E_2$. Therefore, the electric displacements in the media are

$$D_1 = \varepsilon_1 E \quad \text{and} \quad D_2 = \varepsilon_2 E$$

The mean displacement is

$$D = \frac{t_1\varepsilon_1 E + t_2\varepsilon_2 E}{t_1 + t_2}$$

and

$$\varepsilon_{\parallel} = \frac{D}{E} = \frac{t_1\varepsilon_1 + t_2\varepsilon_2}{t_1 + t_2} = f_1\varepsilon_1 + f_2\varepsilon_2$$

Since the index of refraction is related to E by $\eta^2 = \varepsilon$, we find that the system has different indices of refraction depending on the polarization of light. Note that

$$\eta_{\parallel}^2 - \eta_{\perp}^2 = \frac{f_1 f_2(\varepsilon_1-\varepsilon_2)^2}{f_1\varepsilon_2 + f_2\varepsilon_1} > 0 \qquad \text{(for plates)}$$

Therefore, a material which has bodies arrayed like parallel plates in a medium acts like a negative uniaxial birefringent crystal. It can be shown that a material which has bodies which are thin parallel rods occupying only a small fraction of the volume acts like a

positive uniaxial birefringent crystal

$$\eta_{\parallel}^{2} - \eta_{\perp}^{2} = \frac{f_1 f_2 (\varepsilon_1^{2} - \varepsilon_2^{2})^2}{(1+f_1)\varepsilon_2^{2} + f_2 \varepsilon_1^{2}} \qquad \text{(for rods)}$$

3) Dependence of the Index of Refraction on Wavelength

We now consider the variation of the refractive index of a dielectric with changes in wavelength.[11] The basic problem in calculating n is to relate the polarization of the dielectric, P/E, to the frequency of the light field ω.

Suppose there are N electronic oscillators per unit volume, and that each one consists of an electron held by an elastic restoring force and which experiences a damping force which is proportional to the electron's velocity. The equation of motion is therefore

$$m\ddot{r} + g\dot{r} + kr = Xe + Ee$$

where m is the electronic mass, g and k are constants derived from the quantum theory, X the field due to dipoles of the dielectric, and E the externally applied field from the light. X is made up of the average field due to the dipoles very nearby and to the average field from the rest of the dipoles in the medium. The first term is zero by symmetry while the second term is equal to $(4\pi/3)P$. For isotropic media P and E are in the same direction, so Eq. 1 becomes

$$\ddot{r} + \frac{g}{m}\dot{r} + \frac{k}{m} r = \left(E + \frac{4\pi\rho}{3}\right) \frac{e}{m}$$

In the absence of an external field, E = P = 0, and the equation

has a solution

$$r = r_o \exp\left(-\gamma\frac{t}{2} + i\,\omega_o t\right)$$

where

$$\gamma = \frac{g}{m} \quad \text{and} \quad \omega_o^{\,2} = \frac{k}{m} - \frac{g^2}{4m^2}$$

When damping is small, $\omega_o^{\,2} \approx k/m$, and the non-zero field equation takes the form

$$\ddot{r} + \gamma\,\dot{r} + \omega_o^{\,2} r = \left(E + \frac{4\pi}{3}P\right) e/m$$

The polarization P is equal to the dipole moment per unit volume, i.e. $P = Ner$, so multiplying Eq. 5 by Ne we have

$$\ddot{P} + \gamma\,\dot{P} + \omega_o^{\,2}\,\rho = \left(E + \frac{4\pi}{3}P\right)\frac{Ne^2}{m}$$

P should have the same frequency as E, although not necessarily the same phase, so put

$$E = E_o e^{i\omega t}$$

$$P = \alpha E_o e^{i\omega t} \qquad (\alpha \text{ complex})$$

Substituting in Eq. 7, we obtain

$$\alpha(-\omega^2 - i\gamma\omega + \omega_o^{\,2}) = \frac{Ne^2}{m}\left(1 + \frac{4\pi}{3}\alpha\right)$$

or

$$\alpha = \frac{Ne^2}{m}\,\frac{1}{\omega_o^{\,2} - \omega^2 - \frac{4\pi}{3}\frac{Ne^2}{m} + i\gamma\omega}$$

and the refractive index n can be obtained from

$$n^2 = 1 + 4\pi\,\alpha$$

$$n^2 = 1 + \frac{4\pi Ne^2}{M}\;\frac{1}{\omega_o'^2 - \omega^2 + i\gamma\omega}$$

where $\omega_o'^2 \equiv \omega_o^2 - \frac{4\pi Ne^2}{3m}$

If the system contains a fraction f_s of s type electronic oscillators, the equation becomes

$$n^2 = 1 + \frac{4\pi Ne^2}{m}\sum_s \frac{f_s}{\omega_s'^2 - \omega^2 + i\gamma_s\omega}$$

In regions far from the absorption peak, $\omega'^2 - \omega^2$ is large compared to ω, and the equation for one type of oscillator reduces to

$$n^2 = 1 + \frac{4\pi Ne^2}{m}\;\frac{1}{\omega_o' - \omega^2}$$

$$n^2 = 1 + \frac{Ne^2}{\pi C^2 m}\;\frac{\lambda^2\lambda_o^2}{\lambda^2 - \lambda_o^2}$$

where $\lambda_o = \frac{2\pi c}{\omega_o'}$

This may be rewritten in the form

$$n^2 = 1 + A + \frac{B}{\lambda^2 - \lambda_o^2}$$

where $A = \frac{\lambda_o N e^2}{C^2 \pi M}$ and $B = \frac{N e^2}{\pi M C^2} \lambda_o^4$ are constants.

In the region of absorption ($\omega_o' \approx \omega$), the equation

$$n^2 = n_o^2 + 4\pi \frac{Ne^2}{m} \frac{1}{\omega_o'^2 - \omega^2 + i\gamma_s \omega}$$

may be simplified, since $\omega_o'^2 - \omega^2 \approx 2\,\omega_o' (\omega_o' - \omega)$.

$$n^2 = n_o^2 + 4\pi \frac{Ne^2}{M\omega_o'} \frac{1}{2\,(\omega_o' - \omega) + i\gamma_s}$$

Let $n = \eta + i\chi$, where η and χ are real. Then equating real and imaginary parts, we get

$$\eta\chi = \frac{2\pi Ne^2}{M\omega_o'} \frac{\gamma_s}{4\,(\omega_o' - \omega)^2 + \gamma^2} \qquad \text{(a)}$$

$$\eta^2 - \eta^2\chi^2 - \eta_o^2 = \frac{8\pi Ne^2}{M\omega_o'} \frac{(\omega_o' - \omega)}{4\,(\omega_o' - \omega)^2 + \gamma^2} \qquad \text{(b)}$$

If $(\eta - \eta_o)$ and $\eta\chi$ are small compared to η_o, Eq. b can be solved for η

$$\eta = \eta_o + \frac{4\pi Ne^2}{\eta_o m\omega_o'} \frac{(\omega_o' - \omega)}{4\,(\omega_o' - \omega)^2 + \gamma^2}$$

The imaginary part of the refractive index, $\eta\chi$, is the absorption term, while the real part, η, is called the dispersion term. Figure III-1 shows a typical absorption and dispersion curve.

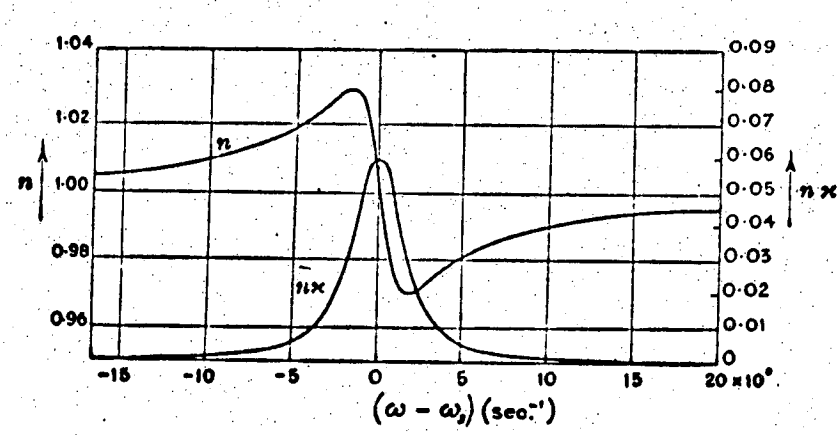

Figure III-1

4) Dependence of Birefringence on Wavelength

We now consider what type of wavelength dependence could be expected for any birefringence changes detected when the nerve fires. In making such a calculation it is necessary to consider the fact that the nerve birefringence arises not only from the active membrane, but also from the axoplasm, the supporting tissues and any inactive membrane.

From Eq. 14, we have that the intensity of light passing through crossed polarizers is related to the birefringence of the object between them by

$$I = I_o \sin^2 \delta/2$$

where δ is the retardation, and is equal to

$$\delta = 2\, e(n_1 - n_2)/\lambda$$

where e is the thickness of the material. Since the birefringence of a layer is determined by how many molecules are contained per unit area rather than by its three dimensional density, it is convenient to set e = kN, where N is the number of molecules per unit cross-sectional area and k is a calculable constant. This step is useful in avoiding problems as to what happens if the membrane changes thickness during the action potential.

$kN(n_1-n_2)$ is the optical path difference, $\overline{\lambda}$, of the two polarization directions in passing through the substance, and is referred to as the retardation. It is important to note that retardation is not a direct function of wavelength but only of refractive index difference. If the indices remain constant over a given portion of the spectrum, so will the retardation $\overline{\lambda}$ while δ will still be wavelength dependent.

$$\delta = 2\, \overline{\lambda}/\lambda \quad .$$

We divide the birefringence of the nerve into two parts, δ_m, due to the part of the membrane region which changes during the action potential, and δ_r due to the rest of the curve. Then

$$I = I_o \sin^2(\delta_r + \delta_m)$$

During the action potential δ_m changes, causing a change in I.

$$\Delta I = I_o 2\sin(\delta_r + \delta_m)\cos(\delta_r + \delta_m)\Delta\delta_m$$

The signal most easily measured experimentally is

$$S = \Delta I/I = \frac{I_o 2\sin(\delta_r + \delta_m)\cos(\delta_r + \delta_m)\Delta\delta_m}{I_o \sin^2(\delta_r + \delta_m)}$$

$$= 2\cot(\delta_r + \delta_m)\Delta\delta_m$$

Since $\overline{\lambda}_r$ has been measured to be 240 Å, and $\overline{\lambda}_m$ even if due to completely oriented lipid or protein would be about 3 Å, then $\delta_m << \delta_r$ and $S \approx 2\cot(\delta_r)\Delta\delta_m$.

For visible light,

$$\delta_r = 240\ \text{Å}/\lambda << 1$$

and $\cot\delta_r$ can be expanded as $1/\delta_r$.

$$S \approx 2\Delta\delta_m/\delta_r = \frac{2\Delta(2\pi\overline{\lambda}_m/\lambda)}{2\pi\ \overline{\lambda}_r/\lambda}$$

$$S \approx 2\Delta(\overline{\lambda}_m)/\overline{\lambda}_r .$$

Note that the $1/\lambda$ dependence cancels out.

We therefore see that if the active membrane has retardation which is a different function of wavelength than that of the bulk of the nerve, it should be detectable and not swamped by a $1/\lambda$ dependence.

Can we tell from the wavelength dependence of $\overline{\lambda}_m$ the absorption spectrum of these molecules? The answer depends on the number of assumptions that one is willing to accept. We would like to assume that $\overline{\lambda}_m$ is directly proportional to the average index of refraction of the molecules, since this is the quantity determining the absorption spectrum of the molecules in solution.

Consider the case when $\overline{\lambda}_m$ arises from an array of dichroic molecules immersed in a medium whose refractive index is not a strong function of wavelength near the molecular absorption peak. If $\Delta\ \overline{\lambda}_m$ is caused by a rotation of the molecules, then it obviously has the same wavelength dependence as the index of refraction.

If $\overline{\lambda}_m$ arose from dichroic molecules, but $\Delta\overline{\lambda}_m$ was due to a chemical change in those molecules, the spectrum obtained would be relatable to the difference in absorption spectra of the two species.

However, it is possible for the molecules to have two absorption centers causing the dichroism, and then n_1-n_2 would not go directly with the average n. In this type of case the interpretation of the data would be more difficult.

IV. TECHNIQUES AND INSTRUMENTATION FOR OPTICAL STUDIES

A. Previous Work

1) Birefringence and Scattering Measurements

Optical studies have been done on nerves for over a century. However, the first recorded attempt to optically study the nerve during the action potential was made in 1939 by F. O. Schmitt and O. H. Schmitt, working on the recently discovered squid axon.[13] They had previously used the polarizing microscope to study nerve structure and the orientation of micelles in the axoplasm. Placing the nerve between crossed polarizers and using white light, they claimed to find no change in light intensity to within .00025%, during the few milliseconds of the action potential.

Faced with no results at such a remarkably high sensitivity, neurophysiologists did not do much more optical work until Solomon and Tobias.[14] Their approach stirred interest primarily because they, unlike others who sent beams through the whole nerve, used an internally placed quartz micropipette as a light source to emit light through just one layer of the nerve. The experiments compared the amount of light emitted before, during and after prolonged stimulation using time resolution of about a second. The emerging light was found to decrease about 2% after 2 minutes of stimulation at 175 pulses per second. The decrease was larger for longer stimulation times, and reversible after many minutes of rest.

Because of the long term nature of these effects, they are most likely due to metabolic changes, and have not given much help in understanding the nerve membrane or the action potential.

2) Ultraviolet Absorption

In 1959, Kaiushin, Lindkovskaia and Shmelev reported changes in ultraviolet absorption of nerves.[15] Using photographic techniques, they took 2 minute exposures of resting nerves and compared them with 2 minute exposures of nerves being excited at 50 times per second. In this experiment, the illumination was at 270 - 280 nm. Absorption increases of 15-30% were measured. At first this effect was reversible and the absorption returned to normal when stimulation ceased. However, after several cycles, the reversibility was lost.

Changes were also detected for broader band UV (250 - 285 nm) measurements, and were also of magnitude 15-30%. However, these results were as often decreases as increases in absorption, which seems to make their significance somewhat dubious. However, the authors claimed that they are significant because their experimental error was significantly less than this.

Shortly after this, Shmelev and Kayushin reported results of a very important extension of their first work.[16] Again using cuttlefish giant axons, they sought to measure absorption changes during the millisecond of the action potential. They devised a rotating disc shutter which had slits to allow 1 msec pulses of light to pass through the nerve fifty times per second. Other slits in the disc allowed light from a second source to be seen by

a photomultiplier, which in turn triggered the nerve stimulus. Adjustments were made to control the time lag between the stimulus and the light flash. The light exposed a photographic plate, and densitometry was used to quantify the results. Total measurement time was one minute.

The results of this experiment seemed quite interesting. The authors claimed that on the average, during excitation, a decrease of 6% in absorption of 265 nm light was measured, although some nerves decreased by as much as 10%. In contrast to this, at 285 nm the absorption during the millisecond of peak action potential increased by as much as 15%, while the average was 6%. Measurements in the millisecond before the action potential or the millisecond after the crest showed no change to within 2%, which is their stated noise level.

B. Introduction to Our Study

It was at this point that our own optical experiments were begun. The approach of searching for optical changes in the nerve during the action potential seemed to us to be sound. Any such change would almost surely be from the membrane region, since this is the only region of the nerve which reacts with such speed. If, for instance, we were fortunate enough to detect a change in absorption with a maximum characteristic of a specific molecule, we would be able to conclude that 1) the membrane contains such a molecule, and 2) that the molecule is active during the action potential.

Polarization studies might also reveal whether the molecule rotates or changes chemically. It is even conceivable that two optical signals would be found: one corresponding to the sodium channel and one to the potassium channel. With such interesting possibilities before us we began our studies with enthusiasm.

It seemed worthwhile to repeat some of the previous optical studies of nerves during excitation using some of the modern averaging techniques which were available in our lab. We decided to use microspectrophotometric techniques similar to those developed for vision research,[17] and which use a photomultiplier rather than a photographic plate as a light detector.

Certain peculiarities in the Russian work led us to have at least some skepticism at their particular experimental results. However, with the superior sensitivity which would be available to us, we felt that we would have a good chance of finding some sort of optical change. Furthermore, it seemed possible to design optics flexible enough to explore several types of optical phenomena which had previously been either neglected or studied with less advanced techniques. Nevertheless, our main hope was to find the absorption changes in the ultraviolet region which would presumably be due to changes in the membrane protein structure.

C. Optical Instrumentation

A) Absorption and Fluorescence Apparatus

The main problem of the optical equipment was to provide high intensity, well polarized light onto the nerve. Several models of

the optical system were used during the course of these experiments. Figure IV-1 shows a block diagram of the original optical setup used for the absorption and fluorescence studies.

The lamp was attached to a Bausch and Lomb 500 mm grating monochromator. The lamp arc was focused on the entrance slit. The light emerging from the monochromator was collimated by a B&L 400 mm projecting lens. The beam was bent into the vertical plane by a 45° first surface mirror and then through a glan polarizing prism.

After leaving the prism, the beam was focused on the nerve by a Zeiss Ultraflurar 10X condenser and collected by a Zeiss Ultrafurar 10X objective. The light was next passed through a second glan prism and then hit the photomultiplier.

2) Light Sources

Several light sources were considered. Since the region of primary interest was 250 - 300 nm, only arc lamps were considered. The brightest source in this region is a Xenon lamp. However, the monochromator available was notorious for stray light, and since Xenon lamps emit a tremendous amount of visible light, heavy filtering of the visible would have been necessary. These ultraviolet transmitting, visible absorbing filters do not have very good transmission in the 250 - 300 nm region, and reduce the useful output of the lamp quite substantially. Xenon arc lamps are low voltage, high current devices, and commercially available power supplies generate ripple of over 1%. This ripple plus the arc instability led to excessive noise which made the lamp unsuitable.

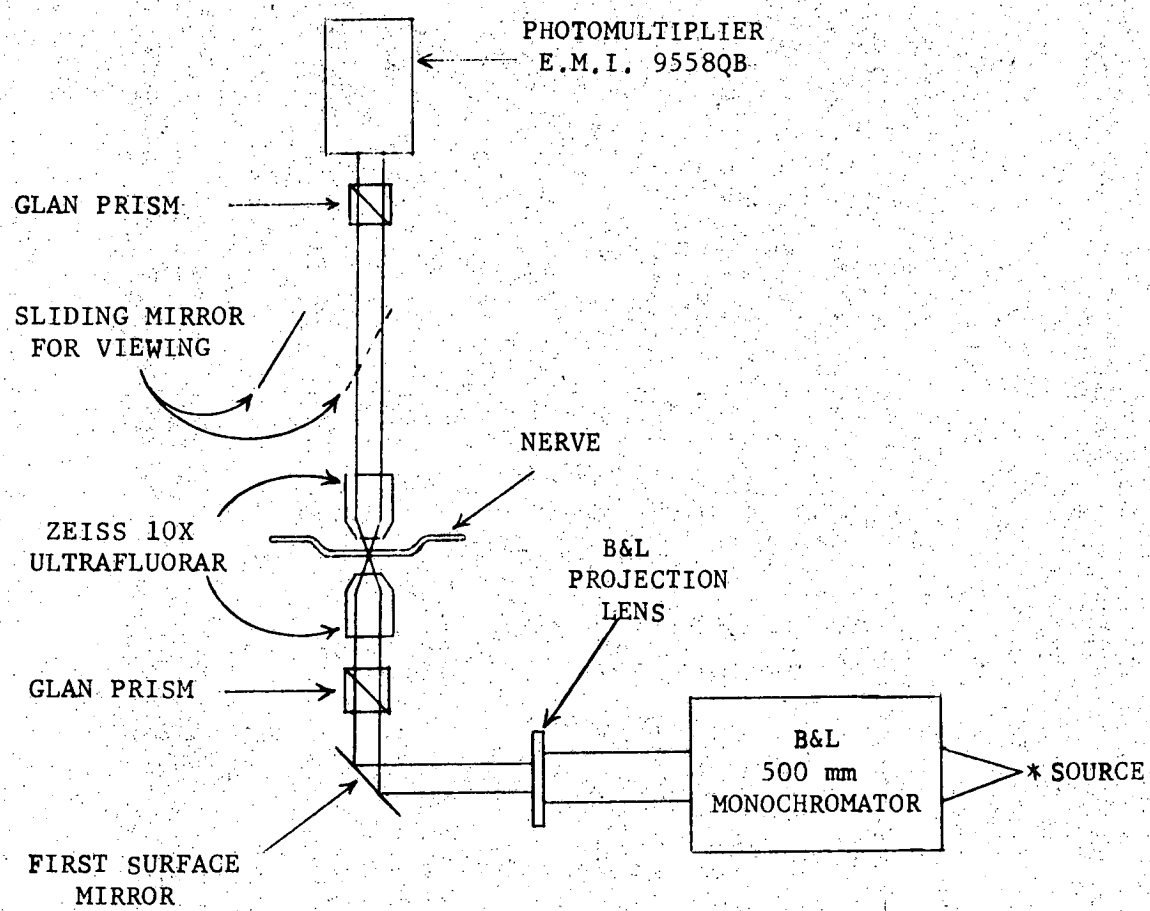

XBL 6910-5329

Figure IV-1. Block diagram of Model 1 (prisms removed for absorption measurements).

Mercury lamps are superior in their stability and power supply specifications, but emit only line spectra. They were ruled out on this basis.

The lamp finally chosen was a WHS-200 200 watt deuterium lamp made by Kern of Germany. This is one of the brightest deuterium lamps available,[18] and provides a nice continuum in the U.V. while emitting little visible. Its output is less than that of a Xenon but needs no filtering other than that provided by the monochromator. This results in the output being almost as much as the useful output of a Xenon. Being a 150 volt 1.3 amp lamp, regulation and ripple control are quite straightforward, and we found this water-cooled lamp well suited for our work.

3) Ultraviolet Polarizers and Lenses

The glan prism has an air gap rather than cement between the two halves, and is therefore suitable for use in the U.V. down to 220 nm. The prism has the disadvantage that the light through it must be well collimated to achieve high extinction ratios. We compared the glan prisms to the more standard polarizing sheet, such as those made by Polacoat Corp. The sheets had much lower transmission (only 30% as much) and an extinction ratio of only 10-1 at 260 nm. We therefore chose the prisms as our polarizing devise.

Zeiss lenses are specifically designed for work in both the visible and U.V. so that they have high transmission and are achromatic. This allows the focusing of the light to be done in the visible while the measurements are done in the U.V.

4) Birefringence Apparatus - Laser

Model 2 of the optics was quite similar to the first model except that the light source was a Spectra-Physics He-Ne gas laser. Since the laser beam is about 1 mm in diameter and well collimated, there was no need to use the lenses, and they were removed from the system. With the removal of these lenses, which were found to have enough undesirable strain to cause them to be slightly birefringent, the extinction ratio of crossed to parallel prisms rose to 10^4.

5) Ultraviolet Birefringence System

Model 3 is illustrated in Figure IV-2. The purpose of the system is to replace the high F number of the monochromator with low F number lenses and interference filters. The light source is placed at the focal point of a 2" diameter F 1 lens to produce a parallel beam for the interference filter and water filter. The beam is collected by a similar lens and recollimated by a 1" diameter F 1 lens for passage through the prisms and the rest of the system. Having the two inch parallel beam provided a very convenient place for combinations of color filters and neutral density filters and also separated the light sources far enough from the microscope to permit easy interchanging from visible to U.V.

Included in this version of the optics was a variable wave plate. This device consists of a fluorite crystal under stress by two bars separated by stacks of piezoelectric crystals. Voltage applied to the stacks causes the bar to exert more or less

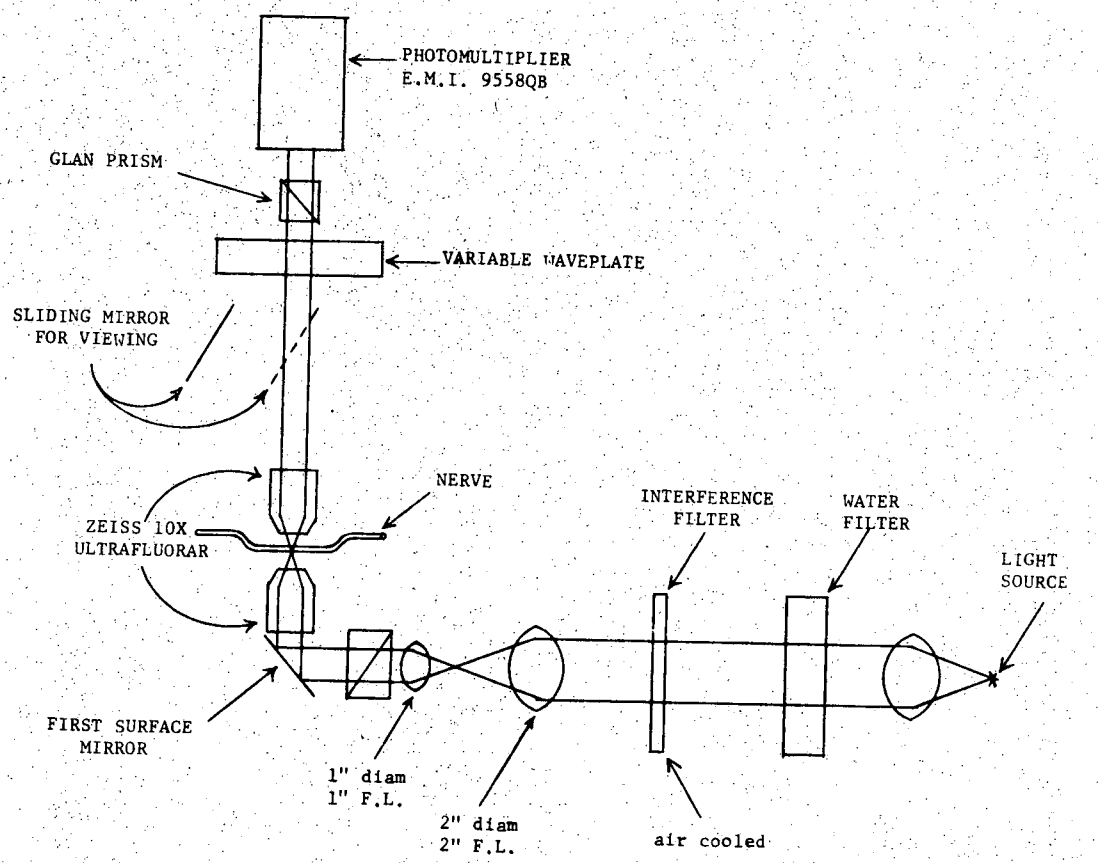

XBL 698-5307

Figure IV-2. Model 3 optics.

force on the fluorite and thereby induces a stress birefringence which is linear with voltage. The purpose of this variable wave plate was to permit quantitative birefringence measurements to be made at different wavelengths.

We also used a new lamp in place of the ribbon filament one. The General Electric ENA 3350°K lamp seems quite well suited to this purpose. It is only 80 watts, has a small filament, and runs on 30 volts. It projects 2-1/2 times the intensity into the system as the T-10 lamp.

6) High Light Intensity Optics for Visible Spectrum

Model 4 of the optics was constructed very near the termination of the work. All hope of using squid axons was gone, so the microscope was no longer necessary. Birefringence measurements in the ultraviolet were also deemed impractical and the prisms were replaced by Zeiss sheet polarizers. The resulting system, Figure IV-3, despite its lack of flexibility, increased the available light intensity so greatly that the signal to noise ratio increased dramatically for the birefringence measurements. Wavelength dependence of the birefringence change and a broad band ultraviolet absorption measurement were done with this system.

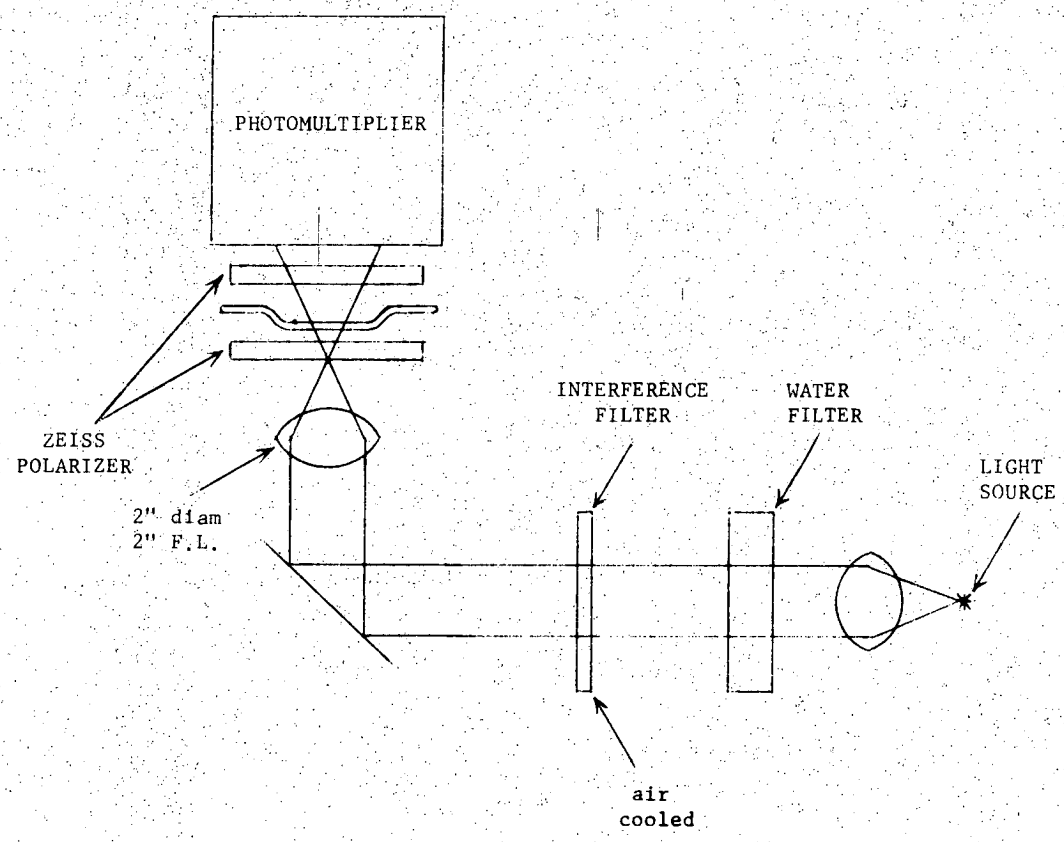

XBL 6911-5351

Figure IV-3. Model 4 optics.

D. Electronic Instrumentation

1) Continuous versus Chopped Light

Three factors were considered in deciding between a D.C. light source and a light source chopped by a shutter system. On one hand, it is better to keep incident radiation on the nerve at a minimum to prevent destruction of the proteins by the U.V. On the other hand, shutter systems complicate both the mechanical and electrical problems. Shutters, whether rotating discs or stepping motors, almost always cause some mechanical vibration. For the sensitivities desired, these effects would be hard to eliminate.

The signal from the photomultiplier in the case of light being chopped would be a square wave of approximately 5 volts. A 10^{-4} change in absorption, for instance, would correspond to only 500 μV, which would have to be separated from the 5 volts and amplified. This separation requires electronic clamps and switching circuits accurate to 1 part in 10^5, while being insensitive to long term changes in the 5 volt signal due to non-action potential changes in the nerve. These requirements are extremely stringent and difficult if not impossible to meet.

However, if one uses a D.C. source, it becomes relatively easy to separate the 5 volt resting signal from the 500 U.V. signal due to the action potential. Only a blocking capacitor and a low noise A.C. amplifier is required. Figure IV-4a shows the types of signal which would come out of the PM under chopped conditions, and Figure IV-4b shows the signal under D.C. conditions. In both diagrams

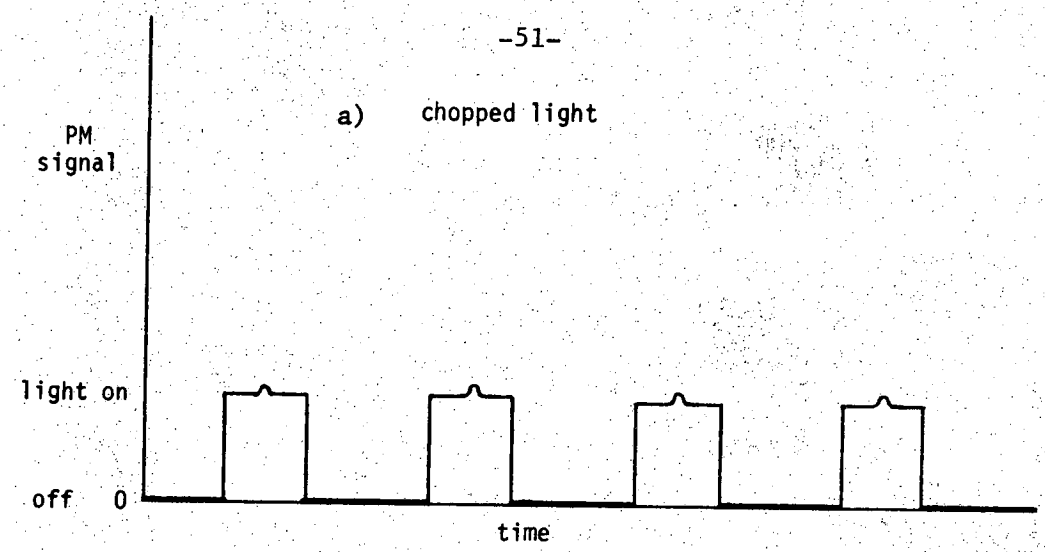

Chopped light makes detection of small signal difficult.

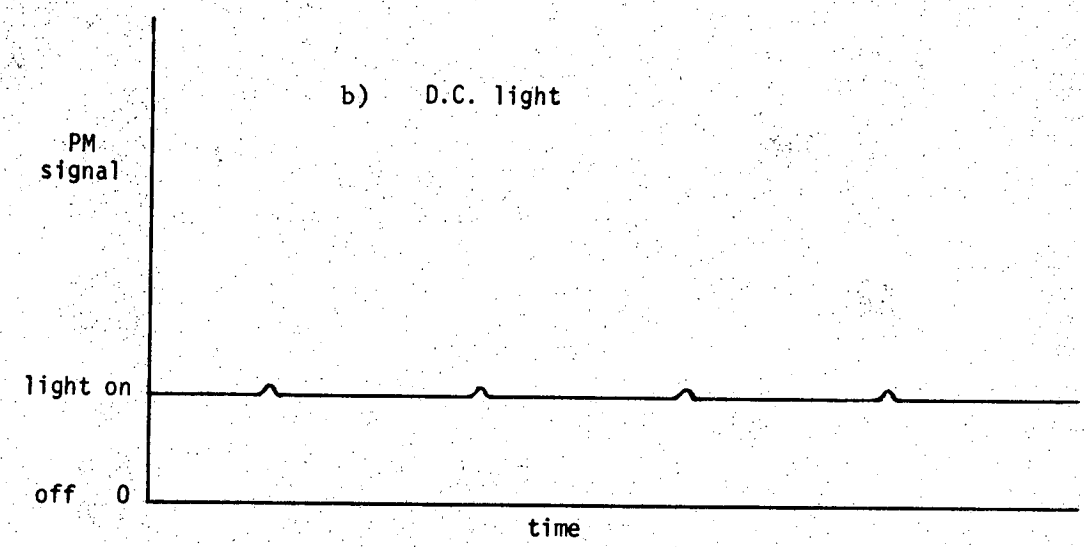

D.C. light signal can be easily blocked by a capacitor, making detection of nerve signal easier.

XBL 692-4114

Figure IV-4. Possible photomultiplier outputs.

the hypothetical optical signal is greatly exaggerated, for illustration.

Nerve action potentials are typically 10 millisec long, including the after potential. Firing rates of 40/sec have been found practical, so the measurement takes 40% of the time the light is on. Therefore, chopping the light could cut down the exposure by at most a factor of 2-1/2, which does not seem to justify the disadvantages of this method. Therefore the light was not chopped.

2) Photomultiplier and Preamplifier

The electronic circuitry was designed with the signal to noise ratio being the primary consideration. As has been described in the optical design section, under proper conditions the signal to noise at the photomultiplier is determined by shot noise. This noise is minimized by using a photomultiplier with a photocathode of high quantum efficiency. The S-20 photocathode has high efficiency in both the red and ultraviolet regions, and was found most suitable for this application. The tube used was an EMI 9558 QB, a 14 stage, quartz windowed, selected tube.

If the PM signal is 5 volts, and the expected shot noise is 5 MV, the amplifier must have its inherent noise less than this in order not to deteriorate the signal. The Philbrick P2A fulfills this requirement, having a noise of 20 μV for the required 10 KC bandwidth. This amplifier is used as a voltage follower to provide low impedance to drive the cable from the PM to the rest of the

electronics and to filter out high frequency noise. Figure IV-5 shows the circuitry for the P2A.

R_1 is used as the PM load resistor and is easily changed if weaker light sources are used. R_2 and R_3 set the gain at 1 since all the necessary voltage gain is available in the PM or R_1. The feedba ck capacitor limits the high frequency response of the system and prevents the P2A from oscillating.

A calibrating pulse is directed to the positive input of the amplifier. Since the signal will be added and averaged over varying lengths of time, and since the CAT computer has no means of normalization, quantitative results can be obtained only by sending a known signal along with the nerve signal through the system and into the averaging computer. The nerve signal is then compared to the known signal. Our calibration was usually a 5 msec square pulse, about 1/4 MV high, but this varied with the experiment.

3) Bandwidth of System

The P2A drives a blocking capacitor differentiator which not only blocks out the voltage due to the D.C. light level, but also the slow changes of light level which occur due to changes in lamp intensity or mechanical vibration. The low frequency cutoff of the differentiator should be as high as possible to reduce light changes not associated with the nerve action potential, but not so high as to distort that signal. The calibrated pulse can be lengthened to measure the distortion caused by this differentiator. For squid nerves the differentiator was set to cause no more than

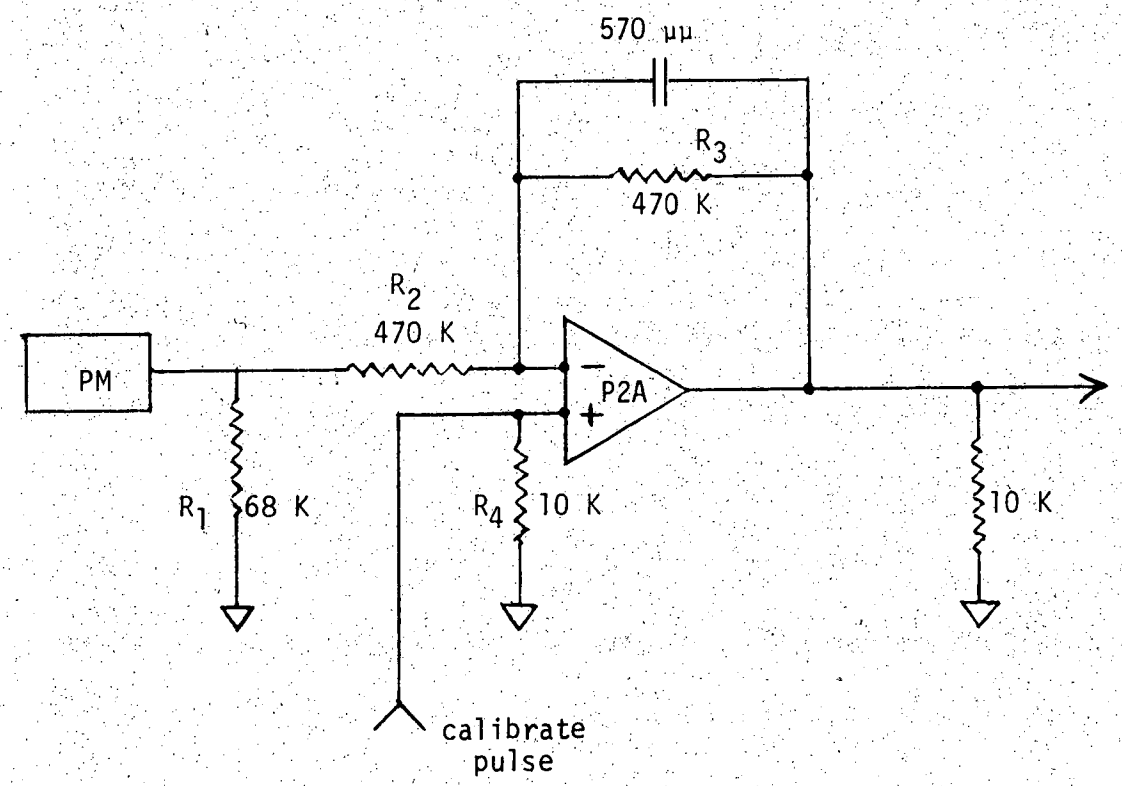

XBL 692-4112

Figure IV-5. P2A voltage follower. Gain of one, impedance reduction, calibration of signal.

a 10% droop on a 10 msec square wave, and for crab nerves no more than a 10% droop for a 40 msec square wave.

Following the differentiator is a Kintel 121-A amplifier which has low noise (3 μV RMS) and gain adjustable from 1 to 1000. The Kintel drives the CAT averaging computer. In later experiments this was replaced by a Tektronix 1A7 preamplifier driving a Philbrick P65A.

4) Synchronization

The system is synchronized by a set of Tektronix pulse generators. Figure IV-6 shows a block diagram of this system. A type 162 waveform generator is used to trigger the system at any desired rate. It drives a second 162 which produces a ramp on which all the other generators can synchronize and establish their individual delays. By using one of the 162's as a clock and the other as a ramp generator, the frequency of firing of the nerve can be changed without affecting the relative timings of the CAT, calibrate pulse and action potential.

The four pulse generators are type 161. Pulse generator 1 fires first and starts the CAT sweep. About 5 msec later, generator 2 emits a calibration pulse. Since the pulse needed is about 0.5 mv, a Hewlett Packard step attenuator plus a resistance voltage divider is used after this generator to allow more accurate control of the calibration pulse amplitude. Shortly after the calibration pulse, the nerve is fired by generator 3. The action potential passes the light beam, causing a change in optical signal which

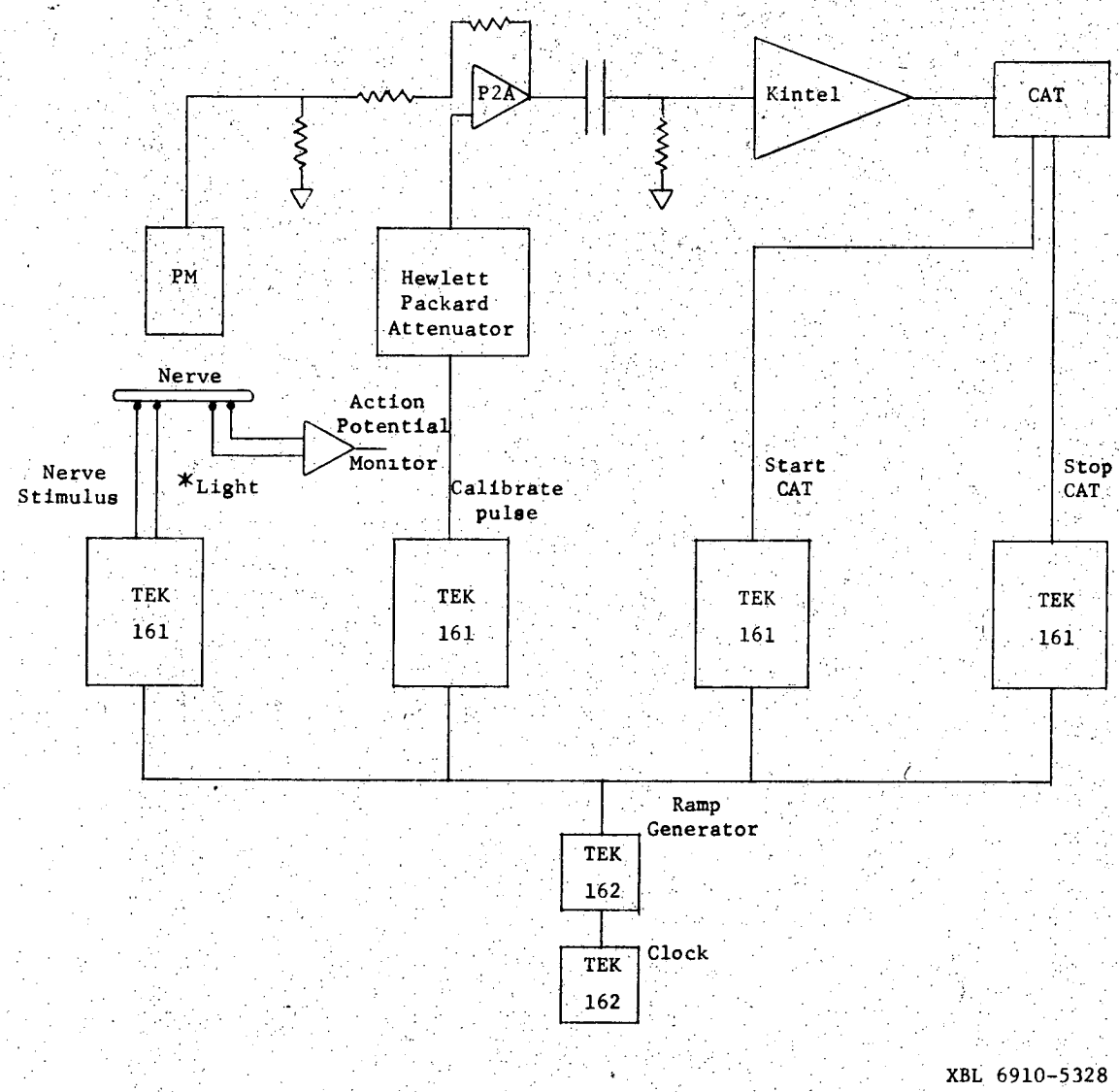

Figure IV-6. Block diagram of electronics.

is recorded on the CAT. The CAT sweep is then reset to zero by generator 4 and is ready to begin a new sweep for the next cycle. Generator 4 is necessary because the CAT is not allowed to complete its normal 400 channel sweep when rapid repetitions are desired.

An interesting problem arises when one considers what happens as a squid axon gets tired and more difficult to fire. During the course of an experiment, as the nerve tires, the delay between the stimulus pulse and the action potential increases. Often this delay can be shortened by raising the stimulus level, but fine control is difficult to obtain.

A varying delay can be quite detrimental to a method of detection like ours which relies on averaging a signal point by point. If the signal occurs later and later with respect to the sweep of the CAT, it no longer gets averaged with the corresponding parts of previous signals but rather is added to parts of previous signals which occurred later in the course of the action potential.

We devised a technique to handle this problem which used a dual time base Tektronix RM35[A] oscilloscope. The method is based on the fact that given a constant stimulus frequency, the time between successive action potentials will always be nearly constant even if a long term increase of delay occurs between each stimulus and action potential. For example, if over the course of a minute, the stimulus-action potential delay has increased by 5 msec, under the old system no useful averaging would take place for an action potential lasting only about 1 msec. However, if we consider the difference in delay between two successive nerve

firings we see that for a firing rate of 30/sec or 1800 per minute, the change in delay is only 5 msec/1800 or only a few microseconds.

Thus if we can start the sweep of the CAT for one pulse by using the previous pulse as a trigger, the pulses will always enter the CAT in the correct channels. Figure IV-7 shows a block diagram of the system used for such triggering.

Time base B is set to trigger on the action potential. B's sweep is slightly shorter than the time between stimuli. B triggers A which sweeps during the following action potential and displays it. During A's sweep, B triggers on the next action potential. The end of each of B's sweeps, a pulse is emitted which triggers A and appears as "A gate" on the front of the scope. This pulse is used to fire the waveform generator and pulser which start the CAT. Thus the sweep of the CAT has been triggered by the previous action potential.

Aside from the primary advantage of the system of insuring accurate averaging, two secondary benefits are accured. First, the CAT sweeps only when the nerve is firing. If for some reason the nerve should die suddenly, the CAT stops immediately and does not accumulate in extra noise. Secondly, the A gate can be used to drive a speaker which permits the experimenter to know if the nerve has ceased firing without having to constantly watch the scope.

5) Lamp Power Supplies

The tungsten light used for the visible absorption and birefringence measurements was a General Electric T10 18 amp ribbon

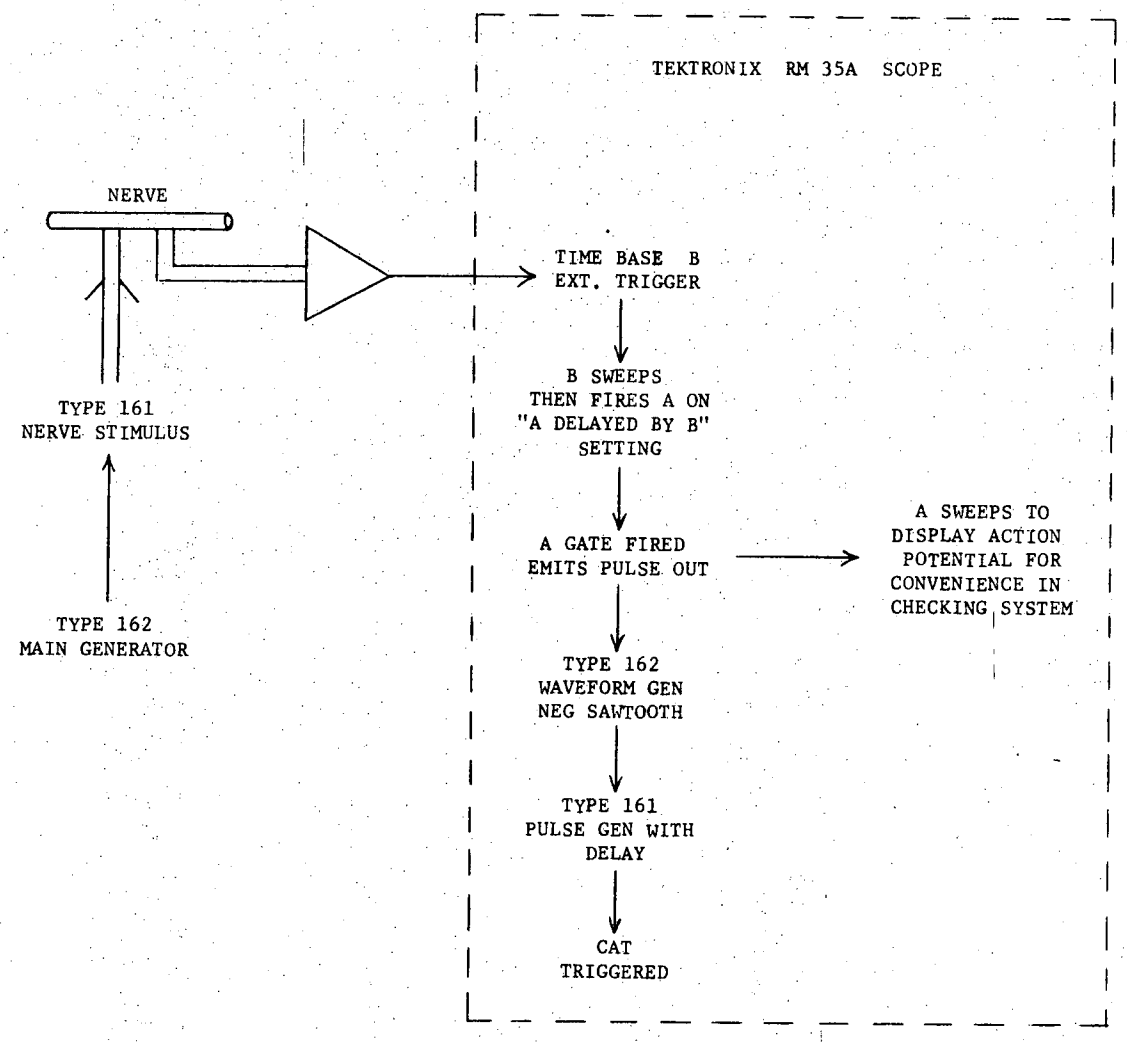

XBL 698-5308

Figure IV-7. Block diagram of synchronization for squid axon.

filament lamp. This lamp burns at 3000°K, is designed to fill the slit aperture of the monochromator, and is fairly homogeneous in its filament intensity. The lamp supply was an Invar 40 volt 40 amp voltage regulated supply with less than 0.1% ripple. Because the tungsten filament intensity tends not to follow rapid changes in voltage, this lamp power supply combination never presented any 60 Hz problems like the arc lamps.

The WHS-200 deuterium lamp requires a high voltage (300 volts) for starting but only 150 volts for running. It was therefore necessary to place three 50 ohm and two 25 ohm 50 watt resistors in series with the lamp. This allows the full 300 volts of the Lambda power supply to appear across the arc for starting but limits the current after the tesla coil has ignited the arc. Toggle switches across each of the resistors permitted the amount of current to be changed and compensated for the fact that the supply could not be varied by more than 25 volts.

The deuterium lamp requires a filament supply. The filament, which insures sufficient ions for both starting and stable running, requires 8 amps at 2 volts. The Armor 30 volt-10 amp power supply which was available objected to regulating at such a low voltage. Therefore a 1/2 ohm, 200 watt resistor was put in series with the filament and the remote sensing pickups were placed across it. This made the filament current-controlled, which reduces the chance of burning it out.

The WHS-200 is a water cooled lamp and destroys itself if the water is not on. A water pressure relay powered by the

filament resistor voltage but in series with the 300 volt supply insured that both the filament and the water were turned on before the lamp was started.

The laser used for the birefringence measurements was a Spectra-Physics He-Ne continuous gas laser Model 115. The output was 6328 Å and had an intensity of 5 mw. Unfortunately, the operation of the laser was somewhat erratic. On some days it was so quiet that noise pulses above a tenth percent were rare. Other days it produced frequent spikes of up to 5% which were sufficient to ruin any experiment in progress at that time. The power supply of the laser has provisions for modulation and it was decided to design an optical pickup and a feedback circuit in order to attempt to control these fluctuations. A type 603 Clerex Cd-Se photoconductive resistor was fastened to the rear exit port of the laser and drove a Philbrick P65 voltage amplifier and a second P65 was used as a driver for the modulator input.

The system worked quite well in regulating the light out of the rear exit port and held the photoresistor current steady to one part in a thousand. However, the main laser beam out of the front port still showed the spikes. Frustrated, we talked to the manufacturer, who confessed to having attempted the same technique and achieving the same unsatisfactory result. The spikes are due to mode jumps and because of mirror alignment, different modes have different front to back light ratios. To regulate the laser properly it would have been necessary to install a beam splitter in the main beam and insure that the two paths were not affected differently by

mechanical vibrations. Since most of the useful data available from monochromatic measurements had already been obtained, it was decided to set aside the laser and return to a tungsten source.

6) Calibration

The system is an inherently linear one as long as the photomultiplier is operating in a proper light and voltage range. With the photomultiplier wired as described in the electronics section, the tube is found to be linear under even our highest light intensity conditions. This could be most easily checked by inserting a series of Kodak neutral density filters OD 0.1 to OD 2 into the beam and measuring the D.C. photomultiplier output voltage.

However, many observers still maintained the position that although the system was linear under static testing, it would not necessarily respond that way to very small changes in light intensity. Inasmuch as all our experiments relied on a calibrating pulse inserted into the system after the photomultiplier, we felt it worthwhile to test the sensitivity of the system directly using a pulsed light.

A source of light was set up next to the monochromator and was adjusted to hit the mirror and send a substantial amount of light into the collecting optics. The intensity of the monochromator beam was set equal to that of the new beam by using the D.C. voltage of the PM as the intensity criterion. A rotating disc was then placed before the second beam and caused the beam to hit the mirror 60 times per second with 5 msec pulses. Neutral density

filters were then used to reduce the light intensity to various low levels. The system linearly detected signals as small as 1 part in ten thousand. It should be stressed that this test was only for linearity, not sensitivity, because for this test we could average the signal as long as we wanted.

E. Biological Specimens - Procurement and Care

1) Squid

The choice of squid giant axons as the specimen most suited for optical nerve studies created some very serious logistical problems. The squid found in California waters grow to a maximum length of only about eight inches. Like all other species of squid, the California Squid, *Logigo opulescens*, are very delicate animals and die very quickly in captivity.

At the time when this research was undertaken, no suppliers of live squid existed on the West Coast. Eventually, two biological suppliers, Mr. Len Rummel of Monterey, California and Dr. Rim Faye of Venice, California, were prevailed upon to attempt such an undertaking. Individual squid were caught at night by hand nets and put into oxygen bubbled sea water in tanks on the boats. During the summer, when the squid were found in Monterey, they were transported to the lab by truck while oxygen was constantly bubbled through their seawater. All squid from Venice, during the winter, were put into plastic bags, half-filled with seawater and half with oxygen. The bags were placed in styrofoam car coolers and shipped air freight to Oakland.

Keeping squid alive in captivity is almost an impossible task. No major aquarium in this country has been able to keep them alive for more than a few days. It is the belief of most marine biologists that the factors which squid are most sensitive to are: 1) insufficient oxygen, 2) extraneous metal ions such as copper or zinc, 3) water temperature above 53°F, 4) organic polutants, usually due to an insufficient volume of water for the number of animals, 5) small tanks (less than several hundred gallons) which lead to the squid running themselves into the walls, and 6) too much light.

2) Home Built Aquarium

A system was built in this laboratory in which the squid would survive an average of four days, with a maximum span of seven days. A block diagram of the system is shown in Figure IV-8. Tank one (115 gal.) in which the squid were kept, was made of redwood with a (0.01") mylar liner. Tank two, a used ice cream cabinet lined with apoxied fiberglass, was used to increase the total volume of water in the system and to hold the temperature at 52°F. The pump, Mansfield Pump Model 8B-75-S2, with a 1/2 horsepower motor, provided a circulation rate of 600 gallons per hour. The 2' x 2' x 2' filter, made of lucite, contained 8 inches of crushed oyster shells and an inch of fine gravel. Aeration was provided by a vibrating diaphragm aquarium air pump with sandstone bubblers. All connecting hoses were of tygon. It continually surprised us just how caustic seawater actually is and any exposed metal, including the stainless steel top of the ice cream cabinet, soon showed heavy rust.

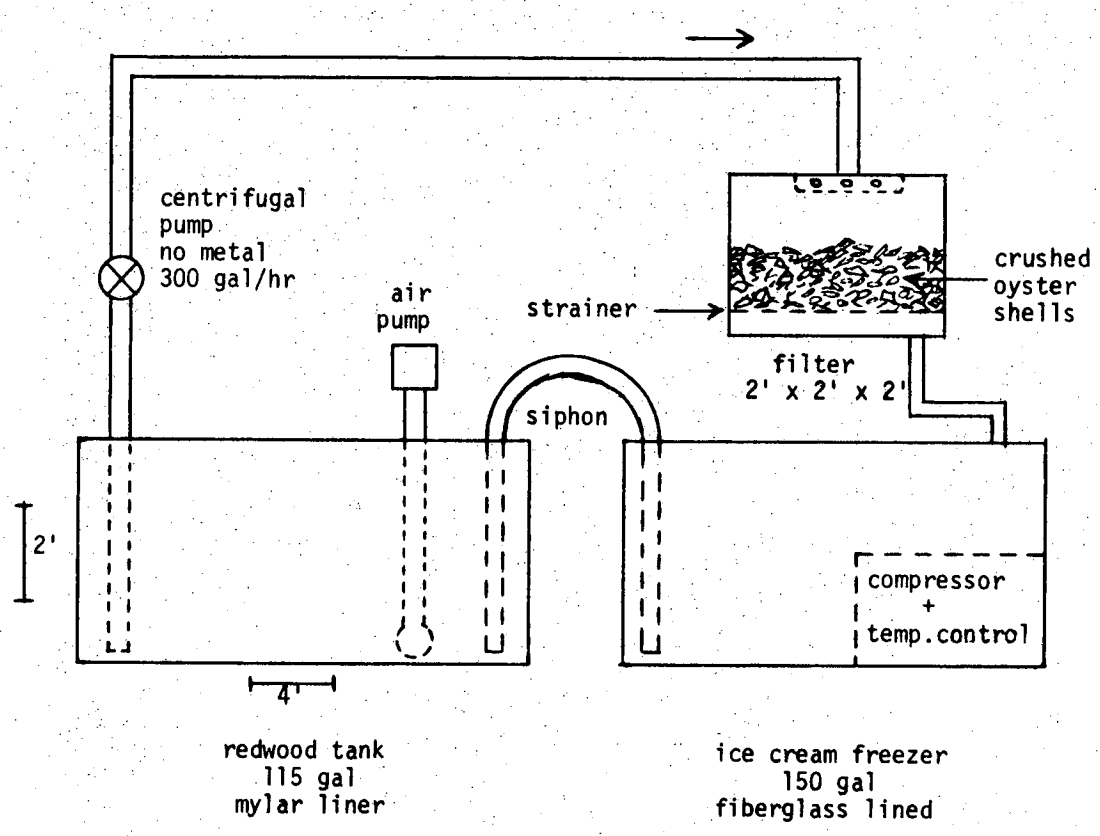

XBL 692-4111

Figure IV-8. Model 1. Sea water aquarium.

The sea water was made of distilled water plus Instant Ocean sea salts. It was usually changed once every month and a half.

The squid, when placed gently in the tank, usually swam around apparently exploring their new surroundings. They seldom ran into the walls of the four foot long rectangular tank. Occasionally one squid would get so nervous upon being transferred to the tank that it would dash back and forth jetting ink. This would trigger the others into doing the same. The ink could be filtered out of the water in about a day.

Getting the squid to eat was quite difficult. Small salt water fish and shrimp did not seem to interest them very much. However, several times they would devour goldfish 1" to 4" long which were put in the tank. Any goldfish not eaten after five minutes were returned to fresh water for recovery until next feeding.

Occasionally crabs were kept in the second tank. They often survived for over a month.

3) Commercial Aquarium

When the ice cream cabinet developed a leak, it was decided to replace the entire system with a more convenient one. Figure IV-9 shows the flow chart and Figure IV-10 the actual tanks. The use of smaller, 80 gallon, tanks instead of the larger ones was prompted by the success of one of our suppliers, Dr. Faye, in maintaining squid for almost three weeks in rather small tanks.

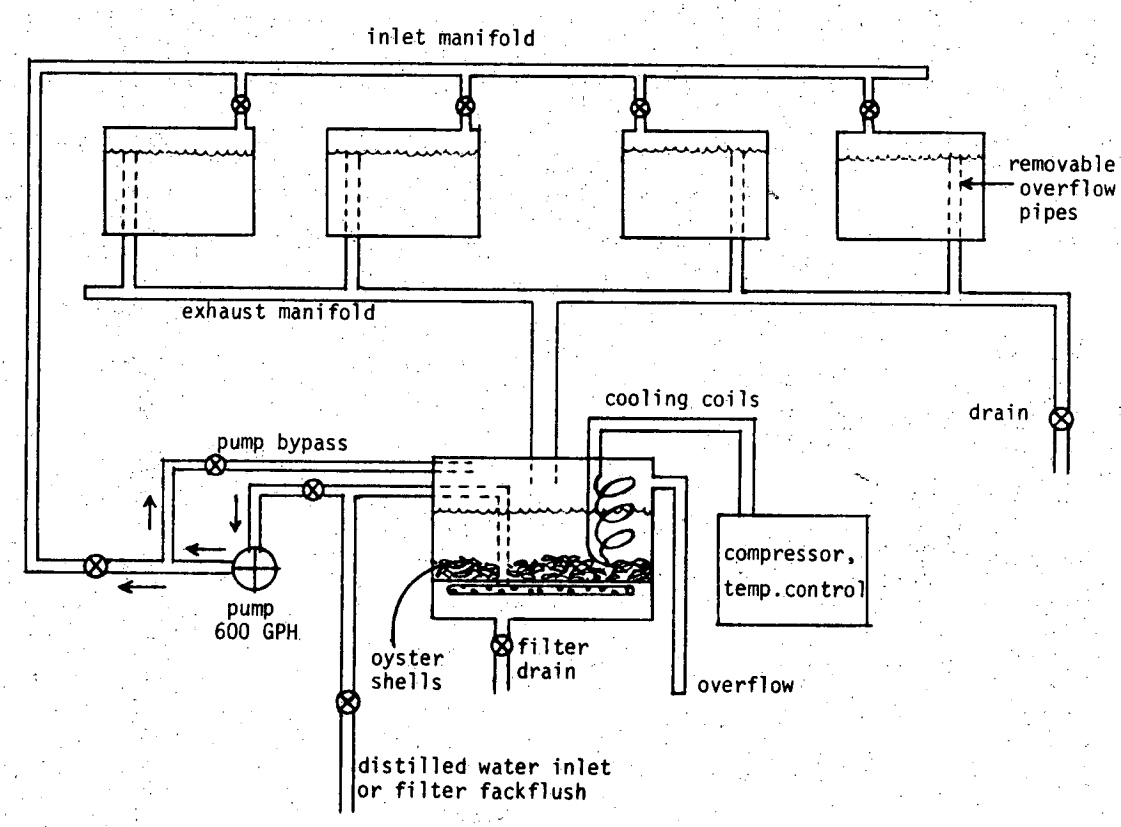

XBL 692-4113

Figure IV-9. Flow chart of sea water aquarium 2.

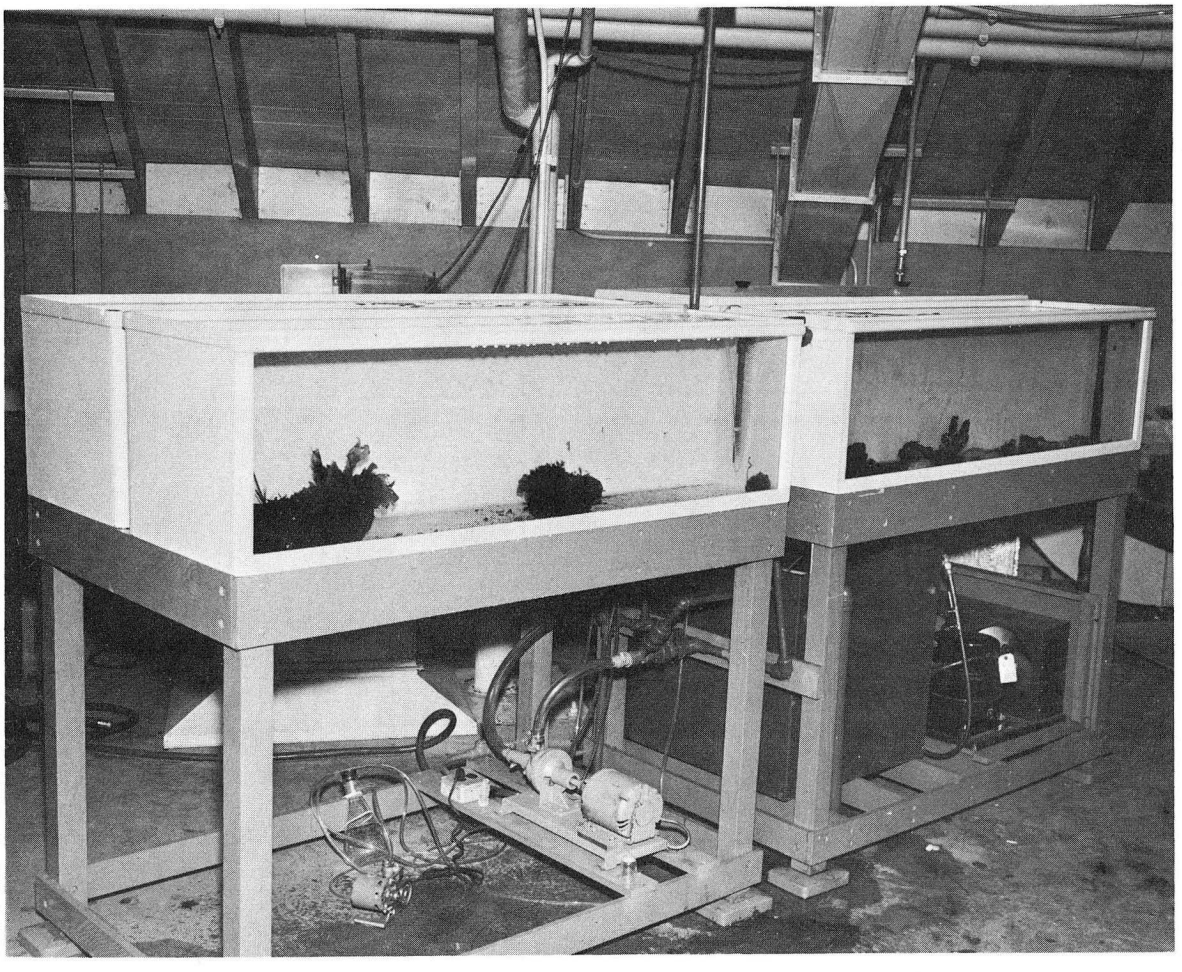

XBB 694-2197

Figure IV-10. Sea water aquarium 2.

4) Imported Axons

During the summer months, squid much larger than those available in California can be found at Wood's Hole, Massachusetts. These Atlantic squid have giant axons which range up to 0.6 mm in diameter or almost four times as large as the axons of the California Squid. Larger axons are much easier to dissect and clean, and therefore we attempted to procure these axons of the Eastern Squid.

Axons were dissected at the Woods Hole, Mass., Marine Biological Laboratory and sent in refrigerated buffer to us. Unfortunately, Woods Hole has no airport and the axons had to be shipped to Boston, Mass. by bus and taxi. The total transit time was 15 to 18 hours. Seven shipments were received. In five shipments, no action potential could be elicited. Two axons of the other shipments, however, displayed excitability over short segments of about one-third of their total length but were unusable for our purposes. Axon death could have been due to packaging, dissection damage, or time, but we do not know which. One moderately successful attempt was made to ship a live squid, but the squid season ended and the experiment was not repeated.

5) Crabs and Lobsters

In contrast to the difficulty in obtaining and keeping live squid, relatively little trouble was found in working with crabs and lobsters. Large crabs weighing about 1-1/2 lbs. each were

easily obtainable at the local fish store during the California crab season of November until June. During the off season crabs were flown in from Los Angeles by Pacific Biomarine. These crabs were much smaller, 1/2 lb. each, but were useable.

Large Maine Lobster, 2-3 lbs. each, were available year round from the Great Atlantic Lobster Company in Oakland. The lobsters were, in general, hostile to each other and it was necessary to keep their claws shut with rubber bands for the total duration of their stay in the tanks.

Both the crabs and the lobsters adjusted well to our aquarium and survived for as long as three months. They were fed once every week and seemed content with fresh meat from the crab or lobster which was used for the experiment on their feeding day.

F. Dissection and Excitation Techniques

1) Squid Dissection

The squid axon, which was chosen as the specimen for our absorption and fluorescence studies, has several advantages over other possible choices. The axon is much larger than any other known fiber, reaching diameters of over 1 millimeter. It may be dissected fairly easily and can withstand surprisingly strenuous handling. When carefully cleaned with fine scissors, the axon is quite homogeneous and very translucent. The axon lies along the

center of the back of the squid and controls the major contractions of the mantle used for escape.

The dissection is performed immediately after the squid is removed from the tank (Figure IV-11). The head is cut off, the mantle slit on the ventral side, and the insides removed. The skin is then peeled away and the mantle is tacked to a cork dissecting tray which has a clear lucite disc in the center to allow light to come from a lamp below (Figure IV-12). If the squid was healthy when removed from the tank, the mantle will be quite translucent and the nerve system will be visible (Figure IV-13). The stellate ganglion is freed by cutting away all the nerve fibers except the giant axon and by cutting away the tissue below it. A thread is then tied around the junction of the ganglion and the axon to prevent the axoplasm from draining out and to provide a convenient way of handling the end of the nerve (Figure IV-14). The axon is then dissected free from the mantle by means of very find iris scissors and tied with thread at the other end. The axon can be manually cleaned of most of its small fibers in a dissecting tray under a low power stereo dissecting scope (Figures IV-15 and IV-16). The average dissecting time is twenty minutes.

A healthy axon will fire as fast as 400 pulses per second although this rate can be maintained for only a few seconds. Rates of 50 pulses per second can be maintained for several hours. Other details of the biological properties of the axons are discussed by Schmitt and Schmitt in Ref. 13.

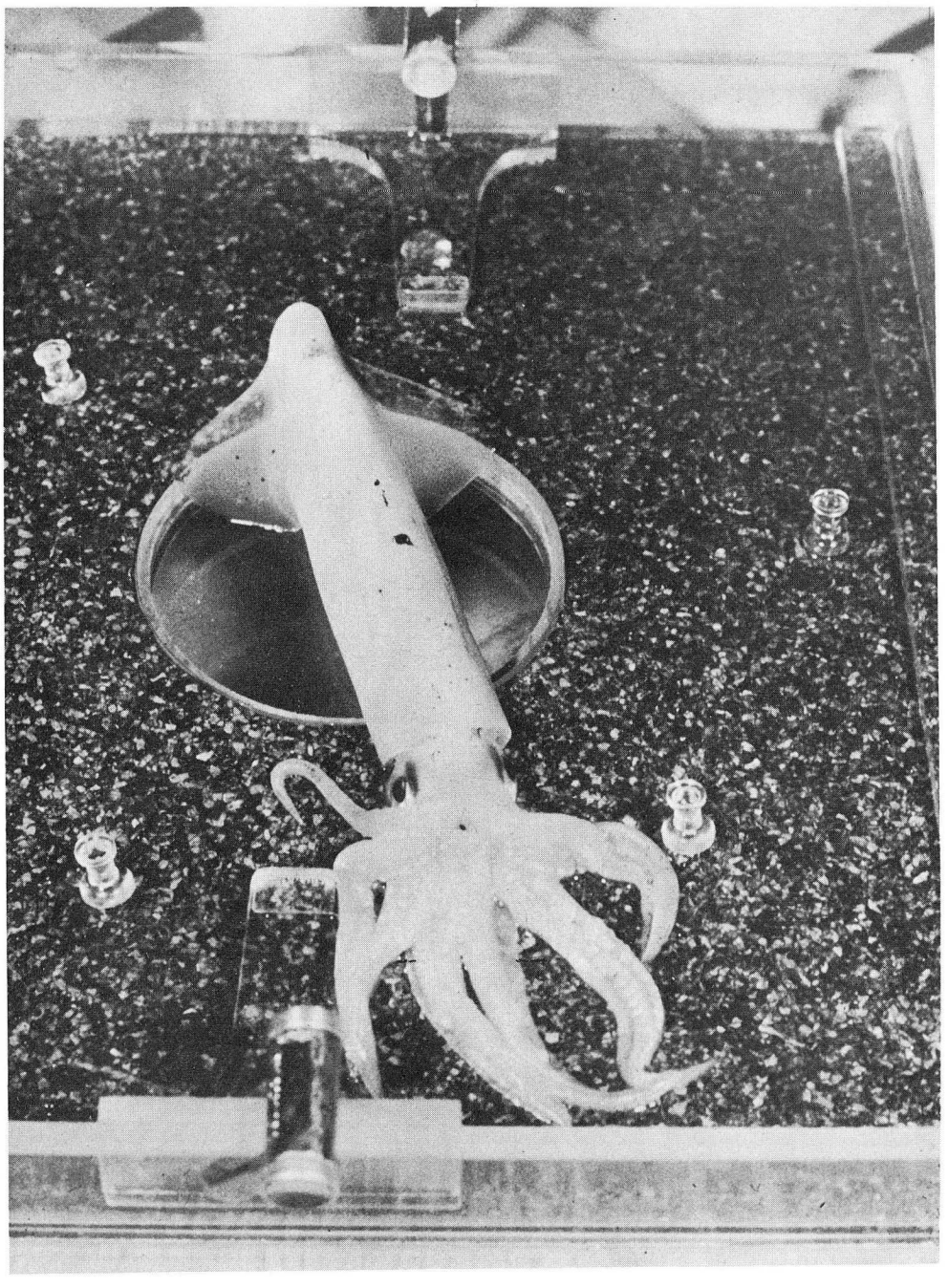

XBC 693-1968

Figure IV-11. Squid on dissecting tray.

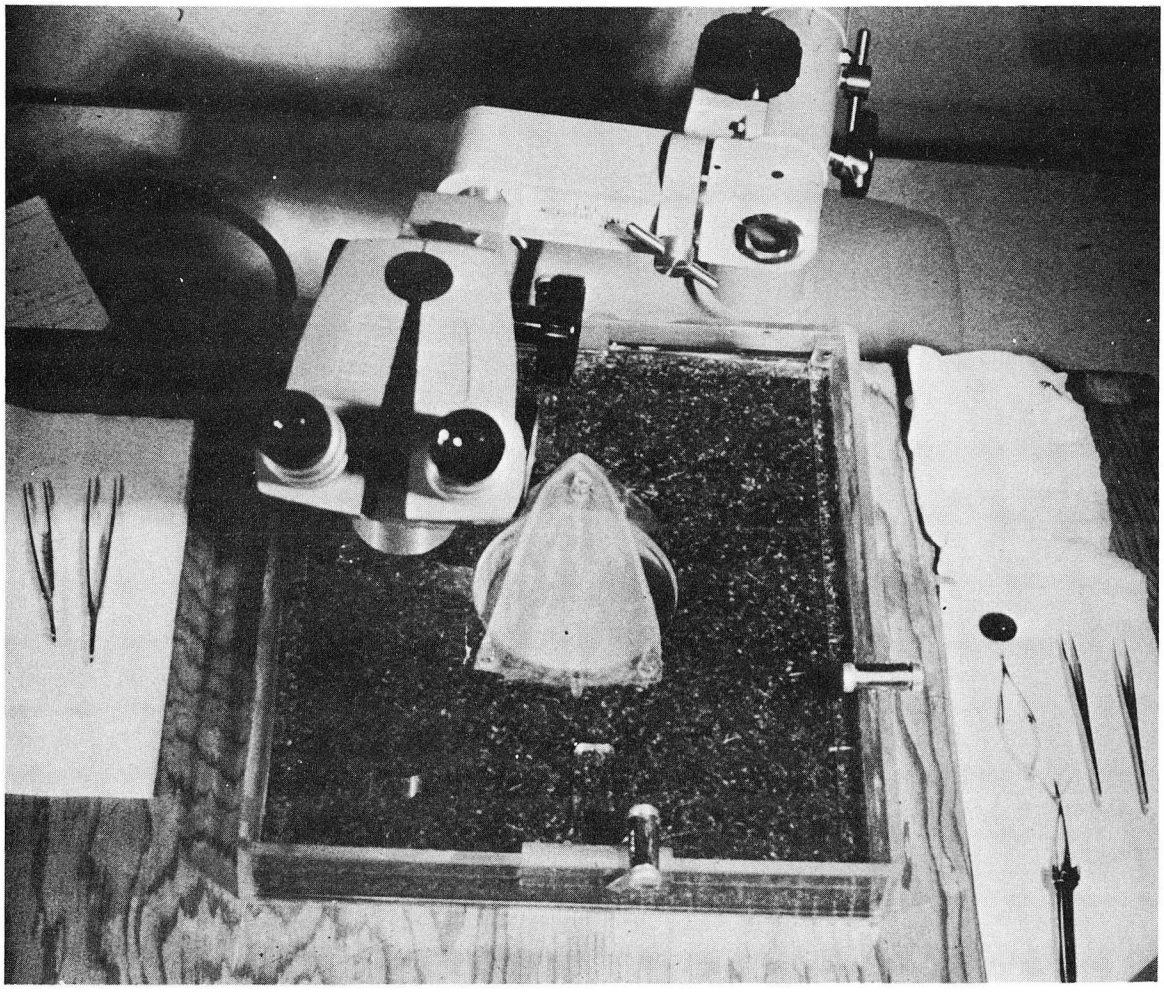

XBC 693-1971

Figure IV-12. Squid mantle is tacked down over clear lucite disc. Dissecting tools are shown near a penny for size comparison.

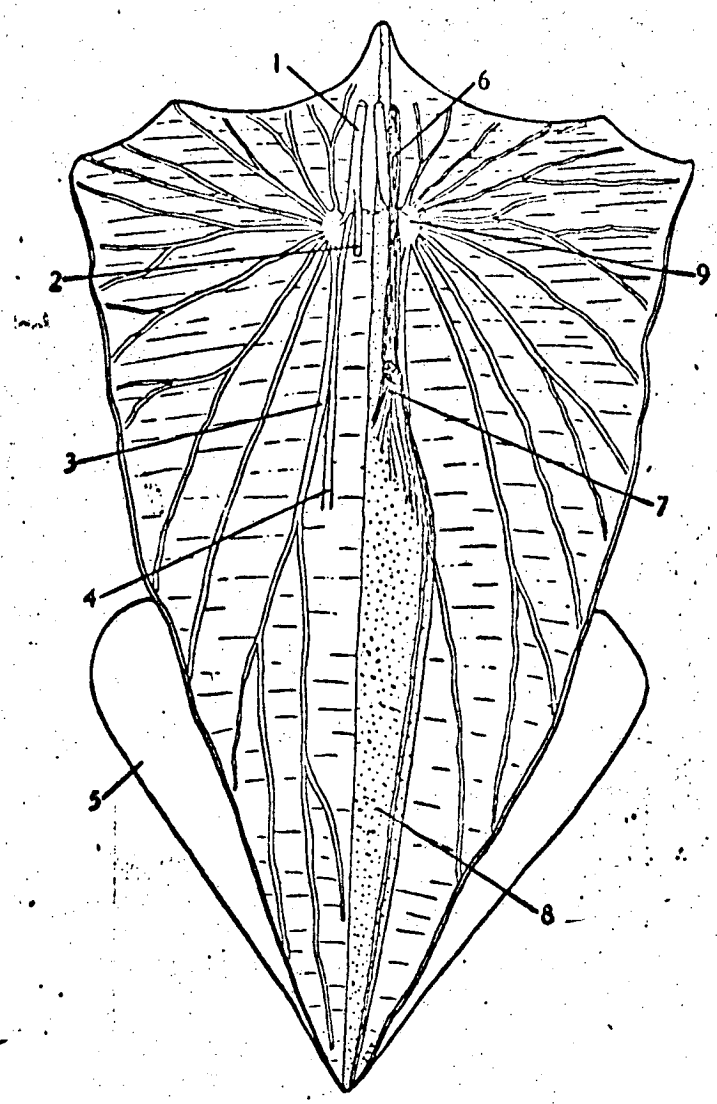

Figure IV-13. Drawing of squid mantle slit ventrally and viewed from ventral size. This drawing is about 3/4 the natural size of West Coast Squid. 9 is the stellate ganglion at which one end of the axon is tied with thread for dissection. 3 is the giant axon (J. Z. Young, 1931).

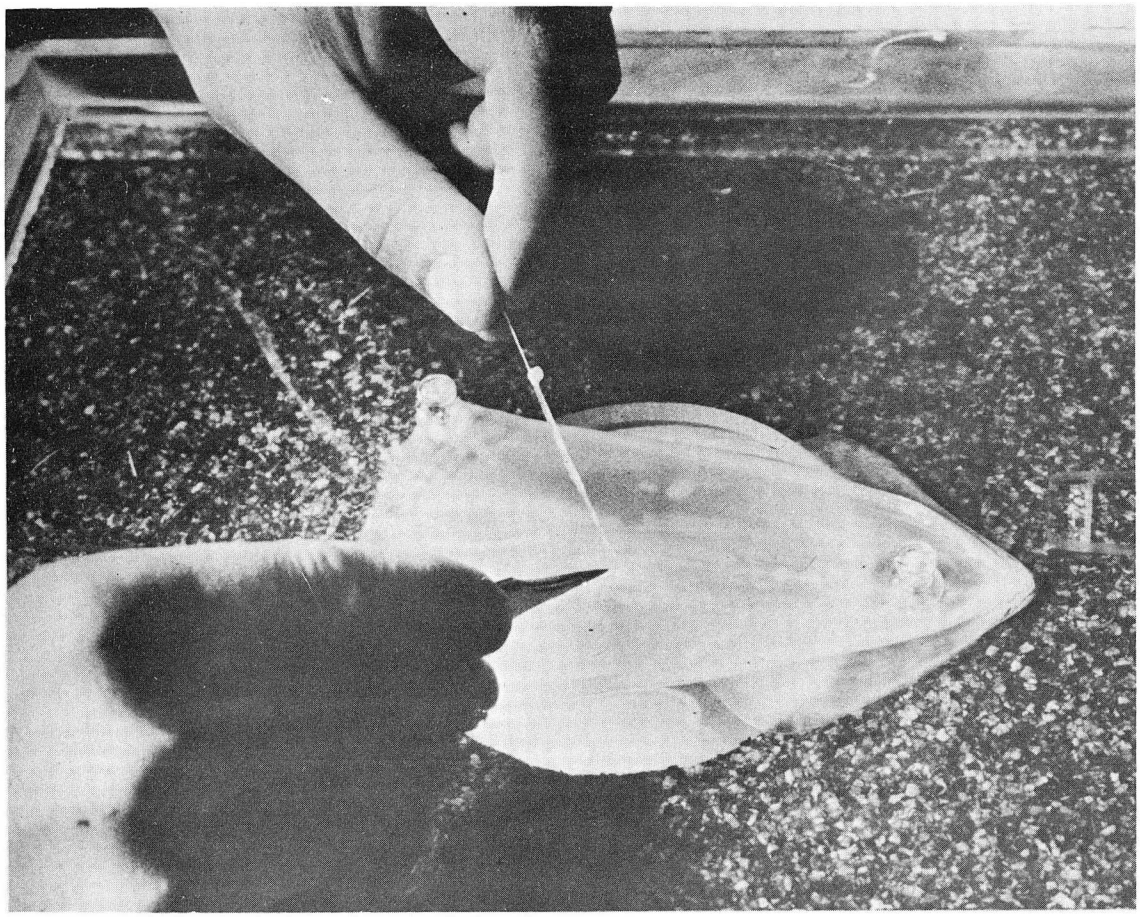

XBC 693-1969

Figure IV-14. Axon partially dissected from mantle. Thread tied to stellate ganglion provides convenient handle.

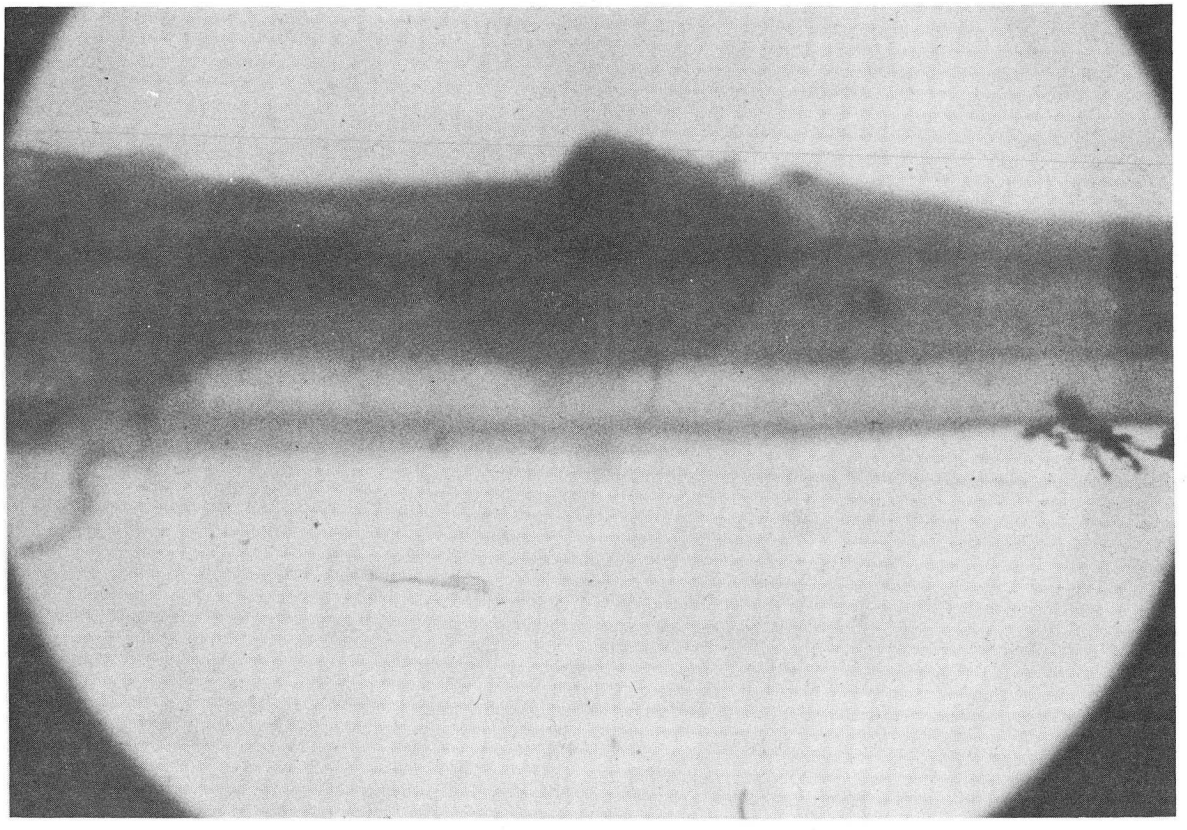

XBC 693-1970

Figure IV-15. Nerve after removal from mantle. Giant axon is surrounded by numerous small fibers and the whole bundle is encased in a sheath.

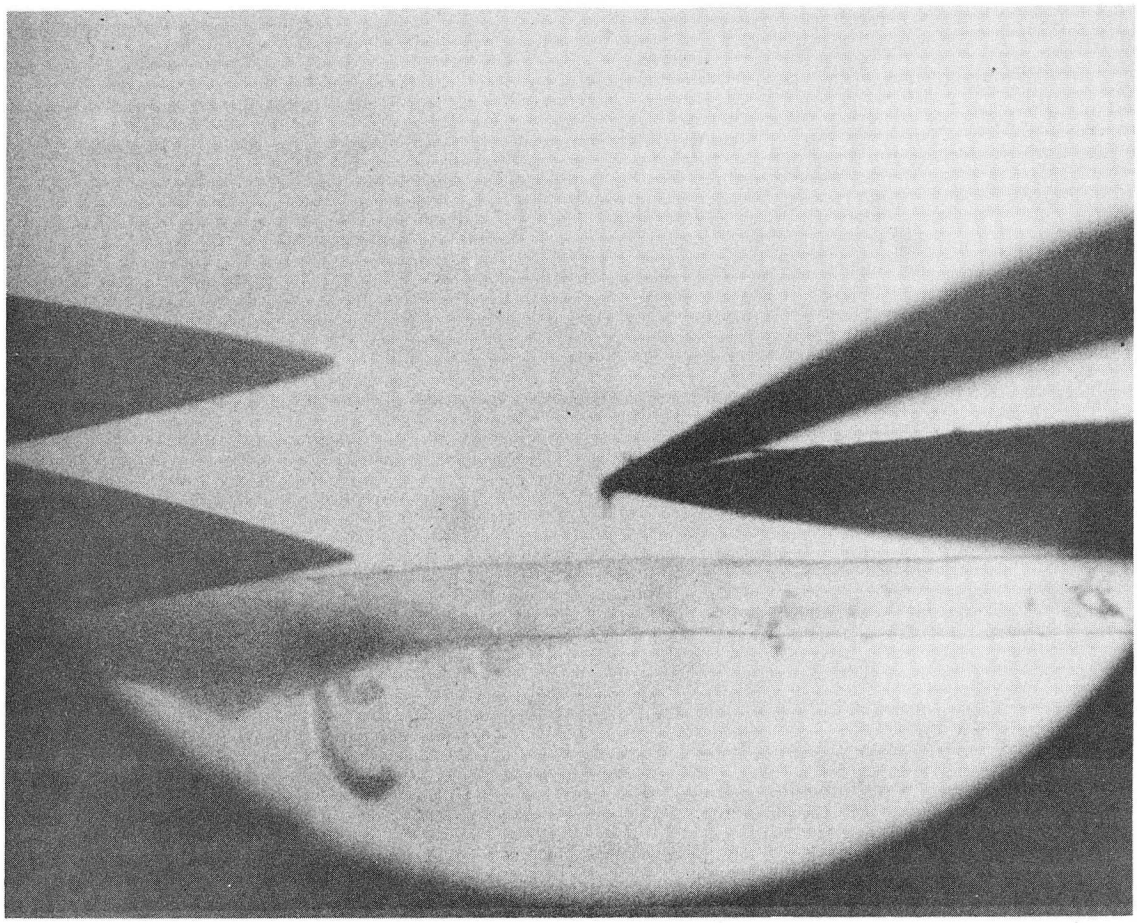

XBC 693-1967

Figure IV-16. Small fibers are cut away with iris scissors and sharpened forceps. This axon is about 175 μ in diameter.

2) Crab and Lobster Dissections

The dissections for both these animals are virtually identical. The walking leg is severed midway between the last joint and the body. The skeletal armor surrounding the joint nearest the toe was cut away with tin snips and strong dissecting scissors were used to sever the cartilage and tendens. The toe is then pulled away from the rest of the leg and the nerve comes away with it. For smaller crabs, the second joint from the toe is used to provide a thicker but shorter section of nerve.

3) Action Potential Excitation and Recording

The cleaned axon was bathed in artificial sea water and put into a quartz bottomed stimulation chamber. In order to prevent the saline solution from shorting out the electrodes, the nerve is allowed to touch pools of fluid only at the middle and the ends. The rest of the nerve is suspended by the five platinum electrodes. Two of the electrodes are recording electrodes and drive the electrometer pre-amp of a Winston Electronics nerve amplifier. The other three electrodes are used for stimulation, the first and third being grounded, the second being the hot line from the Tektronix pulse generator. Two ground electrodes are needed to prevent the stimulus artifact from becoming excessively large.

Occasionally, drops of saline were pipetted onto the nerve, especially at the electrodes, in order to prevent dehydration. Sea water soaked filter paper covered the chamber to maintain high humidity within.

V. RESULTS OF OPTICAL STUDIES

A. Absorption Measurements of Squid Axons

The optical system used was the same as that described as model one except that no polarizing prisms were used. The U.V. measurements were made with the deuterium lamp, while the visible measurements were made with a tungsten lamp. No absorption changes were detected at any of the wavelengths used -- 265 nm, 280 nm, 340 nm, 400 nm, 500 nm, and 600 nm. Sensitivity for the first three measurements was 1 part in 10^4. For the latter ones, 1 part in 10^5.

Replacing the polarizing prism below the condenser, we repeated the measurements at the above wavelengths with the axis of polarization at 0°, 45° and 90° with respect to the long axis of the nerve. Again no changes were detected, although the sensitivity was a factor of two less than the regular absorption measurements because of the reduced light intensity.

B. Fluorescence Measurements of Squid Axons

By replacing the quartz 10X objective with one made of glass, we could look for induced fluorescence changes at any wavelength above 310 nm. In particular, we hoped to study the fluorescence of the amino acid residues, tryptophane and tyrosine, of the

membrane proteins. At first we used the usual optical system with the monochromator set at 265 nm or 280 nm, but this allowed the stray light from the monochromator to reach the PM. We then put the monochromator and light source up on blocks and illuminated the nerve from the side. Nevertheless, no changes in fluorescence were detected.

C. Birefringence of Crab Nerves - Laser Measurement

1) Procedure

Model 2 of the optics with the He-Ne laser was used for our initial birefringence measurements.

With no nerve in the light path, only 10^{-4} of the laser intensity reaches the PM because of the crossed polarizing prisms. A crab nerve placed in the light path causes two opposing effects. The light intensity is decreased by about 30% due to light scattering, and it is increased by as much as a factor of 3 by the birefringence of the resting nerve. This latter effect depends on the angle between the axis of polarization and the long axis of the nerve, and arises from the ellipticity of polarization caused by the birefringent nerve.

Figure V-1 shows the actual experimental setup, and Figure V-2 is a closeup of the nerve chamber. Notice that the crab nerve is still attached to the toe and is composed of about 8 bundles.

2) Results

When the nerve is fired, a very small change in the birefringence occurs which results in the intensity of the light changing

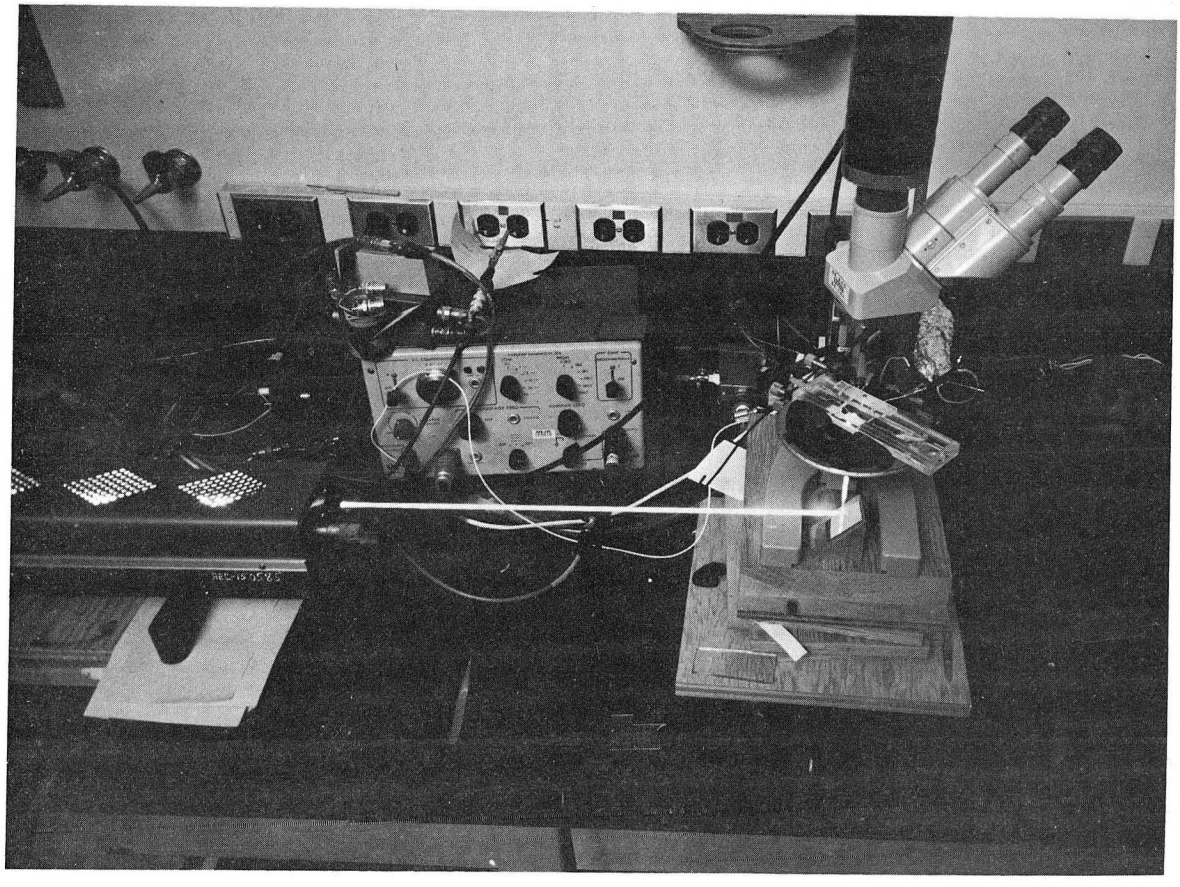

BBC 685-2468

Figure V-1. Laser used to measure nerve birefringence changes.

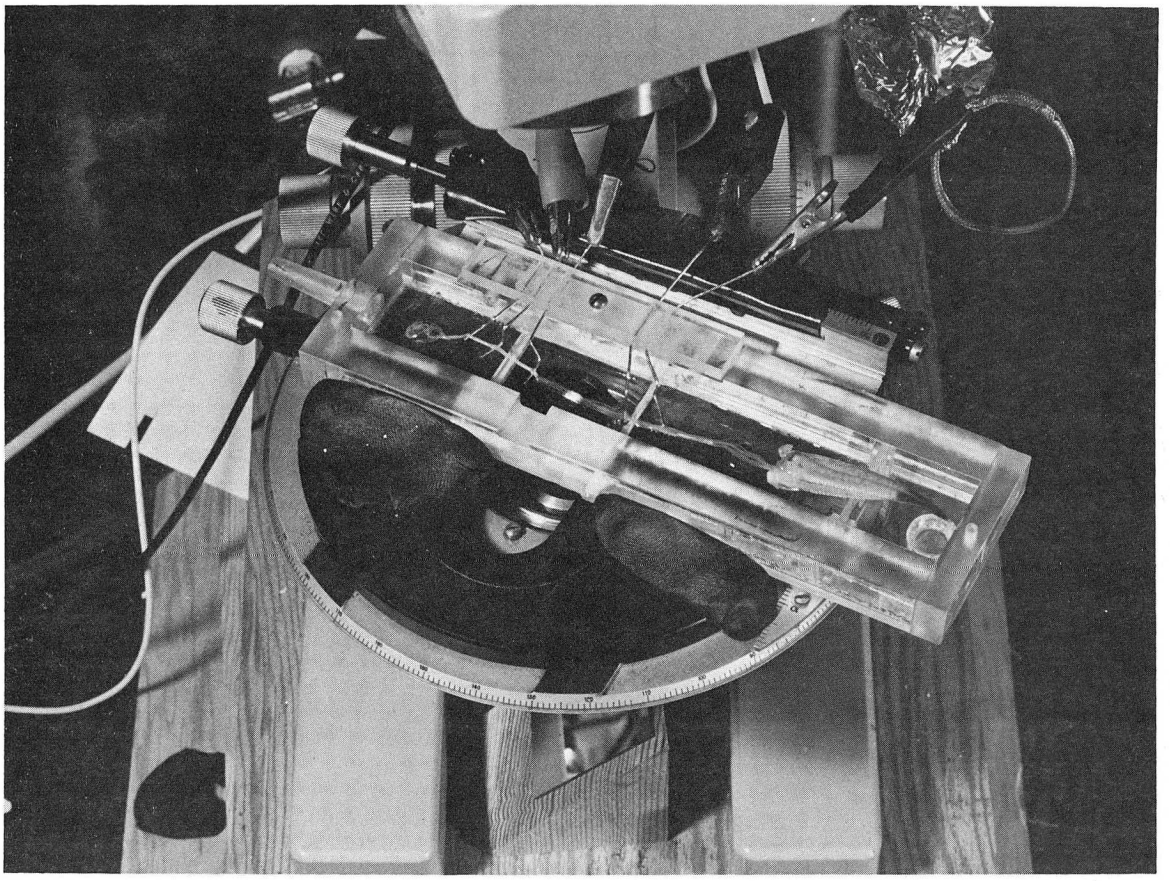

BBC 685-2470

Figure V-2. Closeup of nerve chamber.

by 1 part in 10^{-3}. Figure V-3 shows the time course of the birefringence change. Trace a) is a recording of the electrical action potential plus the calibration pulse. Trace b) shows the optical signal which is slightly larger and much longer than the 0.1%, 5 msec calibration pulse. Trace c) shows the experiment repeated as the nerve is rotated perpendicular to the axis of polarization. The signal virtually disappears. Returning the nerve to its initial 45° orientation restores the signal.

The optical signal cannot be directly correlated with the electrical action potential because the action potential is generated by the largest fibers whereas the optical signal comes from the thousands of very small fibers. By taking measurements as the nerve is rapidly pulsed twice in succession and then allowed to rest before the next pair of pulses, it was hoped that it could be determined whether the optical signal came from the main action potential crest or the after potential. Figure V-4 shows the electrical recording when the two pulses are rather far apart. Trace b) shows the corresponding optical signal. For traces c) and d), the electrical pulses are progressively closer together (not shown), resulting in the two optical signals merging.

Although it appears that the optical signal is due to the action potential crest, bandwidth limitations make this experiment inconclusive. However, as will be pointed out in the section on recent developments, there are better ways of probing this question, and the experiment was not pursued further.

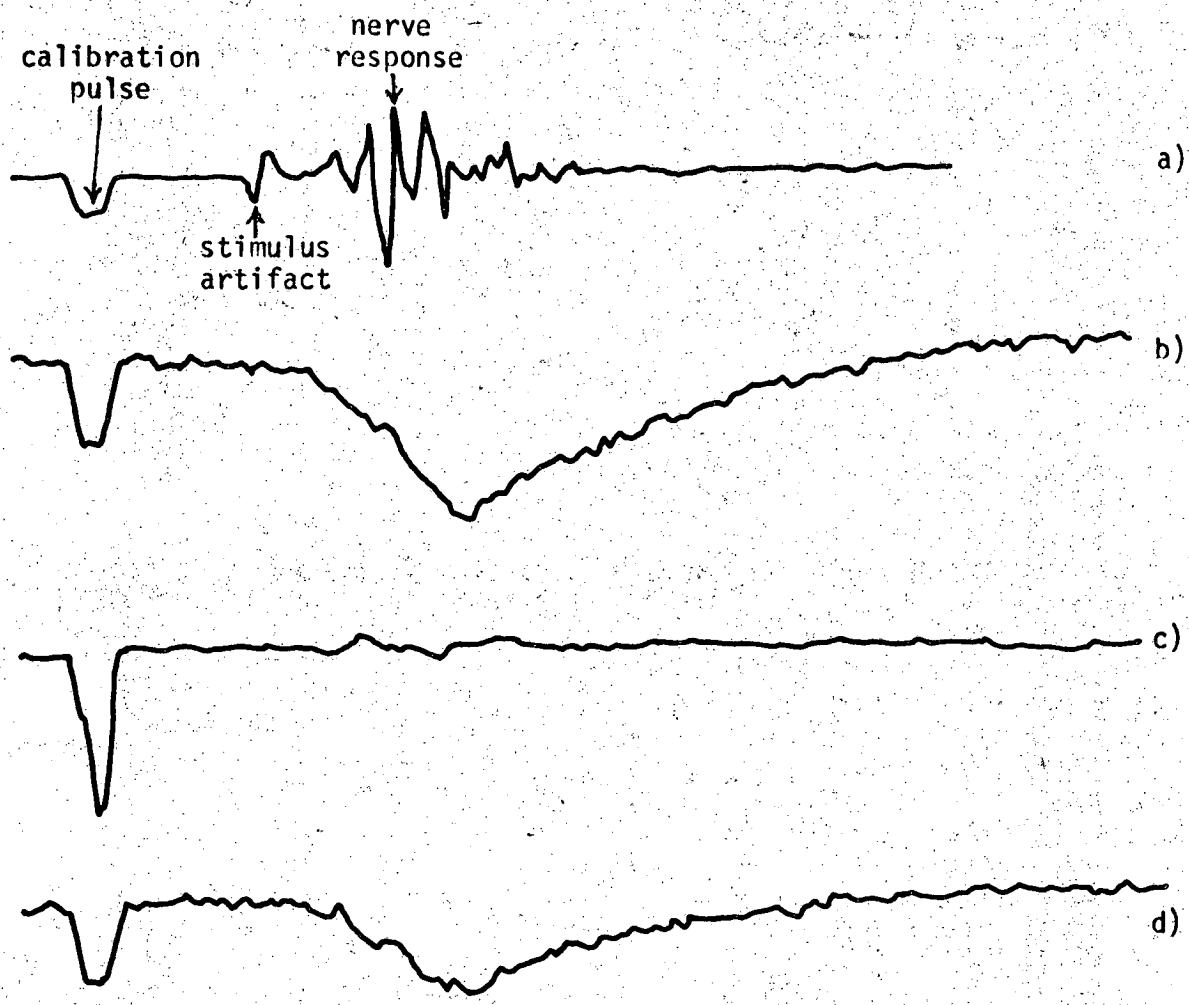

Figure V-3. a) Electrical response. b) Optical signal 45°. c) Optical signal 90°. d) Optical signal 45° (repeat).

XBL 687-4288

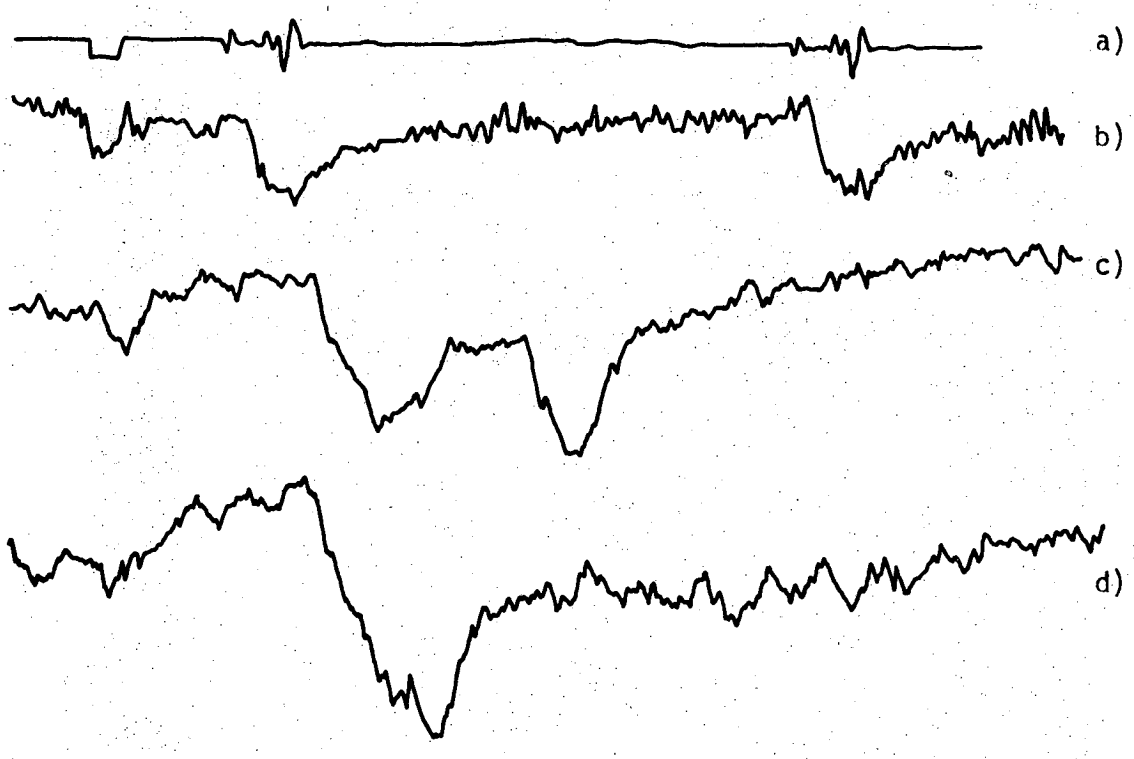

Figure V-4. a) Typical electrical signal. b) Optical signal nerve pulses 80 msec apart. c) Pulses 25 msec apart. d) Pulses 16 msec apart.

XBL 687-4289

D. Birefringence of Crab Nerves - Wavelength Dependence

1) Procedure

The use of model three optics convinced us that we could obtain useable signals without the laser. However, the signal to noise level was not impressive, and the spectacular improvement with model 4 led to its use for the wavelength dependence studies. The optical signal was readily seen on a single sweep of the oscilloscope, but it required sixty sweeps at ten per second to achieve the desired signal readability.

Measurements were made through three sets of broadband interference filters for three regions of the visible spectrum: Red (650 - 700 nm), Green (500 - 550 nm), and Violet (400 - 450 nm). Measurements in the ultraviolet were done with a Kodak Wratten filter 18A (320 - 380 nm), but required 24 seconds of averaging.

2) Results

Figure V-5 illustrates the quality of the signals obtained. Trace a) was measured with green light and averaged for one minute. This much averaging caused the signal to decay about 15% between measurements while achieving an unnecessarily high signal to noise ratio.

Trace b), measured in violet light, was averaged for 6 seconds. Since the light intensity is least in the violet end of the spectrum, this trace typifies our worst signal to noise ratio for the visible measurements. By allowing the nerve to rest for two

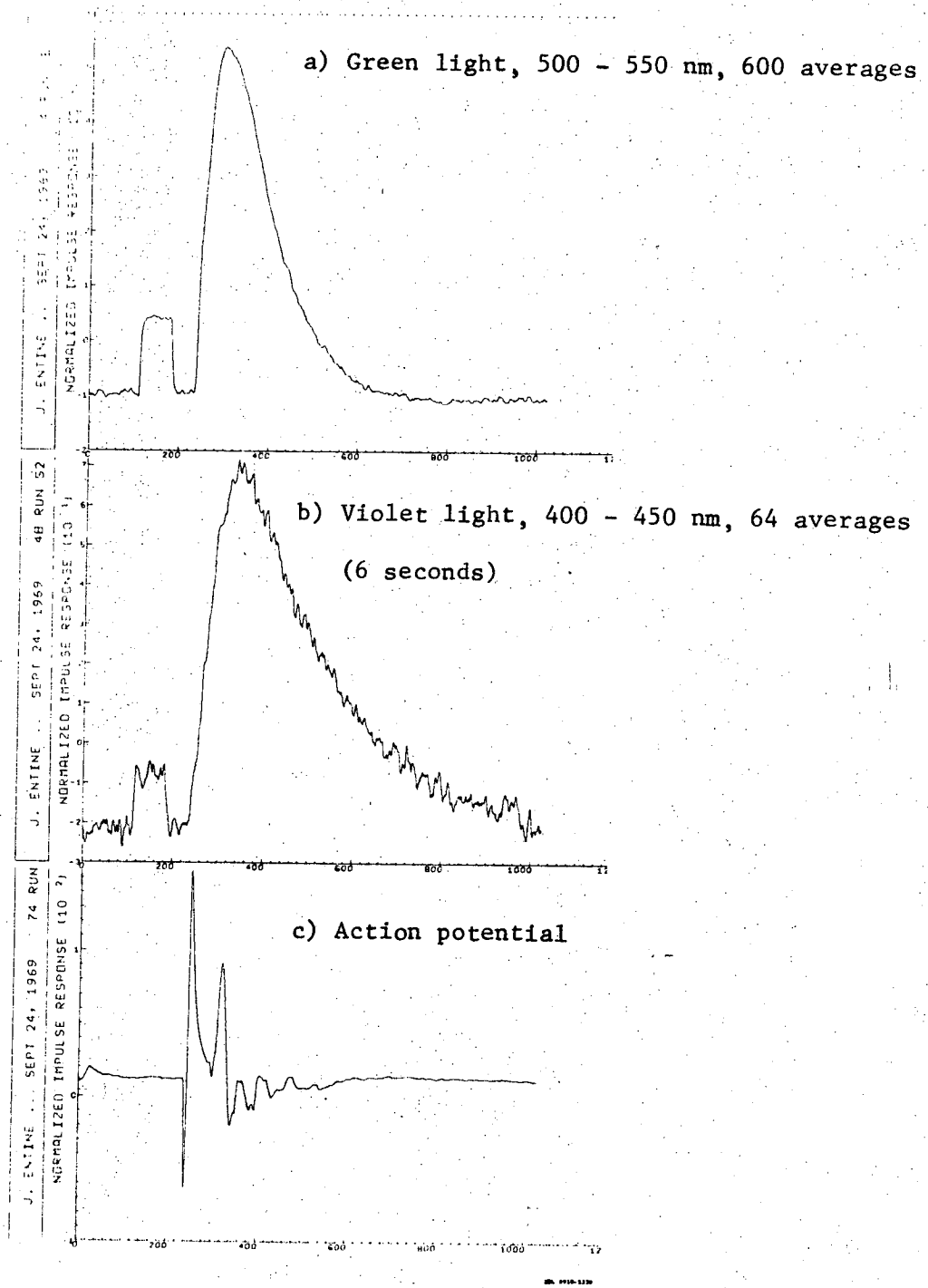

Figure V-5. Birefringence changes of crab nerve. Calibration pulse 5 msec wide, 0.25% high.

minutes between experiments, the nerve could survive for over two hours, allowing sixty color changes to be made.

The third trace shows a typical action potential.

No significant change in the amplitude of the optical signal could be detected in the region between 350 and 675 nm.

VI. DISCUSSION OF RESULTS AND CONCLUSIONS

A. Recent Findings of Other Laboratories

1) Scattering and Birefringence Changes

Approximately the same time as optical studies were begun in our laboratory, Larry Cohen and Richard Keynes decided to look for changes in light scattering of nerves during the action potential. In November of 1967 they reported their initial results from crab leg nerves.[19] They found that concurrent with the compound action potential, the amount of white light scattered at 90° increased by about 5×10^{-5}. They believe that the scattering at 30° and 45° angles decreased, although this result is still a preliminary one.

When dextran was added to their artificial sea water solution in order to raise the refractive index from 1.339 up to 1.353, a significant change in the scattering signal was observed. Unlike the scattering intensity in sea water which first increased and then decreased along with the electrical signal, in the denser medium the intensity increased with the leading edge of the action potential, and then plateaued at well above its initial level. The authors attribute this permanent increase to a reduction in the internal refractive index of the nerve caused by a small increase in the volume of the nerve fibers.

Light scattering measurements were then performed on the giant squid axons available in England. By inserting an electrode directly into the nerve as far as the center of the light beam, direct correlation could be made between the optical and electrical nerve signals. The optical signal was found to follow the action potential almost exactly, except that it lagged the electrical signal by a quarter millisecond. Since this difference in timing represents a conduction distance of over 5 mm, the time lag is not due to misplacement of the electrode.

The amplitude of the scattering signal was proportional to the fourth power of the wavelength. This implies that the scattering probably arises from large macromolecules.

Cohen and Keynes then decided to study birefringence changes.[20] Using white light and apparatus similar to that used in our laboratory, they detected changes in light intensity of 5×10^{-4} when crab nerves were placed between crossed polarizers at 45°, and 5×10^{-6} when squid axons were used. The squid axon provided an opportunity to investigate the phenomena in more detail, and several interesting experiments were performed.

Light was first put through only the outer 100 μ of a 1000 μ axon and the change in intensity measured. Then the beam was centered in the middle 500 μ of the same axon and the measurement repeated. The signal from the strip containing the edge of the nerve produced a signal over twenty times as large as the central strip. This shows that the birefringence change has a radical optic axis and arises from a substance located in the nerve membrane or surrounding cylindrical sheath.

Perfused axons in which at least 95% of the axoplasm was removed showed similar birefringence changes. This indicates that the birefringent micelles of the axoplasm are not the source of the action potential optical signal. Using an internal recording electrode to record the action potential at the point at which the optical measurement was being made showed that the electrical and optical signals have the same time course except for possibly a very small delay for the optical signal. This delay is much less than the quarter millisec described for the scattering work, and the source of the difference between the delays is not at all understood.

Voltage clamps were applied to the nerve during the optical measurement, and birefringence changes were again detected. Hyperpolarizing pulses produced a much larger response than depolarizing pulses of equal amplitude. Furthermore, a plot of birefringence versus membrane potential showed a very nonlinear dependence, with the birefringence changing five to ten times more steeply at 120 MV of hyperpolarization than at 120 MV of depolarization. No symmetry point was found anywhere between these two levels, indicating that the membrane has considerable structural or electrical asymmetry.

The optical signal was compared with the membrane current to determine if the effect was voltage or current related. It appears that the effect is related almost entirely to the voltage rather than to the current. Since it is believed that nerve potential differences exist almost exclusively across the membrane, the

optical effect most likely arises from within the membrane and not from the surrounding tissue.

Tetrodotoxin, the toxin that inhibits the flow of the sodium current, was found to increase the size of the optical signal in voltage clamped axons by as much as a factor of four. However, the change came about several minutes after the sodium currents became blocked and persisted for several minutes after the sodium current resumed when the toxin was washed away. This effect is not understood.

The outer edge of the squid axon has a net axial birefringence of 240 Å. Thus the 4×10^{-5} light intensity decrease corresponds to a 0.005 Å increase in the radial retardation. Although the net birefringence of the axon is axial 240 Å, most of this is form birefringence and the intrinsic birefringence is radial 1-3 Å.[17] The change in radial birefringence is therefore about 0.1% of the intrinsic membrane birefringence.

2). Fluorescence Changes

About a year after Cohen's group reported the initial scattering results, Tasaki *et al.*[21,22] published similar work on turbidity and birefringence changes and new results concerning fluorescent dye studies. Using the dye 8-anilino-naphthalene-1-sulfonic acid (ANS) (0.05 mg/ml), they stained crab, lobster, and squid nerves for about 20 minutes and then examined the 455 nm fluorescence signal while the nerve was being excited.

They found that the fluorescence intensity increased by 1 part in 10^4 with each action potential and had a time course similar to that of the birefringence changes. ANS is known to fluorescesce only when attached to large macromolecules, and it is suggested that the dye might be attached to such molecules in the membrane. However, since the ionic concentrations of the 1 μ on either side of the membrane changes so drastically during the action potential, it is possible that this alteration causes the observed optical effects.

Similar experiments were performed using acridine orange,[23] which also has its emission and absorption spectra affected when it complexes with macromolecules. Again, similar results were obtained. However, neither the polarization of the fluorescence of either of these dyes, nor the spectra were studied because of signal to noise problems.

B. Conclusions

The primary conclusion of this work is that the axon membrane does exhibit a change in optical properties which follows closely the time course of the action potential. As the calculations of the wavelength dependence of birefringence show, it is quite possible that the birefringence changes could reveal the nature of the molecules involved in the membrane change. In our particular experiments, measurements could be made only down to 350 nm. If measurements could be made near the 280 nm protein absorption band,

it would immediately determine whether proteins are the source of the signal. The bulk of the resting nerve birefringence is due to oriented proteins, and thus the measured signal S is actually the ratio of the change in membrane birefringence to protein birefringence. Therefore, if S remains constant throughout the 280 nm region, it would be a strong indication that the active membrane does contain protein, and that the protein is involved in the action potential mechanism. Such a finding would be compatable with the ESR findings discussed in Section VII that a biradical label dissolved in the lipid part of the membrane is unaffected by the action potential. If, on the other hand, S decreased as one approached 280 nm, it would suggest that the signal does not arise from protein but probably lipids which absorb at about 210 nm.

The data of Cohen et al. show convincingly that the birefringence change is directly related to the voltage across the membrane, and probably arises from radially oriented molecules. Their scattering measurements and the fluorescence measurements of Tasaki et al. illustrate that other types of optical phenomena may also be found to change with the action potential. None of these works has revealed the composition, or structure, of the nerve axon membrane or the mechanism of the membrane action potential. However, the fact that direct observations of the changes of the axon membrane have now been achieved is surely grounds for optimism.

VII. BIRADICAL SPIN LABELING OF LOBSTER NERVES[24]

A. Introduction to Biradicals

After the initial results were obtained in the optical experiments, we considered the possibility of applying an analogous technique to study changes of spin labels applied to the nerve membrane. The spin label we first chose was ethelene-di (1-oxy-2,2,5,5-tetramethyl-3-pyrroline-3-carboxamide), denoted biradical A. This probe is a molecule consisting of a flexibly attached pair of nitroxide free radicals in which the variable distance r between the nitrogen atoms is 6.4 A $\leq$ r $\leq$ 12.8 A.

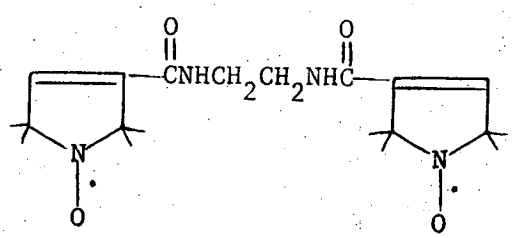

The magnetic interactions between the two unpaired electrons on the nitrogen atoms are large for separations smaller than 10 A and negligibly small for separations exceeding 14 A. The ESR spectrum of the biradical is strongly affected by the intensity of these interactions and thus indicates the conformation of the flexible biradical. If biradicals could be made to adhere to various parts of the nerve membrane, the ESR spectrum would then indicate the geometrical deformations of the membrane.

The details of the ESR spectra[25-27] can be summarized in the following simplified discussion: the electron in an isolated monoradical is subjected to a hyperfine field of 0 ± 15 gauss, corresponding to the Zeeman level occupied by the adjacent N^{14} nucleus. The ESR spectrum of a sample of monoradicals is shown in Figure VII-1a.

A biradical has two sites, at which the N^{14} nuclei may occupy similar or different Zeeman levels. The exchange type of pair interaction, which is of interest here, is equivalent to the electrons exchanging their sites so that each electron is exposed to the hyperfine fields on both sites. The effective hyperfine field seen by an exchanging electron has an average value weighted by the residence times at the two sites. Biradicals in which the two N^{14} nuclei do not occupy similar Zeeman levels contribute interpolated spectral lines which are absent in the monoradical spectrum. Fast exchange results in equal residence times of the electrons at the two sites, in which case the effective hyperfine fields are simple averages. The corresponding ESR spectrum consists of five components with the intensity ratio of 1:2:3:2:1 (Figure VII-2).

B. Basic Quantum Theory of Biradicals

The quantum mechanical calculations for the biradical are somewhat complicated but are soluble. The spin Hamiltonian for the system is:[26]

$$H = g\beta BS_z + a(S_{1z}M_1 + S_{2z}M_2) + J(S_1 \cdot S_2) \text{ where } S = S_1 + S_2$$

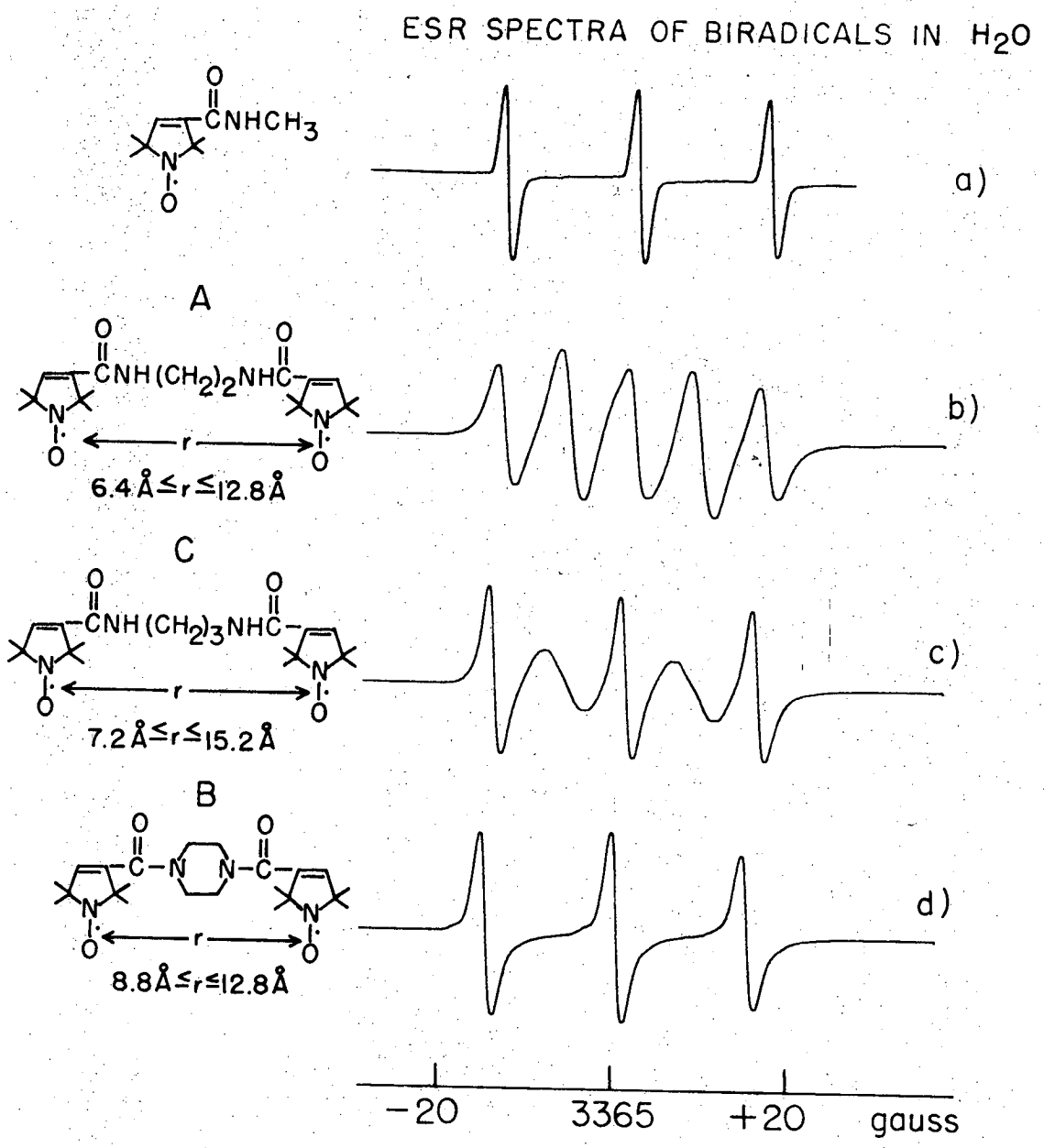

XBL 691-4036

Figure VII-1. ESR derivative spectra of four different nitroxide radicals dissolved in water at room temperature. Biradical A, 6.4 Å ≤ r ≤ 12.8 Å. Biradical C, 7.2 Å ≤ r ≤ 15.2 Å. Biradical B, 8.8 Å ≤ r ≤ 12.8 Å.

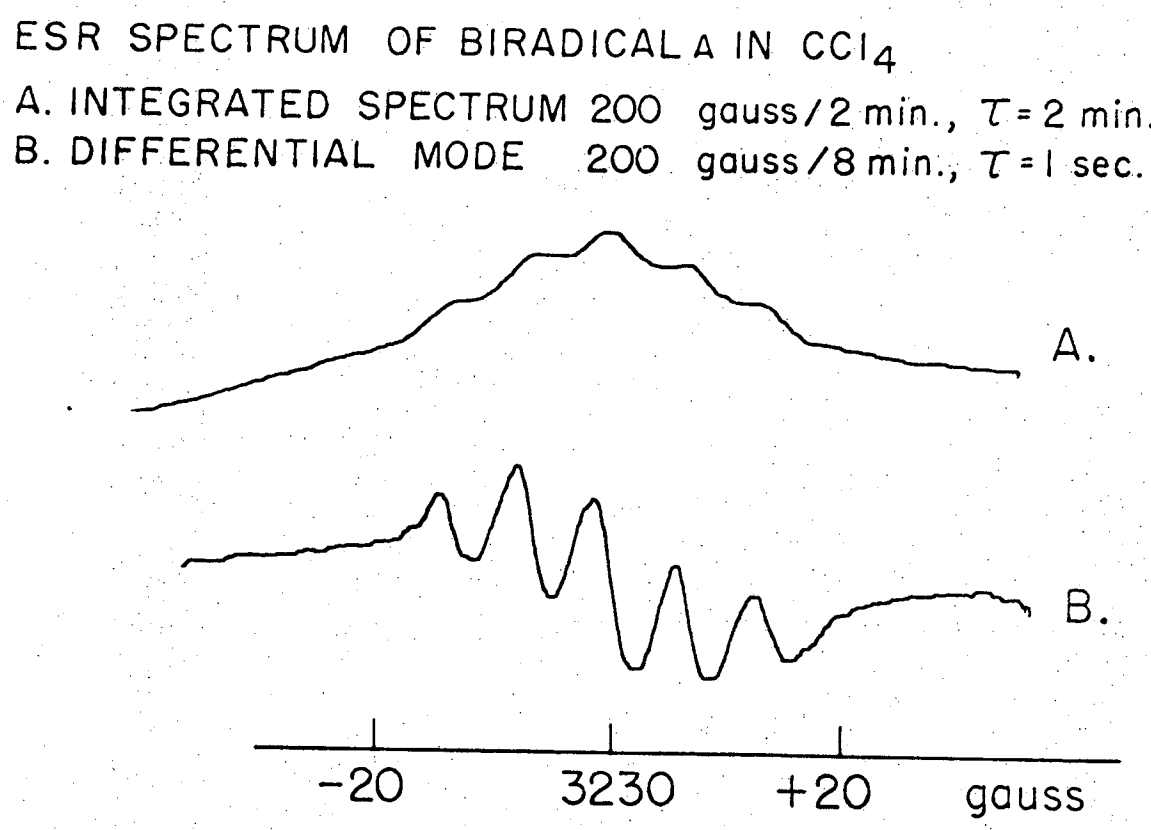

X3L 691-4037

Figure VII-2. ESR of biradical A in CCl_4 at room temperature. This is a representative case of fast exchange resulting in a five line spectrum, the components of which have the intensive ratio of 1:2:3:2:1. The broadening apparent in the spectrum is not dependent on radical concentration. The upper spectrum has been obtained in the integrating mode, whereas the lower one is the derivative spectrum. Integration was attained on the Varian E-3 spectrometer by adjusting the scan rate to 100 gauss/min and the time constant to 100 sec.

The first term is the Zeeman splitting due to the direct interaction between the electron magnetic moments and the external field. The second term, the hyperfine interaction, arises from electron spin, nuclear spin interaction. The third term is the exchange interaction from the symmetry of the wave functions. In our case the S_1 refer to the unpaired electrons on each radical and M_i to the Z component of the nuclear spins of the N^{14} atom which has I = 1.

Since the exchange and hyperfine terms do not commute, the energy levels are strongly affected by the relative magnitudes of these terms. When the electrons are far apart, J is very small and the Hamiltonian is approximated by the first two terms:

$$H = (g\beta B + aM_1)S_{1z} + (g\beta B + aM_2)S_{2z}$$

Since all transitions measured are near the free electron resonance field, for this case only single electron flips are relavent. The energy level diagram is shown in Figure VII-3. Nuclear transitions are forbidden and therefore M_i do not change. From the diagram it is evident that there are three equally intense resonances at energies ($g\beta B + a$), ($g\beta B$), and ($g\beta B - a$). In this case the spectra are identical with a monoradical system.

When the two electrons are close together, their orbitals overlap enough to make J much larger than a. In this case the S_z of each electron is no longer a good quantum number and only the total electron spin S, and its component S_z can be considered.

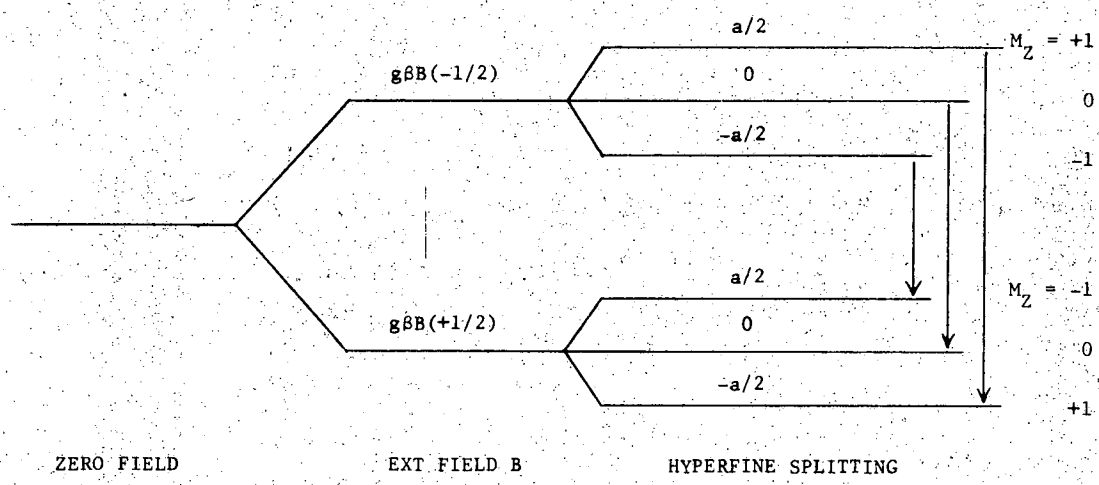

XBL 698-5306

Figure VII-3. Energy level for a biradical when J/a is very small is analogous to that of a monoradical.

With two electrons, only the triplet S=1 and the singlet S=0 are possible. The appropriate triplet wave functions are $|1,M_1,M_2\rangle$, $|0,M_1,M_2\rangle$, and $|-1,M_1,M_2\rangle$. The hyperfine energy is still equal to $a(S_{1z}M_1 + S_{2z}M_2)$ and gives the following energy level diagram (Figure VII-4). Note that the $S_z = 0$ states are degenerate. The singlet state is very slightly mixed with the triplet $S_z = 0$ state by the hyperfine interaction, but because of the exchange separation of the states, transitions between these states are very weak.

The intermediate case when $J/s \approx 1$ can be solved by diagonalizing the appropriate matrices, and the following energy transitions are calculated:

$$E = g\beta B + \frac{1}{2}a(M_1 + M_2) \pm \frac{1}{2}\,|a\Delta M|\,[(1-K\lambda)/(1+K\lambda)]$$

where $\lambda \equiv J/[|a\Delta M| + (a\Delta M)^2 + J^2)^{\frac{1}{2}}]$ and $\Delta M = M_1 - M_2$, $K = \pm 1$.

The relative intensities of the transitions are

$$I = [1 + 2K\lambda/(1 + \lambda^2)] .$$

Figure VII-5, adapted from Le Maire *et al.*, illustrates how the lines vary with J/a.

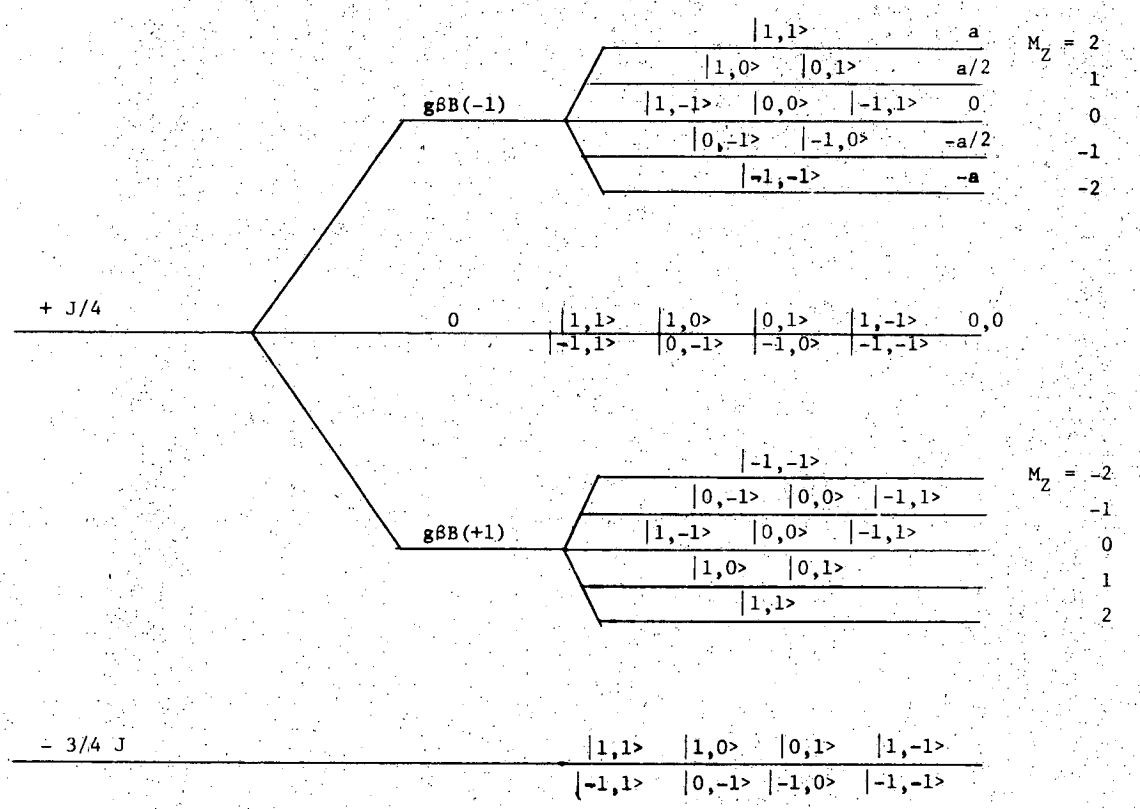

XBL 698-5305

Figure VII-4. Energy level diagram for a biradical when J/a is large.

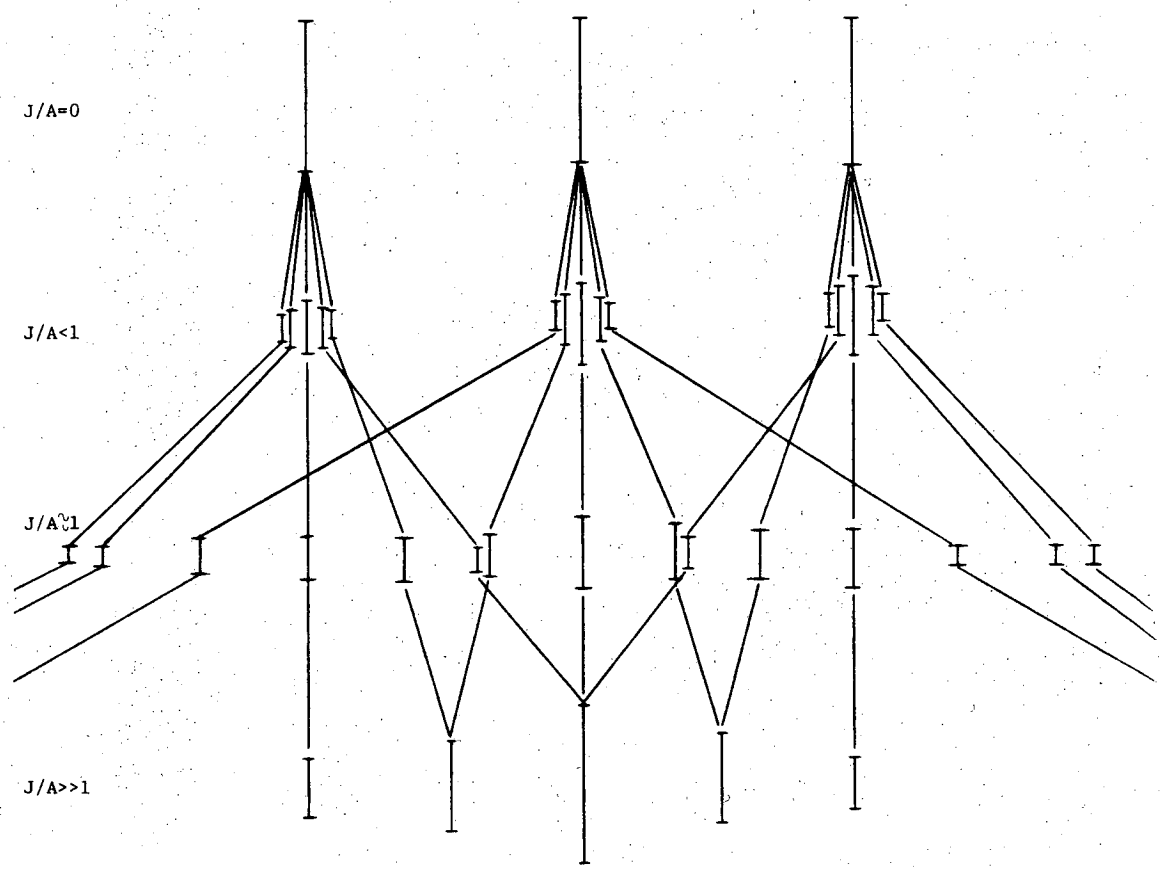

XBL 698-5304

Figure VII-5. Diagram of how EPR spectrum of biradical changes as J/A increases. Lengths of vertical lines indicate amplitude of peak. When J/A = 0 (top) three peaks of equal amplitude are seen. For J/A large (bottom), the 1:2:3:2:1 five peaked spectrum is seen (Le Maire *et al.*, Ref. 28).

C. Effect of Biradical Structure and Solvents on the Electron Interaction

The problem of relating J to the distance between the electrons is a rather difficult one and has not yet been solved directly. We have attempted to determine this relationship empirically by changing the chemical structure, length, and flexibility of the link between the two radicals. Solvent and temperature effects have also been studied, and were found to drastically affect the extent of exchange.

1) Structural Effects

We first consider the effect of the structure of the biradical on the ESR spectrum of the molecules in aqueous solution. The biradical A showed a five line spectrum (Figure VII-1b), indicating fast exchange interactions of the two centers. A rigid biradical (the piperazine analogue of biradical A), henceforth named biradical B showed a three line spectrum (Figure VII-1d), indicating no exchange interaction. Similar solutions of the corresponding trimethylene diamine radical (biradical C) showed a five line spectrum (Figure VII-1c) that was intermediate between the spectrum of the rigid biradical B and that of biradical A. Such an intermediate spectrum indicated that biradical C had a slower rate of exchange than biradical A. The only difference between biradicals A and C is the greater separation of the radical centers due to the addition of one methylene group. These results support the concept

that the rate of exchange interaction is a function of the flexibility of the molecules and the distance between the radical centers.

2) Solvent Effects

We have dissolved biradical A in a large number of solvents which are chemically similar to membrane constituents. The results are:

(a) Water: The exchange at room temperature is intense ($J/A \gg 10$) and does not depend on pH (Figure VII-1b).

(b) Water additives: In saturated solutions of starch, bovine serum albumin, sodium aleate, the exchange is the same as in water. Thus, the biradicals apparently do not interact with these solutes sufficiently strongly to effect the exchange. It is probable that the sodium oleate had formed micelles in water and the biradicals were accomodated inside them, but no effect was seen on the rate of spin exchange.

(c) Pure organic acids (e.g., formic acid, acetic acid, butyric acid and oleic acid): The exchange is fast. However, in pure formic acid the nitroxide groups are destroyed chemically, probably by reduction.

(d) Alcohols: Propanediol, butane-2,3-diol, n-octanol (Figure VII-6), n-decanol and glycerol (Figure VII-7). In all these alcohols the spin exchange is inhibited at room temperature.

(e) The spectra in representative esters, such as olive oil and amyl acetate, are characterized by fast exchange, as are the spectra in dihydrosphingosine.

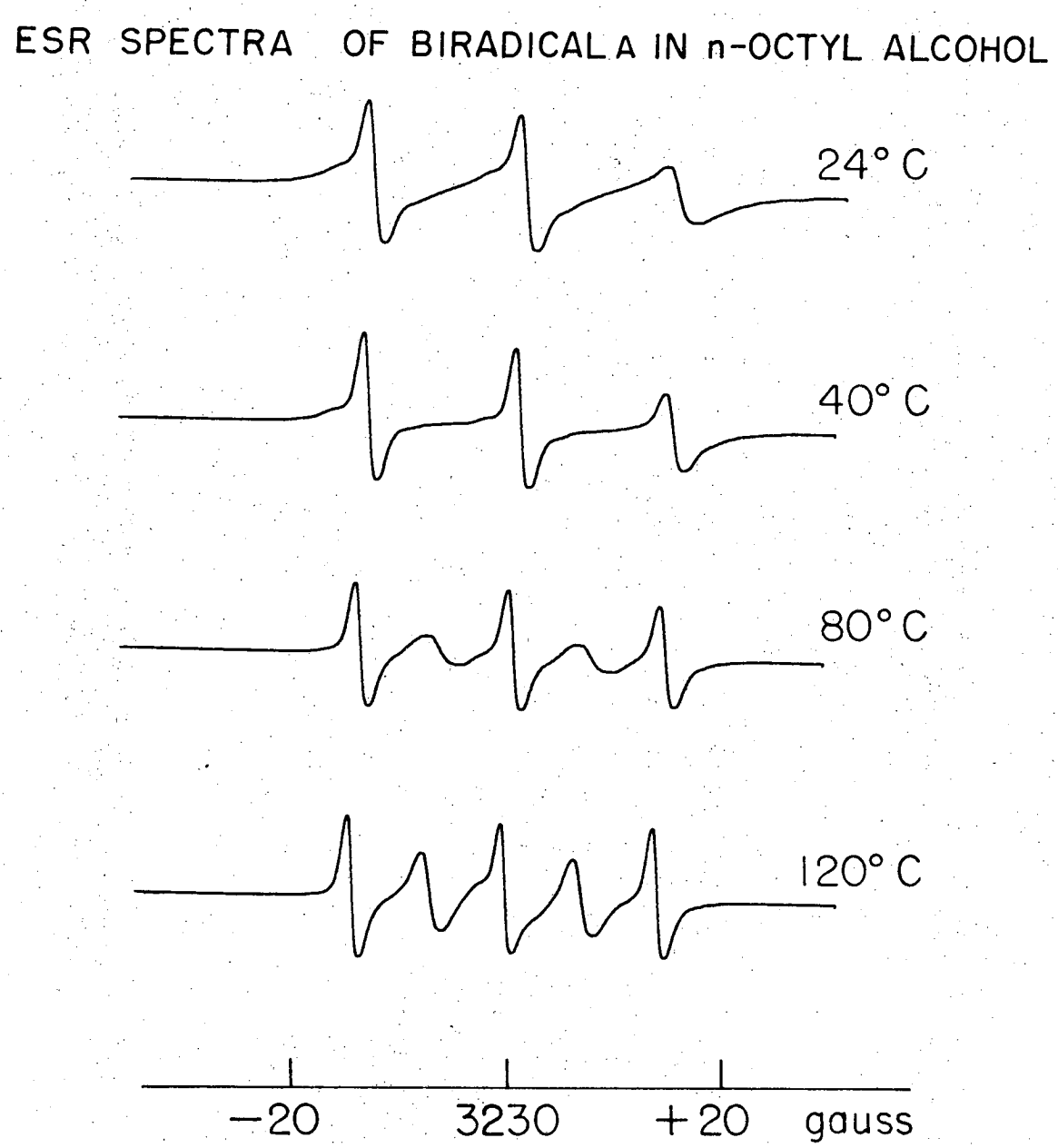

XBL 691-4034

Figure VII-6. The temperature dependence of the ESR of biradical A dissolved in n-octanol. Spin exchange is inhibited. The spectrum at 40° is considered a simulation of the spectrum obtained in the nerve membrane.

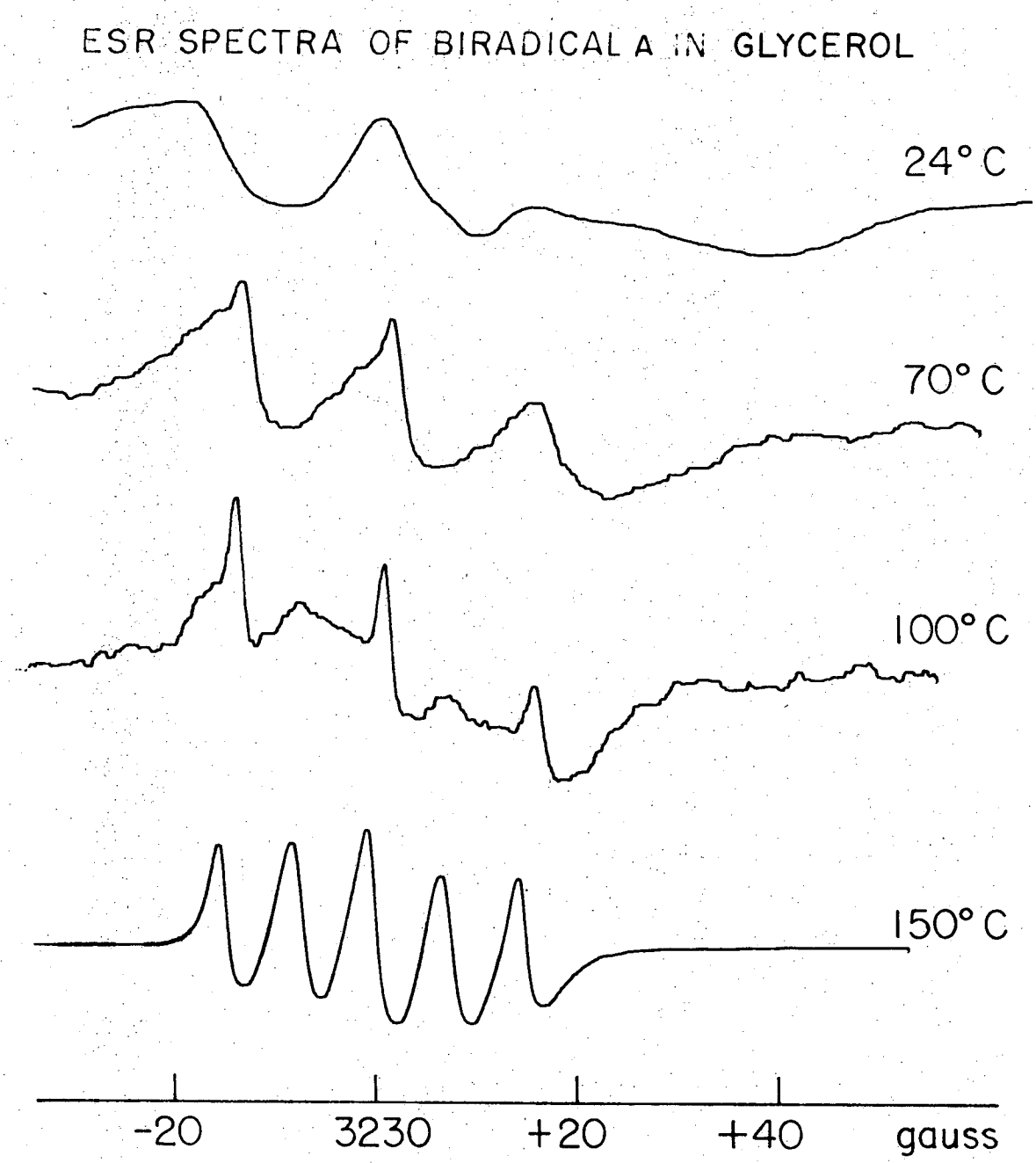

XBL 691-4039

Figure VII-7. The temperature dependence of the ESR of biradical A dissolved in glycerol. Viscosity effects do not mask the absence of pair interactions in the low temperature spectra. The exchange apparent at 150° is believed to result from the presence of trace quantities of water.

3) Conclusions

Viscosity has a strong influence on the spectra, but it is always distinguishable from that of strong pair interactions. Low viscosity spectra on non-interacting biradicals have three components, and this analogy of weakly interacting biradicals with monoradicals is valid through the whole range of increasing viscosity (Figure VII-7, 70° and 24°). In fact, the similarity of the spectra of biradical A in frozen alcohols with the spectra of immobilized monoradicals lends the strongest support to the conclusion that the unpaired electrons of the biradicals in alcohols are far apart. In viscous media the r^{-3} dependent dipole-dipole interaction becomes fully effective at close range, and in combination with spin exchange it would drastically modify the immobilized spectra.[30,31] The resulting line shape (Figure VII-8, 24°), which can be computer simulated, would be sharper than that of the immobilized non-interacting pairs (Figure VII-7, 24° and 70°). Sharpness is actually the main attribute of the ESR spectrum of the immobilized interacting pairs, and it is also significant that these sharp lines pass directly into five line spectra when viscosity is lowered (Figure VII-8).

The addition of water to the alcohols enhances the exchange, probably by displacing the bound alcohols. In one fortunate run with glycerol, the three line spectra were followed all the way to 160°, indicating that the biradicals were girdled even at that temperature. We believe that in that case the sample was water-free, while in the sample reported in Figure VII-7 some

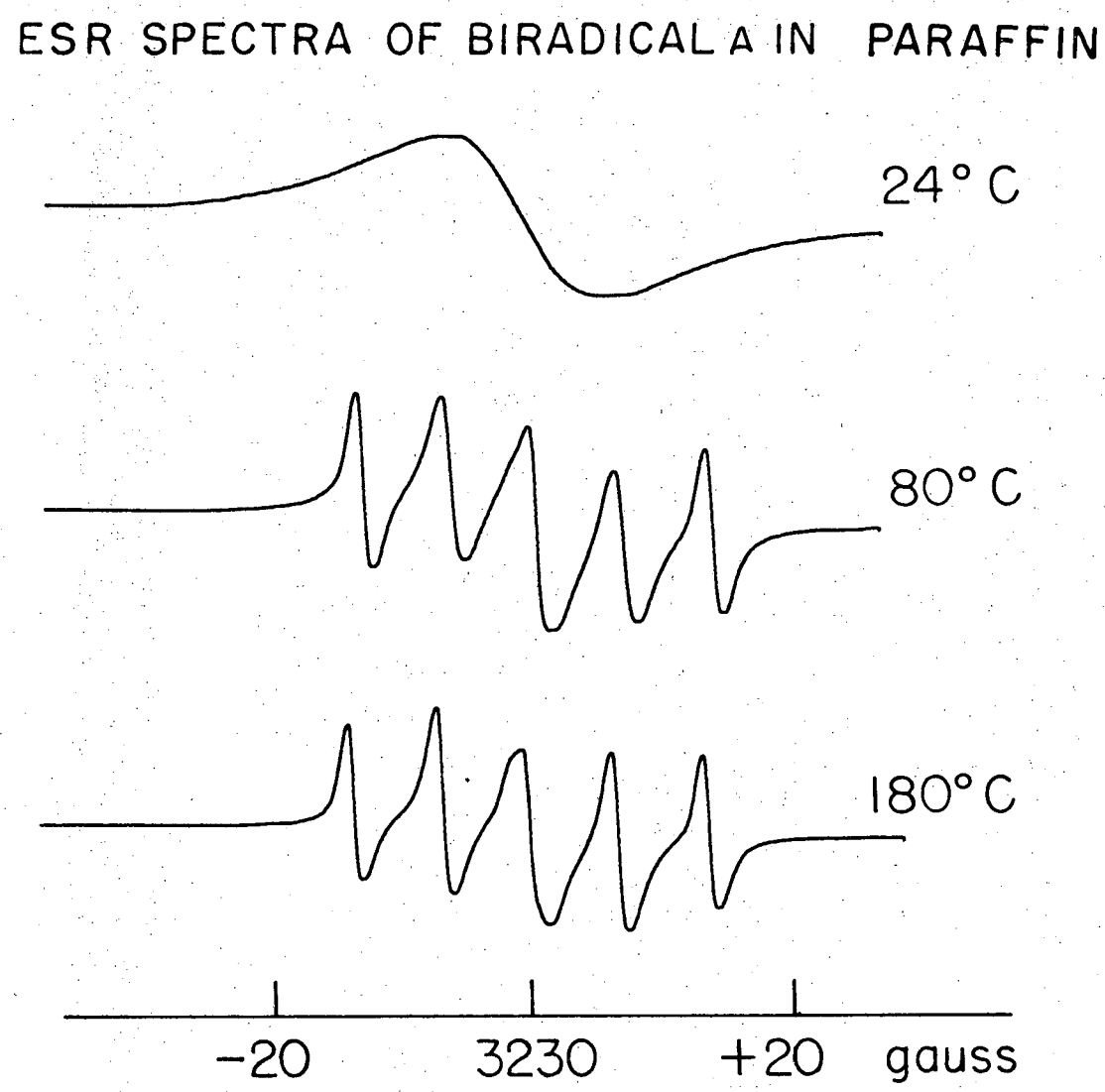

XBL 691-4038

Figure VII-8. The temperature dependence of the ESR of biradical A dissolved in paraffin which is solid at room temperature. The spectra are typical of strong pair interactions in both the solid and fluid phases.

water was present, thus lowering the temperature for the onset of exchange.

The results of the present section allow us to predict the changes in spectrum that one might expect in a satisfactorily bound geometrical probe.

If the biradical probe is bound to a framework so as to reflect its dimensional changes, e.g., two point binding, it may also be free to change its orientation in the external magnetic field rapidly or slowly. If it is the former, the dimensional change should appear as a transition between the three and five line spectrum (Figure VII-6, 40° - 120°). If it is the latter, the change should appear as a transition between a distorted three line spectrum (Figure VII-7, 24°) and an exchange narrowed single line spectrum (Figure VII-8, 24°).

D. Resting Nerve Study

1) Designing an Ideal Biradical Probe

Ideally, the biradicals used for investigating the nerve membrane should be covalently bonded at their two ends to the structural components of the membrane. For instance, if the membrane structure contains protein molecules which change their conformation during the action potential, a biradical which had proteophyllic groups at each end might bind to the proteins and be stretched or compressed as the proteins moved. Lipophillic end groups might be used to study the lipid portion of the membrane. It is conceivable that the time course of the spectrum of

the radical bound to one membrane would be similar to that of the potassium flow and the other to the flow of the sodium. This would directly link the membrane structural changes to the electrical and chemical phenomena.

2) Lobster Nerve Preparation

Because of time difficulties, this study was not pursued beyond the stage of using biradical A. We used the walking legs of Maine Lobster (*Homarus americanus*). These nerves are unmyelinated and consist of about ten bundles of 1000 fibers each. For an EPR experiment it is desirable to have as much membrane per unit volume and this type of nerve is therefore preferable to a squid nerve.

The nerve was bathed in a 10^{-5} m solution of biradical A in artificial sea water. After 5 - 20 minutes the nerve was removed and drawn into a glass tube with a one millimeter constriction at the center. The nerve was tied off at both ends by a nylon thread which was used to center it in the constriction. The tube was then closed with corks and inserted in the cavity of the Varian E-3 spectrometer.

3) Results

The spectrum of the biradical was markedly changed upon contact with the nerve (Figure VII-9). The spectrum indicated that the exchange interaction between the two radical centers was sharply decreased. While it would have been nice to assume that the biradical was bound to the membrane, the line shape of the

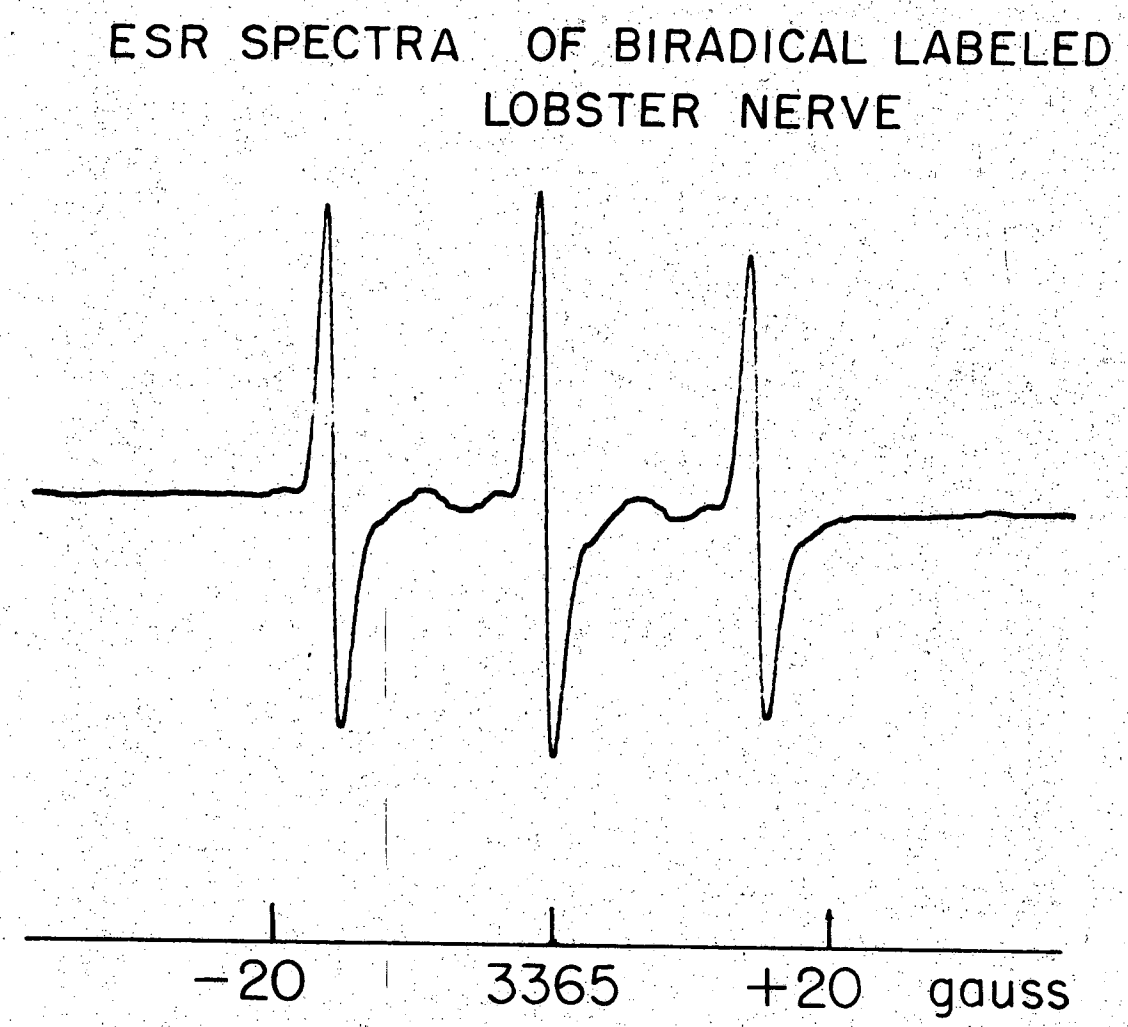

XBL 691-4035

Figure VII-9. ESR spectrum of biradical A labeled lobster nerve.

spectrum indicates a rather high tumbling rate approaching that of a liquid environment. It was for this reason that the above described solvent effect experiments were done. The EPR spectrum of the radical in the nerve most closely corresponds with that of the biradical in the alcohol solvents (Figure VII-6, 40°). It therefore seems likely that the biradical is dissolved in the lipid portion of the membrane.

4) Strength of Binding of Biradical Label

Experiments were done to determine how tightly the radical was bound to the membrane. The nerve was soaked in the biradical solution and then washed in radical-free artificial sea water for periods of 5 minutes to 8 hours. The initial few minutes seemed to rinse the biradical off the surface, but a substantial EPR signal remained. The bulk of the bound biradical took over two hours to wash out. The residue after this washing did not seem to wash out, but rather to be reduced. Total reduction of the biradical in the nerve required about 8 hours, while biradical in sea water solution was stable for weeks. Attempts were made to extract the reductant from the nerve. The nerve was soaked for 30 minutes in a small quantity of sea water and removed. The biradical was then put into the sea water and found to be stable. Thus the reductant was not water soluble.

E. Study of Nerve During Action Potential

1) Apparatus

We then proceeded to develop apparatus to be used for detecting changes in the EPR spectrum during the action potential. A chamber was constructed which contained stimulating and recording electrodes (Figure VII-10). The chamber body is made of an acrylite tube 10 mm O.D. and 7 mm I.D. and 15 cm long. Down the center of the tube was a 4 mm wide strip of lucite 1 mm thick, on which platinum wire electrodes were glued. Part of the center portion of the cylinder was cut away for easy access, while a sliding cover prevented the nerve from drying out during the experiment. The nerve adheres to the strip by surface tension.

The magnetic field was set on the spectral peak under study and the unfiltered output of the spectrometer (scope output jack E-3) was sent to a 1A7 Tektronix preamp. The second input of the preamp was used to inject a calibration pulse. The bandwidth of the system was set on the 1A7 to be 1 Hz to 3 KHz. As can be seen from the block diagram (Figure VII-11), the apparatus is very similar to that used in the optical work.

2) Results

The sensitivity of the system is limited by the inherent electronic noise of the E-3 (probably from the detector diode) which is not a function of the strength of the EPR signal. Thus the signal to noise ratio is a linear function of the size of the EPR signal. For these experiments with biradical A, the

NERVE CHAMBER FOR STIMULATING AND RECORDING THE ACTION POTENTIAL IN THE ESR CAVITY

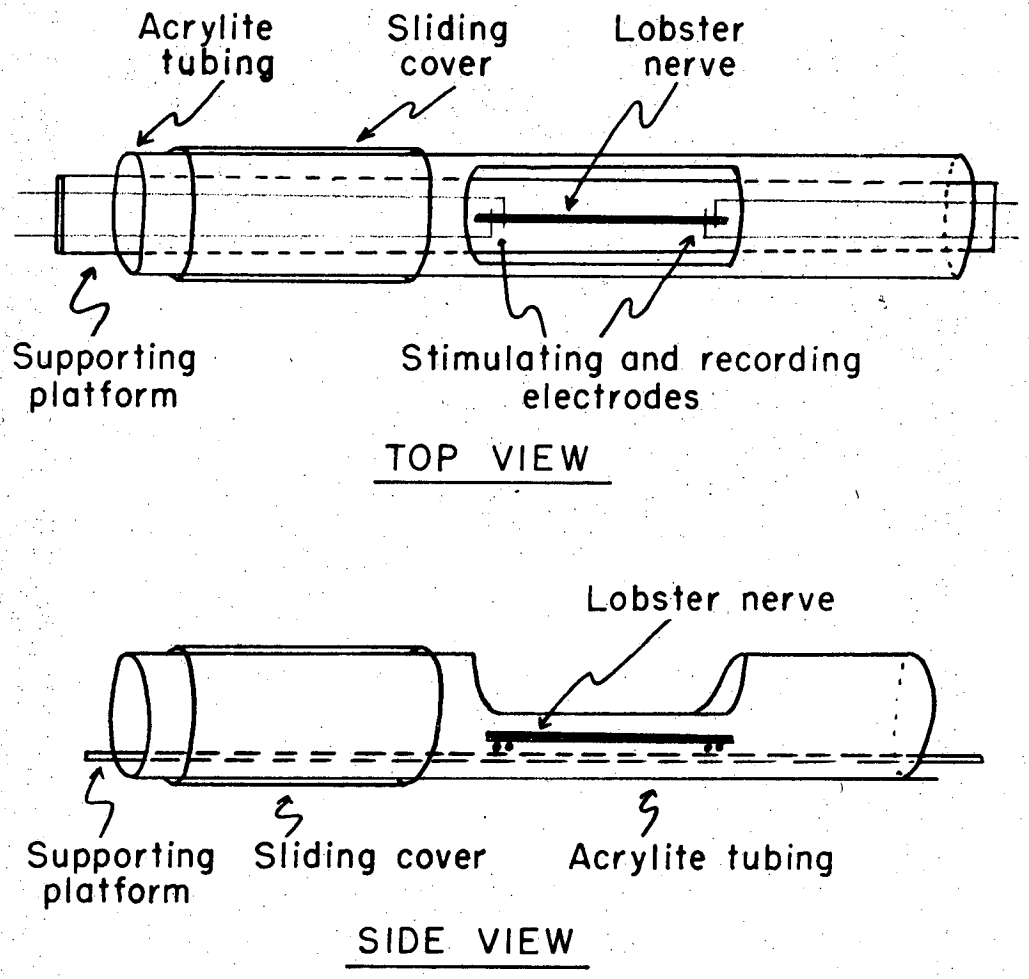

XBL 691-4031

Figure VII-10. Nerve chamber for stimulating and recording the action potential in the ESR spectrometer cavity.

BLOCK DIAGRAM OF SYNCHRONIZING CIRCUITRY FOR STUDYING THE ESR SIGNAL DURING MEMBRANE EXCITATION

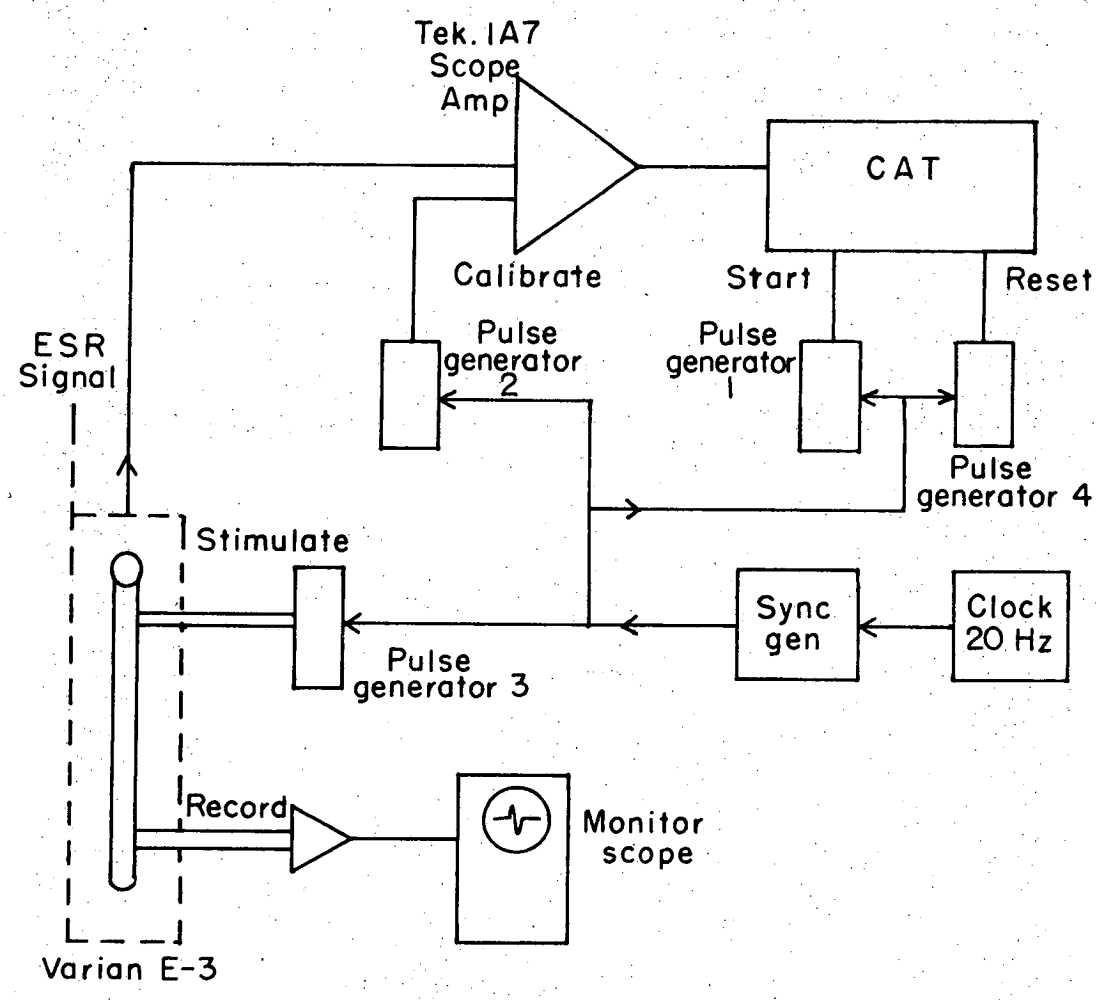

XBL 691-4032

Figure VII-11. Block diagram of synchronization circuitry.

system had sufficient sensitivity to detect a change in signal as small as 1 part in 10^{-3} with a time resolution of 1/6 millisec.

By taking the measurements at different fields, the entire ESR spectrum of the biradical labeled nerve could be studied point by point. Our initial results showed that the ESR spectra of lobster nerves labeled with biradicals A and C (see Figure VII-1) did not change during the action potential. Such a result may be due to the biradical being bound at sites where no conformation changes occur during membrane excitation. This finding is consistent with the idea that these particular biradicals are dissolved in a liquid-like hydrophobic region of the nerve.

F. Future Possibilities

As mentioned above, biradical A is not an ideal membrane probe. There are many variations of backbone structure and end groups which should be much more suitable for this study than the biradical actually used. Figures VII-12 and VII-13 show several of these which have been synthesized in our laboratory but not yet applied to the nerve. Biradical B, for instance, has a long hydrocarbon chain which might bind it more firmly to any lipid in the interior of the membrane. Biradical C, on the other hand, was constructed to have localized charges at each end which might bind to the charged surface of the membrane.

The possibilities of biradical variations seem boundless, and their use as probes for both active and inactive biological structures appears quite promising.

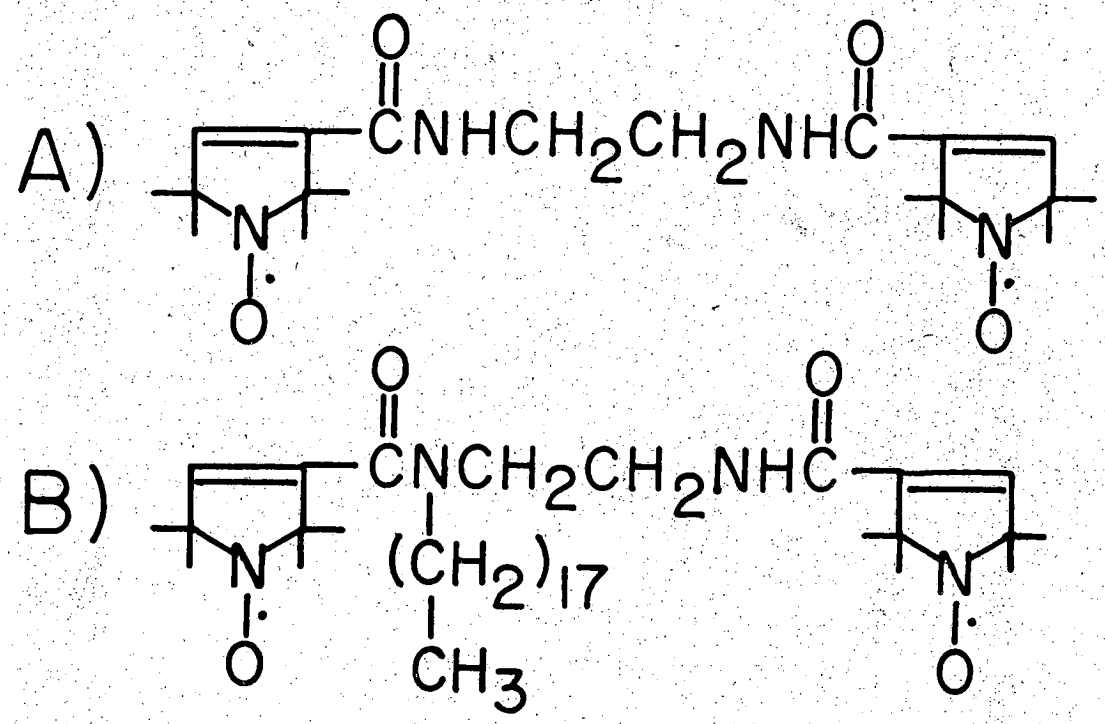

XBL693-4164

Figure VII-12.

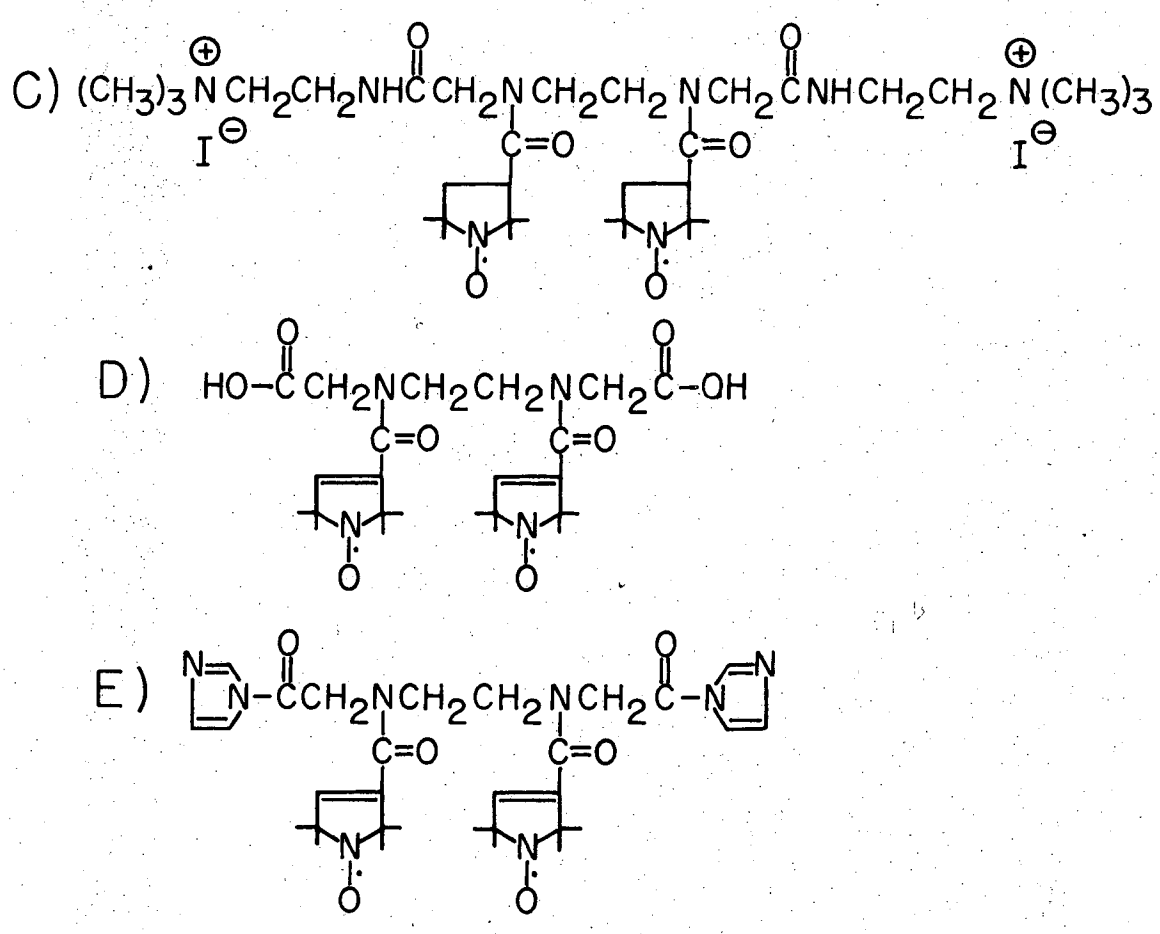

XBL 693-4165

Figure VII-13.

ACKNOWLEDGEMENTS

My graduate career at Berkeley from its inception has been somewhat unorthodox, and has been greatly aided by the understanding and aid of many people.

Dr. Owen Chamberlain, who enticed me here with an offer of great flexibility in my program, has not only fulfilled that promise, but also provided much encouragement and administrative support at crucial times.

During my first year, Dr. Fred Reif allowed me to work with him and his student, Mr. Clifford Surko, on liquid helium vortex rings. Since that time he has helped me at several points in my career--particularly in editing this thesis.

It is hard to describe how just a few words of periodic encouragement from Dr. Melvin Calvin, my research director, were able to undo most of the ill effects of several months of discouraging experiments. This encouragement, along with adequate financial support for equipment and unusual supplies, were very instrumental in this work.

Dr. Howard Wang, who worked with me during the final year of research, and Dr. Claude Lussan, who endured the first year, not only taught me much about fields outside of physics but also provided daily moral support and guidance.

To Gerryann Wulbern, Evie Litton, Susan A. Scharf, Don Phelps, George Ruben, Mel Klein, Dave Downie, Dick O'Brian, Bob Creedy, and Bill McAllister, and the other members of the Biodynamics Laboratory, I express my deep appreciation for your help and special favors.

It must be noted that the National Science Foundation withdrew its support during the last and crucial year of research. It is conjectured that this support was withdrawn because of several critical comments made by me in the required evaluation of the fellowship program requested by NSF. I would, however, like to acknowledge the support of the U. S. Atomic Energy Commission.

REFERENCES

1. A. L. Hodgkin, "Conduction of the Nervous Impulse", Liverpool University Press, Liverpool, England, 1965.
2. R. Pumphrey and J. Young, J. Exp. Biol. 15, 453 (1938).
3. Kenneth S. Cole, "Membranes, Ions and Impulses: A Chapter in Classical Biophysics", University of California Press, Berkeley, 1968.
4. M. I. Tasaki, "Nerve Excitation", Charles C. Thomas Co., Springfield, Illinois, 1968.
5. E. Rojas and I. Atwater, Nature, 215, 850 (1967).
6. B. Hille, J. Gen. Physiol. 50, 1287 (1967).
7. J. Pooler, Biophys. J. 8, 1009 (1968).
8. J. Leonard and S. Singer, Proc. Nat. Acad. Sci. 56, 1835 (1966).
9. J. Kavanau, Nature, 198, 525 (1963).
10. J. Lettvin, W. F. Pickard, W. S. McCulloch and W. Pitts, Nature, 202, 1338 (1964).
11. R. Ditchbourn, "Light", Interscience Publishers, New York, 1959.
12. M. Born and E. Wolfe, "Principles of Optics", Pergamon Press, New York, 1959, p. 702.
13. F. Schmitt and O. Schmitt, J. Physiol. 98, 26 (1940).
14. S. Solomon and J. Tobias, J. Gen. Physiol. 42, 159 (1960).
15. L. Kaoushin, R. Lyudkovskaya and I. Shmelev, Biofizika, 5, 279 (1960).

16. L. Shmelev and L. Kaoushin, Biofizika, 6, 40 (1961).

17. P. Liebman and G. Entine, J. Opt. Soc. Amer. 54, 1451 (1964).

18. P. Liebman and G. Entine, Appl. Optics 8, 1502 (1969).

19. L. Cohen and R. Keynes, Physiol. Soc. Meeting, London, Nov. 1967; J. Physiol. 194, 85P (1968).

20. L. Cohen, R. Keynes and B. Hille, Nature, 218, 438 (1968).

21. A. Watanabe, I. Tasaki and L. Carnay, Biol. Bull. 135, 442 (1968).

22. I. Tasaki, A. Watanabe, R. Sandlin and L. Carnay, Proc. Nat. Acad. Sci. 61, 883 (1968).

23. I. Tasaki, L. Carnay and R. Sandlin, Science 163, 683 (1969).

24. M. Calvin, H. Wang, G. Entine, D. Gill, P. Ferruti, M. Harpold and M. P. Klein, Proc. Nat. Acad. Sci. 63, 1 (1969).

25. R. Briere, R. M. Dupreyre, H. L. Lemaire, C. Morat, A. Rassat and P. Rey, Bull. Soc. Chim. France, 1963, 3290.

26. S. H. Glarum and J. H. Marshall, J. Chem. Phys. 47, 1374 (1967).

27. H. R. Falle, G. a. Lockhurst, H. Lemaire, Y. Marechal, A. Rassat and P. Rey, Molecular Physics, 11, 49 (1966).

28. G. Cauquis, M. Genies, H. Lemaire, A. Rassat and J. P. Ravet, J. Chem. Phys. 47, 4642 (1967).

29. H. Lemaire, A. Rassat and P. Rey, Bull. Soc. Chim. France, 1968, 886.

30. G. E. Pake, "Paramagnetic Resonance", W. A. Benjamin Press, New York, 1962, p. 91.

31. P. W. Anderson and P. R. Weiss, Rev. Mod. Phys. 25, 269 (1953).

32. M. S. Itzkowitz, J. Chem. Phys. 46, 3048 (1967).

SELECTED BIBLIOGRAPHY

AZZI, A., B. Chance, G. K. Radda and C. P. Lee, Proc. Nat. Acad. Sci. 62, 612 (1969). ANS fluorescence.

BEAR, R. and F. Schmitt, J. Opt. Soc. Amer. 26, 363 (1936). Birefringence.

BEAR, R., F. Schmitt and J. Young, Proc. Roy. Soc. London, 123B, 496, 505, 529 (1937).

BENNETT, M., Biophys. J. 7, 151 (1967). Fixed charge analysis.

BINSTOCK, L. and H. Lecar, J. Gen. Physiol. 53, 342 (1969). Ammonium currents.

CHALAZONITIS, N., Photochem. & Photobiol. 3, 539 (1964). Dyeing of nerves.

CHAPMAN, D., "Biological Membranes", Academic Press, New York, 1968.

HANDBUCH der Physik, 22, Chapter 11, G. Szivassy, p. 762. Birefringence.

KORN, E., Science 153, 1491 (1966). General review of membrane models.

LIEBERMAN, E., M. S. Perkins, T. Tomita and E. B. Wright, Science, 156, 240 (1967). Crab nerve.

LYUDKOVSKAYA, R., Biofizika 2, 589 (1957). General review of neurophysiology.

LYUDKOVSKAYA, R. and L. Kaoushin, Biofizika 5, 40 (1960). Nerve damage.

LUTHY, H. and P. Flugers, Archiv. 253, 477 (1951). U.V. nerve absorption.

NACHMANSOHN, D., "Bioelectrogenesis", Elsevier Publishing Company, New York, 1961, p. 237.

PAGANO, R. and T. Thompson, Biochim. Biophys. Acta 144, 666 (1967). Bilipid membranes.

ROJAS, E. and I. Atwater, Proc. Nat. Acad. Sci. 57, 1350 (1967); E. Rojas and J. Tobias, Biochim. Biophys. Acta 94, 394 (1965). Artificial membrane models.

SHASHOUA, V., Nature 215, 846 (1967). Bilipid excited membranes.

TASAKI, I., I. Singer and A. Watanabe, J. Gen. Physiol. 50, 989 (1967). Tracer experiment.

TASAKI, I., I. Singer and A. Watanabe, Proc. Nat. Acad. Sci. 54, 763 (1965). Sodium free media.

TOBIAS, J., Nature 203, 13 (1964). General review of membrane structure.

WATANABE, A., I. Tasaki and L. Lerman, Biol. Bull. 133, 491 (1967). Divalent ions and their effect on the action potential.

WEI, L., Science 163, 280 (1969). Transistor analog of nerve membrane.

YOUNG, J., J. Exp. Biol. 15, 170 (1938). Giant axon.

LEGAL NOTICE

This report was prepared as an account of Government sponsored work. Neither the United States, nor the Commission, nor any person acting on behalf of the Commission:

A. Makes any warranty or representation, expressed or implied, with respect to the accuracy, completeness, or usefulness of the information contained in this report, or that the use of any information, apparatus, method, or process disclosed in this report may not infringe privately owned rights; or

B. Assumes any liabilities with respect to the use of, or for damages resulting from the use of any information, apparatus, method, or process disclosed in this report.

As used in the above, "person acting on behalf of the Commission" includes any employee or contractor of the Commission, or employee of such contractor, to the extent that such employee or contractor of the Commission, or employee of such contractor prepares, disseminates, or provides access to, any information pursuant to his employment or contract with the Commission, or his employment with such contractor.

TECHNICAL INFORMATION DIVISION
LAWRENCE RADIATION LABORATORY
UNIVERSITY OF CALIFORNIA
BERKELEY, CALIFORNIA 94720